



THE HONG KONG  
POLYTECHNIC UNIVERSITY

香港理工大學

Pao Yue-kong Library

包玉剛圖書館

---

## Copyright Undertaking

This thesis is protected by copyright, with all rights reserved.

**By reading and using the thesis, the reader understands and agrees to the following terms:**

1. The reader will abide by the rules and legal ordinances governing copyright regarding the use of the thesis.
2. The reader will use the thesis for the purpose of research or private study only and not for distribution or further reproduction or any other purpose.
3. The reader agrees to indemnify and hold the University harmless from and against any loss, damage, cost, liability or expenses arising from copyright infringement or unauthorized usage.

If you have reasons to believe that any materials in this thesis are deemed not suitable to be distributed in this form, or a copyright owner having difficulty with the material being included in our database, please contact [lbsys@polyu.edu.hk](mailto:lbsys@polyu.edu.hk) providing details. The Library will look into your claim and consider taking remedial action upon receipt of the written requests.

The Hong Kong Polytechnic University  
Department of Applied Biology and Chemical Technology

**Biodegradable Poly(3-hydroxyalkanoate)s  
& Fullerene-Derived Drugs**

A Thesis

Submitted in Partial Fulfillment of the Requirements  
for the Degree of Doctor of Philosophy

by

Jidong He

June 2004



Pao Yue-kong Library  
PolyU · Hong Kong

## **CERTIFICATE OF ORIGINALITY**

I hereby declare that this thesis is my own work and that, to the best of my knowledge and belief, it reproduces no material previously published or written, nor material that has been accepted for the award of any other degree or diploma, except where due acknowledgement has been made in the text.

Jidong He

June, 2004

## ACKNOWLEDGEMENTS

I am grateful to my supervisor, Dr. Man Ken Cheung, who has influenced my scientific development. His novel ideas and devotion to research have made my study a rewarding experience. He has always impressed me with his kindness.

I am also grateful to Dr. Peter H. Yu of the Department of Applied Biology & Chemical Technology, and Dr. Guoqiang Chen of the Department of Biological Sciences & Biotechnology, Tsinghua University, Beijing, for their helpful discussion and for providing biodegradable materials. I would like to express special thanks to Dr. Paul R. Carlier of the Department of Chemistry, Virginia Tech, and Dr. Yongli Mi of the Department of Chemical Engineering, The Hong Kong University of Science & Technology, for their valuable suggestions.

I wish to offer my thanks to colleagues in our laboratory for their valuable advice, discussion and help. They are Professor Qingan Meng, Professor Sidong Li, Professor Zhongyuan Zhou, Dr. Jing Wang, and Dr. Cheng Chen. Thanks are also due to all the technicians, especially Mr. Wing-kong Kwan and Mr. Jimmy Ho, for their assistance.

I am deeply indebted to my wife and my daughter for their support and concern in the past three years.

Finally, I would like to thank the Research Committee of The Hong Kong Polytechnic University for the award of a studentship.

Abstract of thesis entitled '**Biodegradable Poly(3-hydroxyalkanoate)s**

**& Fullerene-Derived Drugs'**

submitted by **Ji-dong HE**

for the Degree of Doctor of Philosophy

at The Hong Kong Polytechnic University in June 2004

---

The major objectives of this dissertation are to assess the structure-properties relationships of (1) polyhydroxyalkanoates (PHAs), and of (2) a new water-soluble [60]fullerol synthesized by me that has potential as a therapeutic agent.

PHAs are biodegradable polyesters that can be synthesized from renewable sources by numerous bacteria. There is considerable potential for the design of PHAs for applications in drug delivery. PHB, P(HB–HV), and P(HB–HHx) are the most commonly found members of the PHA family. PHB has a narrow thermal processing window. However, the properties of P(HB–HV) and P(HB–HHx) vary widely depending on the mole percentage of HV and HHx in the copolymers. So it is important to determine the thermal properties in order to improve the thermal processing of these biopolymers.

Water-soluble C<sub>60</sub> derivatives can interact with DNA, proteins and living cells. Due to their photochemistry and radical quenching, multiple hydroxyl water-soluble fullerol will have broad clinical applications including drug synthesis.

In the first part of the experiment, thermal analyses of PHB, P(HB–HV), and P(HB–HHx) were conducted with thermogravimetry (TG) and differential scanning

calorimetry (DSC). The experimental results show that the incorporation of 30 mol % 3-hydroxyvalerate (HV) and 15 mol % 3-hydroxyhexanoate (HHx) components into the polyester increased the various thermal degradation relative to those of PHB by 3–12°C (measured at  $B = 40^{\circ}\text{C min}^{-1}$ ). DSC measurements showed that the incorporation of HV and HHx decreased the melting temperature relative to that of PHB by 70°C.

In the second part of the experiment, the thermal degradation kinetics of PHB and P(HB–HV) under nitrogen was studied by TG. The thermal degradation mechanism of PHB and P(HB–HV) under nitrogen was investigated with TG–FTIR and Py–GC/MS. The results show that the degradation products of PHB are mainly propene, 2-butenic acid, propenyl-2-butenate and butyric-2-butenate, whereas, those of P(HB–HV) are mainly propene, 2-butenic acid, 2-pentenoic acid, propenyl-2-butenate, propenyl-2-pentenoate, butyric-2-butenate, pentanoic-2-pentenoate and  $\text{CO}_2$ . The degradation is probably initiated from the chain scission of the ester linkage.

In the third part, the experiment focused on the synthesis and characterization of water-soluble ethoxy [60]fullerol. A novel fullerene derivative  $\text{C}_{60}(\text{OCH}_2\text{CH}_3)_8(\text{OH})_{16}$  was synthesized through the substitution of bromine atoms from  $\text{C}_{60}\text{Br}_{24}$  in  $\text{CH}_3\text{CH}_2\text{OH}/\text{H}_2\text{O}/\text{NaOH}$  solution at ambient temperature ( $23^{\circ}\text{C}$ ). Both the results of IR and NMR determination showed that the hydroxyl groups and ethoxy groups were bonded to the [60]fullerene cage. The antioxidant activity of ethoxy [60]fullerol is very weak. Ethoxy [60]fullerol has antitumor activity.

## CONTENTS

|   | <u>Page</u> |
|---|-------------|
| <b>Title.....</b>   | i           |
| <b>Certificate of Originality.....</b>  | ii          |
| <b>Acknowledgements.....</b>  | iii         |
| <b>Abstract.....</b>  | iv          |
| <b>Contents.....</b>  | vi          |
| <b>Abbreviations.....</b>   | xi          |
| <b>List of Figures.....</b>   | xiii        |
| <b>List of Tables.....</b>  | xvi         |
| <b>List of Published Work from Study.....</b>   | xvii        |
| <br>  |             |
| <b>Chapter 1</b>  |             |
| <b>Introduction.....</b>  | 1           |
| 1.1 Progress in Preparation of Water-soluble C <sub>60</sub> Derivatives.....               | 3           |
| 1.1.1 Enhancement of Water-solubility by Supramolecular Chemistry                           |             |
| Method.....   | 3           |
| 1.1.1.1 Inclusion Complexes of C <sub>60</sub> with Cyclodextrin (CD) or<br>Calixarene..... | 3           |
| 1.1.1.2 Preparation of Other Water-soluble C <sub>60</sub> Complexes.....                   | 7           |
| 1.1.2 Preparation of Water-soluble C <sub>60</sub> Derivatives.....                         | 8           |
| 1.1.2.1 Preparation of Multiple Hydroxyl C <sub>60</sub> Derivatives-Fullerol               |             |

|   |           |
|---|-----------|
| C <sub>60</sub> (OH) <sub>n</sub> .....   | 8         |
| 1.1.2.2 Preparation of Aminoacid C <sub>60</sub> Derivatives.....                                   | 9         |
| 1.1.2.3 Preparation of Other Water-soluble C <sub>60</sub> Derivatives.....                         | 10        |
| 1.1.3 Research Perspectives .....   | 14        |
| 1.2 PHAs as Biodegradable Controlled Drug Release Materials.....                                    | 14        |
| <br>  |           |
| <b>Chapter 2</b>  |           |
| <b>Materials and Methods.....</b>   | <b>17</b> |
| 2.1 Thermal Properties of PHAs.....   | 17        |
| 2.1.1 Materials.....  | 17        |
| 2.1.2 Measurements and Equipment.....   | 17        |
| TG analysis .....   | 17        |
| DSC analysis .....  | 18        |
| TG/FTIR analysis.....   | 18        |
| Py–GC/MS analysis.....  | 18        |
| Data processing.....  | 19        |
| 2.2 Synthesis and Characterization of C <sub>60</sub> Br <sub>24</sub> and Ethoxy [60]Fullerol..... | 20        |
| 2.2.1 Reagents.....   | 20        |
| 2.2.2 Synthesis of C <sub>60</sub> Br <sub>24</sub> .....   | 20        |
| 2.2.3 Synthesis of Ethoxy [60]Fullerol.....   | 21        |
| 2.2.4 Characterization of C <sub>60</sub> Br <sub>24</sub> and Ethoxy [60]Fullerol.....             | 21        |
| Liquid <sup>1</sup> H- and <sup>13</sup> C-Nuclear Magnetic Resonance.....                          | 21        |

|   |    |
|---|----|
| Solid <sup>13</sup> C-Nuclear Magnetic Resonance..... | 22 |
| Fourier Transform Infrared Spectrometer.....          | 22 |
| 2.3 Antioxidant Activity of Ethoxy [60]Fullerol.....  | 23 |
| Reagents.....   | 23 |
| DPPH assay.....                                       | 23 |
| FRAP assay.....                                       | 24 |
| Total phenolic content assay .....                    | 25 |

### **Chapter 3**

|  |           |
|--|-----------|
| <b>Thermal Behavior of Poly(3-hydroxybutyrate), Poly(3-hydroxybutyrate-co-3-hydroxyvalerate), and Poly(3-hydroxybutyrate-co-3-hydroxyhexanoate).....</b> | <b>26</b> |
| Introduction.....  | 26        |
| Results and Discussion .....   | 27        |
| Thermal Degradation of PHB.....  | 27        |
| Thermal Degradation of P(HB–HV) (70:30).....   | 28        |
| Thermal Degradation of P(HB–HHx) (85:15).....  | 29        |
| Effects of HV and HHx Incorporation on the Thermal Properties of PHB.....  | 30        |
| Conclusions.....   | 31        |

## **Chapter 4**

|  |           |
|--|-----------|
| <b>Thermal Degradation Kinetics and Mechanism of Poly(3-hydroxybutyrate) and Poly(3-hydroxybutyrate-co-3-hydroxyvalerate) as Studied by TG, TG–FTIR, and Py–GC/MS.....</b> | <b>38</b> |
| Introduction.....  | 38        |
| Results and Discussion.....  | 39        |
| Conclusions.....   | 42        |

## **Chapter 5**

|   |           |
|---|-----------|
| <b>Synthesis, Structure and Properties of Water-soluble Ethoxy [60]Fullerol</b> | <b>51</b> |
| Introduction.....   | 51        |
| Results and Discussion.....   | 52        |
| Synthesis and Characterization of C <sub>60</sub> Br <sub>24</sub> .....        | 52        |
| Synthesis and Characterization of Ethoxy [60]Fullerol.....                      | 55        |
| Evaluation of Ethoxy [60]Fullerol Composition.....                              | 57        |
| Antioxidant Activity of Ethoxy [60]Fullerol.....                                | 59        |
| Antitumor Activity of Ethoxy [60]Fullerol.....                                  | 59        |
| Conclusions.....  | 60        |

## **Chapter 6**

|  |           |
|--|-----------|
| <b>Suggestions for Further Work.....</b>                 | <b>70</b> |
| 6.1 Research of Molecular Recognition by Vancomycin..... | 70        |

|   |            |
|---|------------|
| 6.1.1 Chemical Structure and Resistance.....                                    | 70         |
| 6.1.2 Rational Modification.....  | 72         |
| 6.1.2.1 Modify the Binding Surface.....   | 72         |
| 6.1.2.2 Semi-synthetic Derivatives.....   | 72         |
| 6.1.2.3 Covalent Dimers.....  | 73         |
| 6.2 Ethoxy [60]Fullerol as Carrier with Vancomycin.....                         | 73         |
| 6.3 Purification and Structure Determination of [60]Fullerene Derivatives....   | 74         |
| 6.4 Antibacterial Activity of [60]Fullerene Derivatives.....                    | 74         |
| 6.5 Anticancer Bioactivity of [60]Fullerene Derivatives.....                    | 74         |
| <b>References.....</b>  | <b>75</b>  |
| <b>Appendices.....</b>  | <b>104</b> |
| <b>Appendix 1.</b> Elemental analysis of C <sub>60</sub> Br <sub>24</sub> ..... | <b>104</b> |
| <b>Appendix 2.</b> Elemental analysis of ethoxy [60]fullerol.....               | <b>105</b> |
| <b>Appendix 3.</b> MALDI-TOF reflection mass spectrum of ethoxy [60]fullerol... | <b>106</b> |

## ABBREVIATIONS

|                   |   |
|-------------------|---|
| BHT               | butylated hydroxytoluene                          |
| CD                | cyclodextrin                                      |
| CD-BPE            | cyclodextrin-bis(p-aminophenyl) ether             |
| CDCl <sub>3</sub> | deuteriated chloroform                            |
| CDP               | cyclodextrin polymer                              |
| DMF               | dimethylformamide                                 |
| DMSO              | dimethyl sulfoxide                                |
| DPPH              | 1,1-diphenyl-2-picrylhydrazyl living free radical |
| DSC               | differential scanning calorimetry                 |
| DTA               | differential thermal analysis                     |
| DTG               | derivative thermogravimetry                       |
| FRAP              | ferric reducing antioxidant power                 |
| FTIR              | Fourier transform infrared                        |
| GC                | gas chromatography                                |
| GPC               | gel permeation chromatography                     |
| HB                | 3-hydroxybutyrate or $\beta$ -hydroxybutyrate     |
| HHx               | 3-hydroxyhexanoate or $\beta$ -hydroxyhexanoate   |
| HMB               | hexamethylbenzene                                 |
| HV                | 3-hydroxyvalerate or $\beta$ -hydroxyvalerate     |
| MS                | mass spectrometry                                 |

|           |   |
|-----------|---|
| m/z       | mass-to-charge ratio (in mass spectrometry)   |
| NMR       | nuclear magnetic resonance                    |
| PHAs      | polyhydroxyalkanoates                         |
| PHB       | poly(3-hydroxybutyrate)                       |
| P(HB–HHx) | poly(3-hydroxybutyrate-co-3-hydroxyhexanoate) |
| P(HB–HV)  | poly(3-hydroxybutyrate-co-3-hydroxyvalerate)  |
| PVP       | poly(vinylpyrrolidone)                        |
| TBAH      | tetrabutylammonium hydroxide                  |
| TG        | thermogravimetry analysis                     |
| THF       | tetrahydrofuran                               |
| TMI       | trimethoxyindole                              |
| TMS       | tetramethylsilane                             |
| TPTZ      | 2,4,6-tripyridyl-s-triazine                   |

## LIST OF FIGURES

- Figure 1.1  $\gamma$ -CD
- Figure 1.2  $\gamma$ -CD/C<sub>60</sub> (1:1) and  $\gamma$ -CD/C<sub>60</sub> (2:1)
- Figure 1.3 Reaction scheme for the synthesis of polyfullerene
- Figure 1.4 Synthesis of fullerene-cyclodextrin conjugates
- Figure 1.5 C<sub>60</sub>-trimethoxyindole-oligonucleotide conjugate
- Figure 1.6 Synthesis of C<sub>60</sub>-fused functionalized pyrrolidines
- Figure 3.1 TG curves of PHB thermal degradation
- Figure 3.2 DTG curves of PHB thermal degradation
- Figure 3.3 Relation of thermal degradation temperatures and  $B$  for PHB thermal degradation
- Figure 3.4 TG curves of P(HB–HV) (70:30) thermal degradation
- Figure 3.5 DTG curves of P(HB–HV) (70:30) thermal degradation
- Figure 3.6 Relation of thermal degradation temperatures and  $B$  for P(HB–HV) (70:30) thermal degradation
- Figure 3.7 TG curves of P(HB–HHx) (85:15) thermal degradation
- Figure 3.8 DTG curves of P(HB–HHx) (85:15) thermal degradation
- Figure 3.9 Relation of thermal degradation temperatures and  $B$  for P(HB–HHx) (85:15) thermal degradation
- Figure 3.10 TG curves of PHB, P(HB–HV), and P(HB–HHx) thermal degradation at 40°C min<sup>-1</sup>

- Figure 3.11 DTG curves of PHB, P(HB–HV), and P(HB–HHx) thermal degradation at  $40^{\circ}\text{C min}^{-1}$
- Figure 4.1 TG curves of PHB thermal degradation at five heating rates
- Figure 4.2 TG curves of P(HB–HV) thermal degradation at five heating rates
- Figure 4.3 TG–FTIR stack plots for PHB under nitrogen at a heating rate of  $40^{\circ}\text{C min}^{-1}$
- Figure 4.4 TG–FTIR stack plots for P(HB–HV) under nitrogen at a heating rate of  $40^{\circ}\text{C min}^{-1}$
- Figure 4.5 FTIR spectra of gases evolved from PHB degradation at various temperatures
- Figure 4.6 FTIR spectra of gases evolved from P(HB–HV) degradation at various temperatures
- Figure 4.7 Chromatograms of products from pyrolysis of PHB in nitrogen at  $590^{\circ}\text{C}$
- Figure 4.8 Chromatograms of products from pyrolysis of P(HB–HV) in nitrogen at  $590^{\circ}\text{C}$
- Figure 4.9 Major products from thermal degradation of PHB and P(HB–HV) under  $\text{N}_2$
- Figure 5.1 FTIR spectrum of  $\text{C}_{60}\text{Br}_{24}$
- Figure 5.2 Solid-state  $^{13}\text{C}$ -NMR spectrum of  $\text{C}_{60}\text{Br}_{24}$  at spinning rate of 4 kHz
- Figure 5.3 Solid-state  $^{13}\text{C}$ -NMR spectrum of  $\text{C}_{60}$  at spinning rate of 4 kHz
- Figure 5.4 FTIR spectrum of ethoxy [60]fullerol
- Figure 5.5  $^{13}\text{C}$  CP/MAS spectrum of ethoxy [60]fullerol at MAS rate of 5 kHz

- Figure 5.6  $^1\text{H}$ -NMR spectrum of unpurified ethoxy [60]fullerol in  $\text{CDCl}_3$
- Figure 5.7  $^1\text{H}$ -NMR spectrum of purified ethoxy [60]fullerol in  $\text{CDCl}_3$
- Figure 5.8  $^1\text{H}$ -NMR spectrum of purified ethoxy [60]fullerol in  $\text{CDCl}_3$  with one drop  $\text{D}_2\text{O}$
- Figure 5.9  $^{13}\text{C}$ -NMR with proton decoupling spectrum of ethoxy [60]fullerol in  $\text{C}_6\text{D}_6$
- Figure 5.10  $^{13}\text{C}$ -NMR spectrum of ethoxy [60]fullerol in  $\text{C}_6\text{D}_6$  with Lorentzian line fitting
- Figure 5.11  $^1\text{H}$ -NMR spectrum of purified ethoxy [60]fullerol in  $\text{CDCl}_3$  with Lorentzian line fitting
- Figure 6.1 Chemical structure of vancomycin
- Figure 6.2 Final stage of peptidoglycan biosynthesis

## LIST OF TABLES

- Table 3.1 Thermal Degradation Temperatures of PHB, P(HB–HV), and P(HB–HHx) at a  $B$  of  $40^{\circ}\text{C min}^{-1}$
- Table 3.2  $T_g$  and  $T_m$  of PHB, P(HB–HV), and P(HB–HHx)
- Table 4.1 Relation between Heating Rate ( $B$ ) and Weight Loss Percentage ( $C$ ) for PHB and P(HB–HV) Degradation
- Table 4.2 Reaction Order and Activation Energy for PHB Degradation
- Table 4.3 Reaction Order and Activation Energy for P(HB–HV) Degradation
- Table 4.4 Products in the Py–GC/MS of PHB and P(HB–HV) at  $590^{\circ}\text{C}$  in  $\text{N}_2$
- Table 5.1 Antioxidant Activity of Ethoxy [60]Fullerol
- Table 5.2 Cytotoxic Property of Ethoxy [60]Fullerol against Human Breast Carcinoma (cell line: MCF-7)

## LIST OF PUBLISHED WORK FROM STUDY

1. “Thermal analyses of poly(3-hydroxybutyrate), poly(3-hydroxybutyrate-co-3-hydroxyvalerate), and poly(3-hydroxybutyrate-co-3-hydroxyhexanoate)”, He Jidong, Cheung Man Ken, Yu Peter H., Chen Guo Qiang. *Journal of Applied Polymer Science*, **2001**, 82(1):90-98 (# of times cited: 5)
2. “Thermal degradation of poly(3-hydroxybutyrate) and poly(3-hydroxybutyrate-co-3-hydroxyvalerate) as studied by TG, TG–FTIR, and Py–GC/MS”, Li Sidong, He Jidong, Yu Peter H., Cheung Man Ken. *Journal of Applied Polymer Science*, **2003**, 89(6):1530-1536
3. “Thermal stability and crystallization kinetics of isotactic polypropylene/organomontmorillonite nanocomposites”, He Jidong, Cheung Man Ken, Yang Ming Shu, Qi Zongneng. *Journal of Applied Polymer Science*, **2003**, 89(12):3404-3415

# Chapter 1

## Introduction

The major objectives of this dissertation are to assess the relationships between the structure and properties of (1) polyhydroxyalkanoates (PHAs), and of (2) a new water-soluble [60]fullerol I have synthesized that has potential as a therapeutic agent.

PHAs are new kind of biodegradable polyester that can be synthesized from renewable sources by numerous kinds of bacteria. They have many characteristics of conventional semi-crystalline thermoplastics. PHAs are not hydrophilic, and therefore are preferable to other biodegradable polymers in food and drug-controlled release applications, where moisture resistance is important.<sup>[1, 2]</sup> They also have better ultra-violet stability than conventional plastics such as polystyrene, poly(vinyl chloride), and poly(ethylene terephthalate), because PHAs are aliphatic polyesters. Poly(3-hydroxybutyrate) (PHB), the most commonly found PHA, does not possess the desirable material properties for use in a wide range of applications. PHB is brittle, thermally unstable above its melting point, and has a very narrow thermal processing window. Fortunately, the ability to control the properties of PHAs has been achieved in recent years by manipulating the average side-chain length or the co-monomer ratios. For example, adding a co-monomer such as 3-hydroxyvalerate (HV) or 3-hydroxyhexanoate (HHx) to the PHB chain decreases the melting point

and increases the thermal stability.<sup>[3, 4]</sup> The average side-chain length determines a variety of properties: strength, toughness, surface energy, biodegradability, water vapor permeability, melting point, glass transition, crystallization and thermal degradation.

Buckminsterfullerene ( $C_{60}$ )<sup>[5, 6]</sup> is a special spherical  $\pi$ -electron carbon cluster, which has exhibited the most attractive chemical and physical properties in the large family of room temperature, atmosphere-stable all-carbon hollow clusters. It is hydrophobic, however, and to be useful in biological applications, it must be made water-soluble. The commonly employed methods for achieving this are (1) encapsulation with cyclodextrins<sup>[7-10]</sup> or calixarenes;<sup>[11, 12]</sup> (2) water suspension;<sup>[13]</sup> (3) chemical functionalization with water-soluble appendages.<sup>[14-16]</sup> Derivatives obtained through the third method have additional interesting properties due to fullerene's electron accepting and photodynamic properties.

PHAs copolymers are particularly interesting candidates for drug delivery in view of their chemical and physical properties. Research into water-soluble fullerene derivatives led to the discovery of the interaction of organofullerenes with DNA,<sup>[17-19]</sup> enzymes<sup>[20-22]</sup> and living cells,<sup>[17, 23]</sup> which could yield some interesting biological and medical applications. So it is very important to explore the possibility of conjunction between PHAs and water-soluble fullerene derivatives.

## **1.1 Progress in Preparation of Water-soluble C<sub>60</sub> Derivatives**

Since Kroto et al.<sup>[5]</sup> discovered C<sub>60</sub> in 1985, research into this fascinating carbon cage has made great progress.<sup>[24, 25]</sup> Owing to its unique structure, C<sub>60</sub> reveals diverse reactivity such as Diels-Alder reactivity, Bingel reactivity etc., and it is a potent matrix for the design of medicines. Since a C<sub>60</sub> molecule has the approximately same radius as the cylinder that describes the active site of the HIV-1 protease and since C<sub>60</sub> (and its some derivatives) is primarily hydrophobic, a strong hydrophobic interaction between the C<sub>60</sub> derivatives and the active site surfaces should covert C<sub>60</sub> derivatives into effective inhibitors of the HIV-1 protease.<sup>[20, 21]</sup> In addition, light radiation effectively excites the C<sub>60</sub> molecules to the triplet state,<sup>[26]</sup> which can, in turn, convert molecular oxygen to singlet oxygen with a quantum yield of nearly unity.<sup>[27]</sup> Due to the high reactivity of singlet oxygen, C<sub>60</sub> can be used in photodynamic therapy.<sup>[17]</sup> Study of the biological application of fullerenes has attracted broad attention, but its hydrophobic nature has hindered the further development in this field. It is therefore very important to increase its solubility in aqueous solution.

### **1.1.1 Enhancement of Water-solubility by Supramolecular Chemistry Method**

#### **1.1.1.1 Inclusion Complexes of C<sub>60</sub> with Cyclodextrin (CD) or Calixarene**

The preparation of a supramolecular system by including C<sub>60</sub> with  $\gamma$ -CD or calixarenes is an effective method to improve the water-solubility of C<sub>60</sub>. A

cyclodextrin supermolecule formed by supermolecular chemistry in aqueous solution can be used in many biomedical fields. For instance, a nonpolar medicine can dissolve in water by forming a complex with CD. CD is a ring-shaped sugar compound formed from D-glucopyranose linked through  $\alpha$ -1,4 glucoside bond (Fig. 1.1), and is found in three forms:  $\alpha$ -CD,  $\beta$ -CD and  $\gamma$ -CD.  $\alpha$ -CD (cavity diameter 5–6Å) and  $\beta$ -CD (7–8Å) cannot discern  $C_{60}$  molecule easily because of its small cavity. Only  $\gamma$ -CD (9–10Å) can form an inclusion complex with  $C_{60}$  easily.<sup>[7-10]</sup> In 1992, Andersson et al.<sup>[7]</sup> prepared a water-soluble  $C_{60}$  complex through refluxing a solution of  $\gamma$ -CD with solid  $C_{60}$ , but this component has yet to be verified by experiment method. Boulas<sup>[8]</sup> and Priyadarsini<sup>[9]</sup> improved the preparation method of  $\gamma$ -CD- $C_{60}$  complex. Boulas prepared the complex of  $\gamma$ -CD with  $C_{60}$  by grinding, and found neutral  $C_{60}$  as well as its negative ion can be included by  $\gamma$ -CD. Priyadarsini put  $5.0 \times 10^{-7}$  mol of solid  $C_{60}$  into 25 ml  $\gamma$ -CD methanolic solution ( $5.4 \times 10^{-4}$  mol L<sup>-1</sup>) and stirred the mixture for 1 h. The resulting insoluble powder was separated and washed by methanol to remove pure CD, yielding the inclusion complex of  $C_{60}$  with  $\gamma$ -CD. This simple method produces  $C_{60}$  with solubility of up to  $1.0 \times 10^{-4}$  mol L<sup>-1</sup>. Zhang et al.<sup>[10]</sup> prepared discernible  $\gamma$ -CD/ $C_{60}$  (1:1) and  $\gamma$ -CD/ $C_{60}$  (2:1) solid complexes (Fig. 1.2) by the grinding method also. These two complexes were in accord with two types of complex structure proposed by Andersson and co-workers.<sup>[7]</sup>

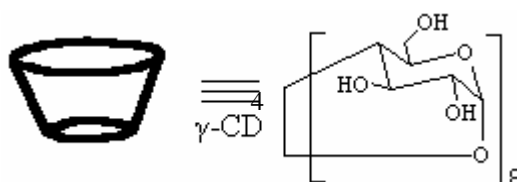


**Figure 1.1**  $\gamma$ -CD

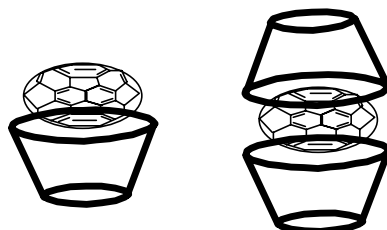


**Figure 1.2**  $\gamma$ -CD/ $C_{60}$  (1:1) and  $\gamma$ -CD/ $C_{60}$  (2:1)<sup>[10]</sup>

Because  $\beta$ -CD is very cheap, it has a good application outlook in enhancing the water-solubility of  $C_{60}$  and studying the possibility of aqueous reaction of  $C_{60}$ . Liu et al.<sup>[28]</sup> used the water-soluble  $\beta$ -CD polymer ( $\beta$ -CDP) crosslinked by epoxy chloropropane as main body to prepare the inclusion complex of  $\beta$ -CDP with  $C_{60}$ . Murthy et al.<sup>[29]</sup> reported that a stable water-soluble inclusion complex of  $\beta$ -CD with  $C_{60}$  was prepared by homogeneous reaction of  $\beta$ -CD and  $C_{60}$  for two weeks in the mixed solvent of DMF and toluene. Its solubility in water is up to  $4 \text{ g L}^{-1}$ . This kind of complex has low toxicity, and  $\beta$ -CD can be removed by normal metabolism and at the same time  $C_{60}$  in the  $\beta$ -CD cavity can retain the ability to eliminate free radicals in biological body. In addition, Samal et al.<sup>[30]</sup> prepared the first water-soluble polyfullerene (Fig. 1.3). A similar reaction between the inclusion complex

CD-bis(*p*-aminophenyl) ether (CD-BPE, N-N distance 968 pm) and C<sub>60</sub> produced polymer **1**, (poly[( $\beta$ -cyclodextrin-bis(*p*-aminophenyl) ether)-*co*-[60]fullerene]) that exhibited a high solubility in water (>10 mg ml<sup>-1</sup>). In exploring the application potential of this novel polymer, the preliminary results have shown that the material could be useful in biological and biomedical fields. The polyfullerene was found to strongly scavenge the 1,1-diphenyl-2-picrylhydrazyl living free radical (DPPH), even more strongly than [60]fullerene itself. Furthermore, this specific polymer was

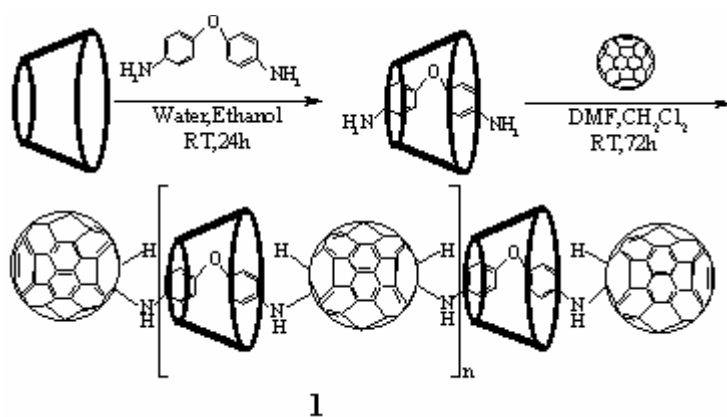


**Figure 1.3** Reaction scheme for the synthesis of polyfullerene<sup>[30]</sup>

also found to cleave DNA oligonucleotide in the presence of light, which was ascertained from the GPC studies in conjunction with membrane filtration of the nucleotide before and after cleaving experiments. These experiments indicate that the polymer has retained the properties of the pristine [60]fullerene.

Calixarene is a kind of bowl-shaped macrocycle with hydrophobic cavity, which is adjustable. It has variable conformation and good selectivity, and can form complexes with ion and neutral molecule. In 1992, Williams and Verhoeven<sup>[11]</sup> first reported that a sulfonic acid derivative of calix[8]arene can form a water-soluble donor-acceptor complex with C<sub>60</sub>, which allows extraction of C<sub>60</sub> from the organic phase into the aqueous phase. Molecular modeling calculations indicate that the complex has a core-shell structure. Consequently, Atwood et al.<sup>[12]</sup> reported that both C<sub>60</sub> and C<sub>70</sub> could form discrete complexes with calixarenes, in which *p*-tert-butyl calix[8]arene and calix[6]arene formed complexes (1:1 and 1:2) with C<sub>60</sub>, respectively.

#### **1.1.1.2 Preparation of Other Water-soluble C<sub>60</sub> Complexes**

Hungerbühler et al.<sup>[31]</sup> found that the water-soluble complexes can be prepared by incorporating C<sub>60</sub> into vesicular and micellar membranes in aqueous environment. For example, a solution of C<sub>60</sub> in an aqueous Triton X-100 micellar system exhibits a brownish color. It is concluded that C<sub>60</sub> is incorporated into the micelle since C<sub>60</sub> is not at all dissolved in water alone or below the critical micellar concentration ( $3.1 \times 10^{-4}$  M). By the analysis of UV spectrum, C<sub>60</sub> is not located in the inner hydrophobic part of the micelle. This is an only interaction of the polar polyethylene glycol units with the  $\pi$ -systems of C<sub>60</sub>.

Yamakoshi et al.<sup>[32]</sup> have found that C<sub>60</sub> and C<sub>70</sub> can be dissolved in water with poly(vinylpyrrolidone) (PVP), and the aqueous solutions of C<sub>60</sub> and C<sub>70</sub> are applied to haemolysis test using sheep-red blood cells. Both of C<sub>60</sub> and C<sub>70</sub> have no effect on haemolysis.

### **1.1.2 Preparation of Water-soluble C<sub>60</sub> Derivatives**

Some fullerene derivatives containing polar groups such as amino, hydroxyl, polar side chain can be prepared by addition reaction to enhance their water solubility.

#### **1.1.2.1 Preparation of Multiple Hydroxyl C<sub>60</sub> Derivatives-Fullerol C<sub>60</sub>(OH)<sub>n</sub>**

The main preparation method of water-soluble C<sub>60</sub> derivatives is to prepare fullerol C<sub>60</sub>(OH)<sub>n</sub> by a wide variety of addition reaction. Fullerol has allyl hydroxyl and medium electron affinity, so it can act as radical clearing agent and water-soluble antioxidant in physiological media.

In 1992, Naim et al.<sup>[33]</sup> reported that fullerol precipitates were prepared when a highly colored solution of C<sub>60</sub>/C<sub>70</sub> (30.2 mg) in toluene (30 ml) was heated in the presence of excess solid KOH under vacuum. This was the first report about C<sub>60</sub> bonding hydroxyl. Schneider et al.<sup>[34]</sup> synthesized water-soluble fullerols through the reaction of C<sub>60</sub> with an excess of BH<sub>3</sub>-THF complex followed by hydrolysis with

either glacial acetic acid, NaOH-H<sub>2</sub>O<sub>2</sub> or NaOH. Chiang et al.<sup>[14]</sup> described the synthesis and characterization of new polyhydroxyorganocarboxylated fullerene derivatives through the electrophilic addition of nitronium tetrafluoroborate onto fullerenes in the presence of arenecarboxylic acid in a nonaqueous medium. Hydrolysis of the ester moieties of these new fullerene derivatives in alkaline aqueous solution affords the corresponding water-soluble fullerols consisting of 18–20 hydroxyl groups per C<sub>60</sub> molecule on average. Li, J. et al.<sup>[35]</sup> reported that C<sub>60</sub> fullerol with 24–26 hydroxyl groups was synthesized directly by the reaction of fullerene with aqueous NaOH in the presence of tetrabutylammonium hydroxide (TBAH), which was the most effective catalyst under aerobic conditions at ambient temperature. Li, T. B. et al.<sup>[36]</sup> added H<sub>2</sub>O<sub>2</sub> to replace O<sub>2</sub> in the air as the oxidant, so developed a rapid method for the preparation of water-soluble C<sub>60</sub> fullerol which has stable structure and properties, can be widely used in many fields such as biology, medicine, and polymers.

#### **1.1.2.2 Preparation of Aminoacid C<sub>60</sub> Derivatives**

C<sub>60</sub> can react with many biological molecules, such as  $\alpha$ -aminoacids, polypeptides and proteins. Scientists<sup>[15, 16]</sup> pay more attention to C<sub>60</sub> aminoacid and peptide derivatives because they have unique biological activities and can be used in photodynamic therapy or as inhibitors of the HIV-1 protease. Zhou et al.<sup>[37]</sup> have prepared a water-soluble C<sub>60</sub> sodium glycinate derivative with C<sub>60</sub> and glycine

sodium. This derivative was characterized by IR, TG–DTA and XPS spectra. Gan et al.<sup>[38]</sup> have also prepared a water-soluble derivative  $C_{60}(NHCH_2CH_2CO_2Na)_x(H)_x$  with  $C_{60}$  and  $\beta$ -alanine sodium. Acidification of this derivative yields  $C_{60}(NHCH_2CH_2CO_2H)_x(H)_x$ . Elemental analysis suggests x is equal to 9.  $^1H$ - and  $^{13}C$ -NMR spectra show that the addition of the amino acid proceeded through its amino group. These amino acid derivatives are air-stable and may be used as precursors for further reaction. Kotelnikova et al.<sup>[39]</sup> have studied the modifying effects of the products of the equimolar addition of DL-alanine and DL-alanyl-DL-alanine to  $C_{60}$  on the structure and permeability of the lipid bilayer of phosphatidylcholine liposomes. The results show that these water-soluble amino acid and dipeptide derivatives of fullerene are able to localize inside the artificial membrane, to penetrate into the liposomes through the lipid bilayer and to perform activated transmembrane transport of bivalent metal ions. Prato et al.<sup>[40]</sup> have reported the preparation and the full characterization of the first peptide-containing fullerene derivative which possesses both  $C_{60}$  and peptide properties.

### 1.1.2.3 Preparation of Other Water-soluble $C_{60}$ Derivatives

Cyclodextrins (CD) can be used to prepare not only water-soluble inclusion complex  $C_{60}$ –CD, but also water-soluble  $C_{60}$  derivatives by covalent binding of fullerene with CD. These derivatives have high water solubility and biocompatibility. Samal et al.<sup>[41]</sup> prepared CD-amine-fullerene by nucleophilic addition of

cyclodextrin-R-monoamines to C<sub>60</sub>, where R represents iminoalkyl and iminoaryl residues (Fig. 1.4). The stable free radical DPPH has been used to study the antioxidant activities of phenols and catechol.

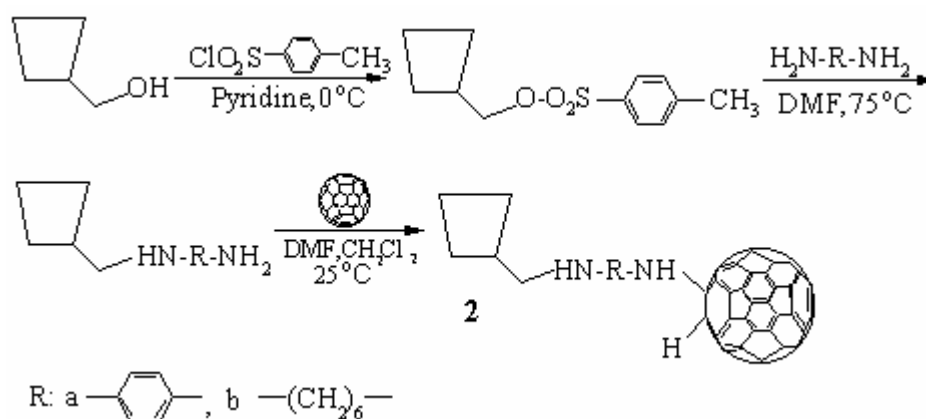


**Figure 1.4** Synthesis of fullerene-cyclodextrin conjugates<sup>[41]</sup>

The result indicated that **2a** was an effective radical scavenger. They also conducted a screening experiment in which a sample of DNA oligonucleotide, which was purified by membrane filtration prior to use, was treated with **2a** in aqueous media. The UV-Vis spectrum of the solution mixture indicated that there had been a reaction with the DNA in which **2a** was gradually consumed and DNA had undergone cleavage.

One of the problems of the photodynamic therapy is the addressed delivery of a photoactive agent to its target. So the conjugates of fullerene with molecules

possessing biological affinity to certain nucleic acids, proteins, cell types, organelles, etc. might be of particular interest. Recently, some conjugates between C<sub>60</sub> and nucleic acid specific agents have been reported, with the aim of better understanding the mechanism of action and to increase their cytotoxic properties and specificity. In order to achieve these goals, Bergamin et al.<sup>[42]</sup> synthesized a hybrid fullerene-trimethoxyindole(TMI)-oligonucleotide conjugate (Fig. 1.5). The TMI unit is characteristic of a class of natural antibiotics named duocarmycins, possessing antitumor activity in the picomolar range. The effect of the oligonucleotide chain could be considered both to induce high sequence-selectivity and to increase water solubility.

Ros et al.<sup>[43]</sup> found an easy access to water-soluble fullerene derivative by 1,3-dipolar cycloadditions of N-substituted glycine **3** to C<sub>60</sub> (Fig. 1.6). All compounds **4a-c** exhibit moderate solubility in a 9:1 ratio of water-DMSO. In preliminary biological tests, **4c** was found to be active against a variety of microorganisms. Different species of bacteria and different fungi strains were killed in a slightly modified agar diffusion test.

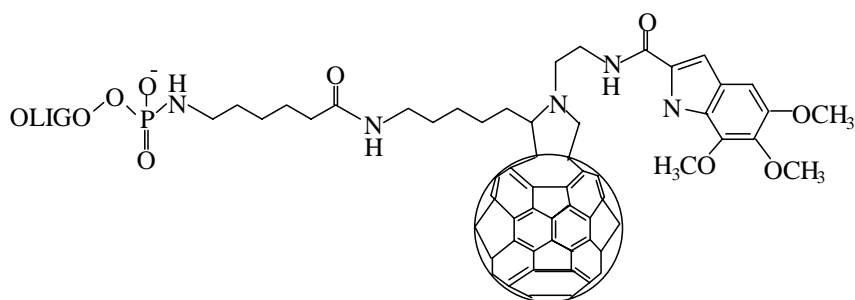


**Figure 1.5 C<sub>60</sub>-trimethoxyindole-oligonucleotide conjugate<sup>[42]</sup>**

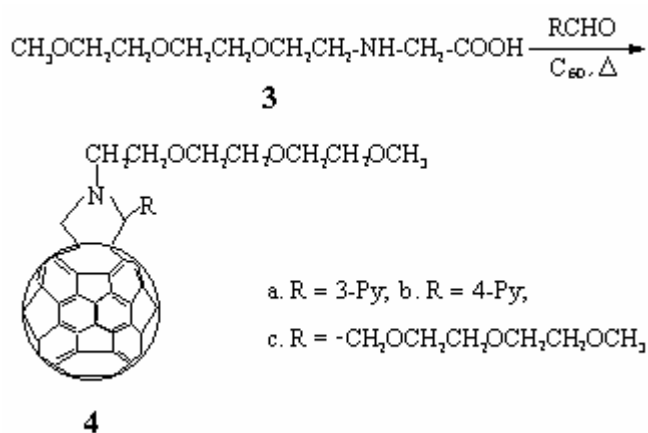


**Figure 1.6 Synthesis of C<sub>60</sub>-fused functionalized pyrrolidines<sup>[43]</sup>**

Bingel reaction is a kind of reaction that C<sub>60</sub> react with 2-bromomalonate esters. It is a good way to prepare methanofullerene derivatives. Richardson et al.<sup>[44]</sup> reported that a series of amino-substituted methanofullerene were prepared by mono-, tris-, and hexa- Bingel-Hirsch reactions using an N-protected malonate derivative. 64 g L<sup>-1</sup> of monoadduct, 152 g L<sup>-1</sup> of tris adduct, and 418 g L<sup>-1</sup> of hexa adduct were found to be soluble in water at room temperature. In addition, Brettreich and Hirsch<sup>[45]</sup> reported a polycarboxylated fullerene dendrimer with a water solubility of 254 g L<sup>-1</sup> using a similar method.

### **1.1.3 Research Perspectives**

The study of C<sub>60</sub> bioactivity has made a great achievement, and many water-soluble C<sub>60</sub> derivatives have been prepared. These water-soluble C<sub>60</sub> derivatives have special application in the fields of anti-HIV, photodynamic therapy and DNA cleavage. Thereby, the preparation of water-soluble C<sub>60</sub> derivatives, the development of its bioactivity and its wide application in many fields such as biological chemistry, biomedical and medical materials are very important.

### **1.2 PHAs as Biodegradable Controlled Drug Release Materials**

One of the enduring features of drug delivery technology is the central role that polymers play in control of drug release, and fabrication of drug delivery devices. Parenteral systems need to be biocompatible, and in many cases, are required to be biodegradable. The most well known class of biodegradable materials for controlled release is poly(lactide-co-glycolide)s, which were originally synthesized for use in manufacture of resorbable sutures. These copolymers have been developed as commercial products for sustained delivery of therapeutic peptides by careful control of polymer molecular weight, copolymer ratio, drug loading and device fabrication.<sup>[46, 47]</sup> Poly(3-hydroxybutyrate) (PHB) is a close chemical relative. PHB has been produced in ton quantities by biosynthesis as a potential biodegradable commodity polymer. This material has been available for

several years and awaits the right socio-economic conditions to fulfil its full potential in bulk packaging, but its applications in biomedical technology would certainly not be inhibited by cost. PHB is one of a broader group of PHAs, which can be synthesized by many bacteria as intracellular carbon and energy storage granules under conditions of restricted growth.<sup>[48-51]</sup>

PHAs may contain units other than 3-hydroxybutyrate (HB), such as 3-hydroxyvalerate (HV) and 3-hydroxyhexanoate (HHx).<sup>[3, 4]</sup> In recent years, much effort has been spent optimizing PHB bioproduction process and blending PHB or P(HB–HV) with other polymers to improve the physical and mechanical properties.<sup>[52-61]</sup> PHB is a relatively stiff and brittle material, and its melting point is about 180 °C.<sup>[62, 63]</sup> However, the properties of P(HB–HV) and P(HB–HHx), including the melting point, mechanical strength, and biodegradability, vary widely depending on the mole percent of HV and HHx in the copolymer.<sup>[64-73]</sup> These biopolymers are biocompatible, and may be used as artificial bones tissue scaffolds and drug delivery devices.<sup>[1, 2]</sup> Copolymers that have on average more than 4 carbon atoms in the side-chain, such as those with octanoate, nonanoate or decanoate units are elastomers at room temperature, and they behave as tacky gels during solvent extraction from the bacteria cells. These medium chain length PHAs are not widely available.



## Chapter 2

### Materials and Methods

#### 2.1 Thermal Properties of PHAs

##### 2.1.1 Materials

Biosynthesized PHB and P(HB–HV) were purchased from Fluka (product numbers 81329 and 27819, respectively). P(HB–HHx) were biosynthesized at Tsinghua University in Beijing, China with bacterial strain *Pseudomonas stutzeri* 1317 in a glucose mineral-salt medium.<sup>[74]</sup> P(HB–HV) (70:30) stands for the statistically random copolymer with a molar ratio of HB:HV of 70:30, and P(HB–HHx) (85:15) stands for HB:HHx = 85:15. The weight-average molecular weights ( $M_w$ ) of PHB and P(HB–HV) were 400–700 kDa, according to the supplier. The exact  $M_w$  depended on the lot number. The  $M_w$  of P(HB–HHx) was about 750 kDa.

##### 2.1.2 Measurements and Equipment

###### TG analysis

TG analyses were carried out with a Perkin–Elmer TGA-7 thermal gravimetric analyzer. The mass of each sample was about 5–6 mg, and the reaction environment was flowing nitrogen ( $50 \text{ ml min}^{-1}$ ).  $B$  ranged from 10 to  $50^\circ\text{C min}^{-1}$ .

TG and derivative thermogravimetry (DTG) curves were recorded in the course of heating from 50°C to 500°C.

### **DSC analysis**

Glass-transition temperature ( $T_g$ ) and melting temperature ( $T_m$ ) were measured by a Mettler Toledo DSC30 differential scanning calorimeter under a nitrogen atmosphere.

### **TG/FTIR analysis**

TG was performed under a nitrogen environment at a heating rate of 40°C min<sup>-1</sup> over a range of 50°C–500°C. The TG outlet was coupled on-line with the spectrometer through a gas cell, which was warmed up to 230°C and stabilized for 2 h before the running of TG. Subsequently, the stack plots of the TG–FTIR spectra were recorded.

### **Py–GC/MS analysis**

Py–GC/MS experiments were carried out with a Japan Analytical Industry JHP-3S Curie point pyrolyzer coupled to a HP6890 gas chromatograph linked to a 5973 quadrupole mass spectrometer. The samples were pyrolyzed at 590°C for 10 s.

The carrier gas was high-purity nitrogen at a flow rate of 50 ml min<sup>-1</sup>. The GC column was a HP-5 fused silica capillary column. The GC column temperature was initially held at 50°C for 2 min; then, at a rate of 5°C min<sup>-1</sup>, it was raised to 280°C and held there for 30 min. The GC–MS interface was set at 230°C. Mass spectra were recorded under an electron impact ionization energy of 70 eV. The total flow was split at a ratio of 50:1. The mass of each sample was 0.10–0.20 mg.

### Data processing

The reaction kinetic parameters were obtained by the processing of TG data through the Coats–Redfern integral method.<sup>[75]</sup> Integrating the reaction kinetic equation

$$d\alpha/dt = k(1 - \alpha)^n \quad (1)$$

and using the Arrhenius equation

$$k = Ae^{-E/RT} \quad (2)$$

the following equations can be obtained:

$$\ln\{[1 - (1 - \alpha)^{1-n}]/[T^2(1 - n)]\} = \ln[(1 - 2RT/E)AR/BE] - E/RT \quad (n \neq 1) \quad (3)$$

and

$$\ln[-\ln(1 - \alpha)/T^2] = \ln[(1 - 2RT/E)AR/BE] - E/RT \quad (n = 1) \quad (4)$$

where  $n$  is the reaction order,  $\alpha$  is the reaction degree,  $T$  is the absolute temperature,  $B$  is the heating rate,  $E$  is the reaction activation energy,  $R$  is the gas constant, and  $A$  is the frequency factor. Where  $n \neq 1$ , a line can be obtained from the plot of  $\ln\{[1 - (1 - \alpha)^{1-n}]/[T^2(1 - n)]\}$  versus  $1/T$ , of which the slope is  $-E/R$ , and the intercept is  $\ln[(1 - 2RT/E)AR/BE]$ . Where  $n = 1$ , a line can be obtained from the plot of  $\ln[ - \ln(1 - \alpha)/T^2]$  versus  $1/T$ , of which the slope is  $-E/R$ , and the intercept is  $\ln[(1 - 2RT/E)AR/BE]$ . Adopting the least-squares fitting method with different values of  $n$ , the  $n$  with the maximum correlated coefficient ( $r$ ) is the reaction order, and the corresponding  $E$  is the apparent activation energy.

## 2.2 Synthesis and Characterization of C<sub>60</sub>Br<sub>24</sub> and Ethoxy [60]Fullerol

### 2.2.1 Reagents

C<sub>60</sub> (purity > 99.9%) was purchased from Wuhan University, China. All the other reagents were of analytical grade.

### 2.2.2 Synthesis of C<sub>60</sub>Br<sub>24</sub><sup>[76]</sup>

A reaction flask (100 ml) charged with liquid bromine (65 ml) and C<sub>60</sub> (500 mg). The mixture was stirred at 30°C under nitrogen for 4 days to give a homogeneous orange yellow powder. The solid product was isolated by filtration

and dried under vacuum at 65°C for 4 days. The elemental analysis gave a average composition of C<sub>60</sub>Br<sub>25.5</sub>.

### **2.2.3 Synthesis of Ethoxy [60]Fullerol**

A reaction flask (100 ml) charged with ethanol (25 ml), water (40 ml), sodium hydroxide (6 g) and C<sub>60</sub>Br<sub>24</sub>(Br<sub>2</sub>)<sub>x</sub> (500 mg). The mixture was stirred at ambient temperature (23°C) for 6 h to give a homogeneous red brownish solution. Adding hydrogen chloride water solution (37%) into flask to make the solution pH<7, salts were precipitated. The solvent was evaporated by placing the sample under a flow of air, and then extracted and evaporated with acetone, tetrahydrofuran and benzene, respectively. The separation and purification of the solid thus obtained were performed by solubility differences in solvents of differing polarity, followed by thin-layer chromatography (E. Merck: Analytical Aluminum Backed Plates/Silica Gel 60 F254; developing solvent, dichloride methane/methanol (20/80, v/v)).

### **2.2.4 Characterization of C<sub>60</sub>Br<sub>24</sub> and Ethoxy [60]Fullerol**

#### **Liquid <sup>1</sup>H- and <sup>13</sup>C-Nuclear Magnetic Resonance**

The identify of the component of ethoxy [60]fullerol was confirmed by liquid 500 MHz proton and carbon nuclear magnetic resonance (NMR). Sample of suitable weight was placed into the NMR tube and 1 ml deuteriated solvent was

added to dissolve the sample for measurement.  $^1\text{H}$ - and  $^{13}\text{C}$ -NMR spectra were recorded at ambient temperature ( $23^\circ\text{C}$ ) on a Varian AS500 high-resolution spectrometer (Varian, USA) in the pulse Fourier transform (FT) mode.

### **Solid $^{13}\text{C}$ -Nuclear Magnetic Resonance**

The identify of the component of  $\text{C}_{60}$ , [60]fullerene bromide and ethoxy [60]fullerol was confirmed by solid carbon nuclear magnetic resonance (NMR). Sample of 500 mg was placed into 7.5 mm Chemagnetics<sup>TM</sup> Pencil<sup>TM</sup> rotor for measurement. The spinning rates were stable within  $\pm 1$  Hz.  $^{13}\text{C}$ -NMR spectra were recorded at ambient temperature ( $23^\circ\text{C}$ ) on a Varian INOVA<sup>TM</sup> high-power, wide-bore, 400 Mz spectrometer (Varian, USA). The  $^{13}\text{C}$  chemical shift scale was set using a solid external reference, hexamethylbenzene (HMB). The  $^{13}\text{C}$  groups of HMB resonate at 17.35 ppm relative to tetramethylsilane (TMS).

### **Fourier Transform Infrared Spectrometer**

Fourier transform infrared (FTIR) measurements were performed on a Nicolet AVATAR360 infrared spectrometer. The spectra were recorded at a resolution of  $4\text{ cm}^{-1}$  and averaged 64 scans. Samples were prepared by mixing [60]fullerene bromide or ethoxy [60]fullerol with KBr, which was stressed into a thin layer under a suitable pressure. The sample layer was subjected to IR analysis.

### **2.3 Antioxidant Activity of Ethoxy [60]Fullerol**

#### **Reagents**

1,1-diphenyl-2-picrylhydrazyl (DPPH, Sigma-Aldrich, Germany), 2,4,6-tripyridyl-s-triazine (TPTZ, Fluka, Switzerland), Folin-Ciocalteu's reagent (BDH, England), gallic acid (Advanced Technology and Industrial Co. Ltd., Hong Kong), ascorbic acid (Panreac Quimica SA, Spain) and butylated hydroxytoluene (BHT, Acros Organics, New Jersey, USA). All the other reagents were of analytical grade.

#### **DPPH assay**

In this assay, antioxidants in the sample scavenge free radical DPPH,<sup>[77, 78]</sup> which has a maximum absorption at 515 nm. Scavenging results in the drop in absorbance, the size of which is proportional to the antioxidant capacity of the sample. In the experiment, the absorbance value of 1.95 ml of DPPH (24 mg L<sup>-1</sup>) in methanol was measured as control, and then 50 µl of each sample solution at a concentration of 7.5 mg ml<sup>-1</sup> were mixed and the absorbance change was measured using a UV-Vis spectrometer (Perkin-Elmer Lambda 35, USA) at 515 nm. The change in absorbance was determined at 2, 3, 4 and 5 minutes, and then at 5 min interval until the absorbance change was not more than 0.003 absorbance units per min. The final absorbance reading of the sample was used to calculate the percentage free radical scavenging capacity (SR%) as follows:

$$\text{SR}\% = (1 - A_{\text{sample}}/A_{\text{control}}) \times 100\%$$

$A_{\text{control}}$ : the absorbance value of the DPPH solution before addition of sample solution or reference antioxidant solution.

$A_{\text{sample}}$ : the final absorbance value of DPPH solution after addition of sample solution or reference antioxidant solution.

### **FRAP assay**

The ferric reducing antioxidant power (FRAP) assay is a direct test of 'total antioxidant power', which uses antioxidant as reductant in a redox-linked colorimetric method, employing an easily reduced oxidant ( $\text{Fe}^{3+}$ ) present in stoichiometric excess.<sup>[79]</sup> At low pH, the ferric tripyridyltriazine ( $\text{Fe}^{3+}$ -TPTZ) complex is reduced by antioxidants in the sample to the ferrous form ( $\text{Fe}^{2+}$ -TPTZ), which appears an intense blue color. The reaction can be monitored at 593 nm. The assay was performed as described by Benzie and Strain<sup>[79, 80]</sup> using a Cobas Fara centrifugal analyzer (Roche Diagnostics Ltd. Basel, Switzerland). In the experiment, 300  $\mu\text{l}$  freshly prepared FRAP reagent, 25 ml acetate buffer (300  $\text{mmol L}^{-1}$ , pH = 3.6), 2.5 ml TPTZ (10  $\text{mmol L}^{-1}$ ) in 40  $\text{mmol L}^{-1}$  HCl, and 2.5 ml  $\text{FeCl}_3 \cdot 6\text{H}_2\text{O}$  solution (20  $\text{mmol L}^{-1}$ ) were mixed as required to prepare working FRAP reagent. It was warmed to 37°C and a reagent blank reading was taken at 593 nm, and then 10  $\mu\text{l}$  of each sample solution of an appropriate concentration was added along with 30  $\mu\text{l}$   $\text{H}_2\text{O}$ . The 0–4 min absorbance change ( $A_{593\text{nm}}$ ) was calculated for each sample

and related to  $A_{593\text{nm}}$  of a  $\text{Fe}^{2+}$  standard solution tested in parallel to obtain the FRAP value of each sample. The FRAP values of ascorbic acid and BHT were obtained by the same procedure.

### **Total phenolic content assay**

The total phenolic content in the samples was measured by the Folin-Ciocalteu method, following the procedure of Singleton et al.<sup>[81]</sup> In brief, phenolic groups are oxidized by phosphomolybdic and phosphotungstic acids in Folin-Ciocalteu reagent, forming a green-blue complex detectable at 750 nm. In the test, 200  $\mu\text{l}$  of each sample solution of an appropriate concentration was mixed with 1 ml of Folin-Ciocalteu reagent (1:10 diluted with  $\text{H}_2\text{O}$ ) and 800  $\mu\text{l}$  of  $\text{Na}_2\text{CO}_3$  (75.05 g  $\text{L}^{-1}$ ). The absorbance at 750 nm was measured after 2 h reaction at room temperature. The aqueous gallic acid solution was freshly prepared in a series of concentrations (10–80  $\mu\text{g ml}^{-1}$ ) and tested in parallel to establish the standard curve. The total phenolic content of each sample was calculated as gallic acid equivalents.

## **Chapter 3**

### **Thermal Behavior of Poly(3-hydroxybutyrate), Poly(3-hydroxybutyrate-co-3-hydroxyvalerate), and Poly(3-hydroxybutyrate-co-3-hydroxyhexanoate)**

#### **Introduction**

PHAs are naturally occurring biodegradable polyesters produced as energy storage materials by many bacteria. Their macroscopic properties are controlled by their chemical structure and composition.<sup>[58, 82, 83]</sup> PHB, P(HB–HV) and P(HB–HHx) possess the physical properties and processability of conventional thermoplastics and yet are fully biodegradable when disposed of in a microbially active environment.<sup>[84, 85]</sup> PHB is a isotactic semi-crystalline polyester with great potential as a biodegradable commodity and appears to be biocompatible. Hydrolytic degradation occurs by surface erosion, which makes it an attractive material for controlled release applications. The homopolymer PHB has a relatively high melting point and crystallizes rapidly, making entrapment of drug technically difficult. The related copolymers P(HB–HV) and P(HB–HHx) have similar semi-crystalline properties though their slower rates of crystallization result in matrices with different properties, which merits further investigation.

In this study, the thermal behavior of PHB, P(HB–HV) and P(HB–HHx) were investigated with dynamic thermogravimetry (TG). The effects of the heating rate ( $B$ ) on the degradation temperature ( $T$ ) and the effects of HV and HHx incorporation on the thermal properties of PHB were considered.

## Results and Discussion

### Thermal Degradation of PHB

Figures 3.1 and 3.2 show the TG and DTG curves from the thermal degradation of PHB at five different values of  $B$ . The TG curve is a smooth weight-loss curve. The DTG curve shows only a single rate of weight loss ( $dW/dt$ ) peak. This indicates that the degradation consisted of one weight-loss step. With increases in  $B$ , the TG and DTG curves shift toward the high-temperature zone. The degradation behavior at all five  $B$  values was similar.

Figure 3.3 shows the effect of  $B$  on  $T$ .  $T_o$  is the temperature at the onset of weight loss.  $T_p$  is the temperature at the maximum  $dW/dt$ , the tip of the DTG curve peak, and  $T_f$  is the temperature at complete degradation.  $T_o$  and  $T_f$  were obtained from the TG curve with a bitangent method. The peak width of the DTG curve can be expressed as  $T_f - T_o$ .

It can be seen from Figure 3.3 that  $T$  increased with  $B$ , indicating that  $B$  was the main factor affecting  $T$ . These factors were related as follows:

$$T_o = 0.75B + 311$$

$$T_p = 0.91B + 320$$

$$T_f = 1.00B + 325$$

The thermal degradation temperature could be expressed more exactly as an equilibrium degradation temperature  $T(0)$  when  $B$  approached zero:  $T_o(0) = 311^\circ\text{C}$ ,  $T_p(0) = 320^\circ\text{C}$ ,  $T_f(0) = 325^\circ\text{C}$ . The peak width  $T_f - T_o = 0.25B + 14$  and increased with  $B$ .

### **Thermal Degradation of P(HB–HV) (70:30)**

Figures 3.4 and 3.5 show the TG and DTG curves for the thermal degradation of P(HB–HV) (70:30) at five different values of  $B$ . Like that of PHB, the DTG curve of P(HB–HV) (70:30) consists of one peak.

Figure 3.6 illustrates that the thermal degradation temperature increased linearly with  $B$ . The equations are as follows:

$$T_o = 0.96B + 308$$

$$T_p = 0.99B + 320$$

$$T_f = 1.09B + 325$$

The equilibrium thermal degradation temperatures were  $T_o(0) = 308^\circ\text{C}$ ,  $T_p(0) = 320^\circ\text{C}$ , and  $T_f(0) = 325^\circ\text{C}$ , respectively. The peak width could be expressed as  $T_f - T_o = 0.13B + 17$ , which increased with  $B$ .

### **Thermal Degradation of P(HB–HHx) (85:15)**

Figures 3.7 and 3.8 show the TG and DTG curves for the thermal degradation of P(HB–HHx) (85:15) at five different values of  $B$ . Like that of PHB and P(HB–HV), the DTG curve of P(HB–HHx) (85:15) consists of only one peak.

Figure 3.9 illustrates that the thermal degradation temperature increased linearly with  $B$ . The equations are as follows:

$$T_o = 1.11B + 305$$

$$T_p = 1.10B + 319$$

$$T_f = 1.16B + 325$$

The equilibrium thermal degradation temperatures were  $T_o(0) = 305^\circ\text{C}$ ,  $T_p(0) = 319^\circ\text{C}$ , and  $T_f(0) = 325^\circ\text{C}$ , respectively. The peak width could be expressed as  $T_f - T_o = 0.05B + 20$ , which increased with  $B$ .

### Effects of HV and HHx Incorporation on the Thermal Properties of PHB

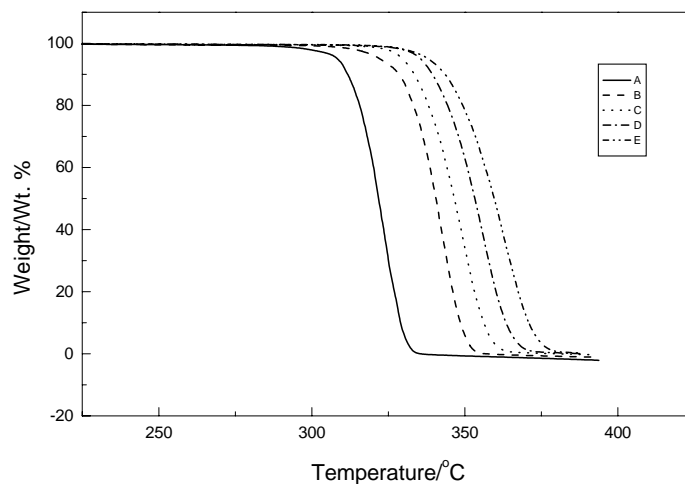
Figures 3.10 and 3.11 show the TG and DTG curves of PHB, P(HB–HV) (70:30), and P(HB–HHx) (85:15) at  $B = 40^\circ\text{C min}^{-1}$ . Table 3.1 lists the thermal degradation temperatures  $T_o$ ,  $T_p$ , and  $T_f$  for the three polyesters. The molecular weights of the polymers were of the same order of magnitude. Therefore, it is obvious from the figures and Table 3.1 that the thermal stability of the polyesters increased with increasing number of structural carbon units in the polymers.

Table 3.2 lists  $T_g$  and  $T_m$  for the three polyesters. It is obvious from Table 3.2 that P(HB–HV) and P(HB–HHx) had a lower  $T_g$  and  $T_m$  than PHB. Furthermore, the literature shows that P(HB–HV) has a lower degree of crystallinity and a lower  $T_m$ <sup>[62, 63, 71]</sup> but only a slightly lower mechanical strength than PHB. It is also known from the literature that the homopolymer PHB is thermally unstable at temperatures just slightly above a melting point of about  $180^\circ\text{C}$ . It has been reported that a PHB sample stored at  $190^\circ\text{C}$  for 1 h degraded to half its original molecular weight.<sup>[86]</sup> It is unfavorable for the processing of polymers when  $T_m$  and  $T_p$  are very close. PHB is limited to a narrow melt-process window of short residence times, and stabilizers have had little effect.<sup>[87]</sup> Incorporating HV units in 10–50 mol % reduces the melting point to  $150$ – $100^\circ\text{C}$ , respectively.<sup>[62]</sup> This study showed that the copolymers have higher thermal degradation temperatures relative to PHB at any given nonzero  $B$ . Extrapolating back to zero  $B$  allows us to calculate the peak width at zero  $B$ ,  $T_f(0) - T_o(0)$ , which gives us an index of how thermally stable the polymers are. The peak widths at zero  $B$  for PHB, P(HB–HV), and P(HB–HHx) were 14, 17, and  $20^\circ\text{C}$ ,

respectively. It was clear that the copolymers degraded slower than the homopolymer.

## **Conclusions**

The weight loss of PHB, P(HB–HV), and P(HB–HHx) caused by thermal degradation was a one-step process. The thermal degradation temperatures of the polymers increased with increasing  $B$ . The peak width of the DTG curves increased with  $B$ . The peak widths at zero  $B$ ,  $T_f(0) - T_o(0)$ , for PHB, P(HB–HV), and P(HB–HHx) were 14, 17, and 20°C, respectively. The incorporation of HV and HHx into the homopolymer rendered the polymer chain more flexible, as indicated by the decrease in  $T_g$  and  $T_m$ ; therefore, P(HB–HV) and P(HB–HHx) were more thermally stable than PHB.



**Figure 3.1** TG curves of PHB thermal degradation: (A)  $B = 10^{\circ}\text{C min}^{-1}$ , (B)  $B = 20^{\circ}\text{C min}^{-1}$ , (C)  $B = 30^{\circ}\text{C min}^{-1}$ , (D)  $B = 40^{\circ}\text{C min}^{-1}$ , and (E)  $B = 50^{\circ}\text{C min}^{-1}$ . The weight is expressed on the vertical axis as a percentage of the initial weight (wt %). The temperature ( $^{\circ}\text{C}$ ) is expressed on the horizontal axis.

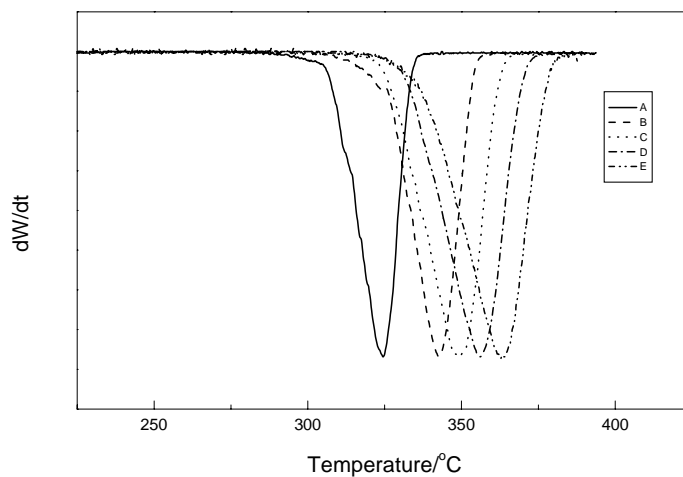


**Figure 3.2** DTG curves of PHB thermal degradation: (A)  $B = 10^{\circ}\text{C min}^{-1}$ , (B)  $B = 20^{\circ}\text{C min}^{-1}$ , (C)  $B = 30^{\circ}\text{C min}^{-1}$ , (D)  $B = 40^{\circ}\text{C min}^{-1}$ , and (E)  $B = 50^{\circ}\text{C min}^{-1}$ .  $dW/dt$  is shown on the vertical axis. The temperature ( $^{\circ}\text{C}$ ) is expressed on the horizontal axis.

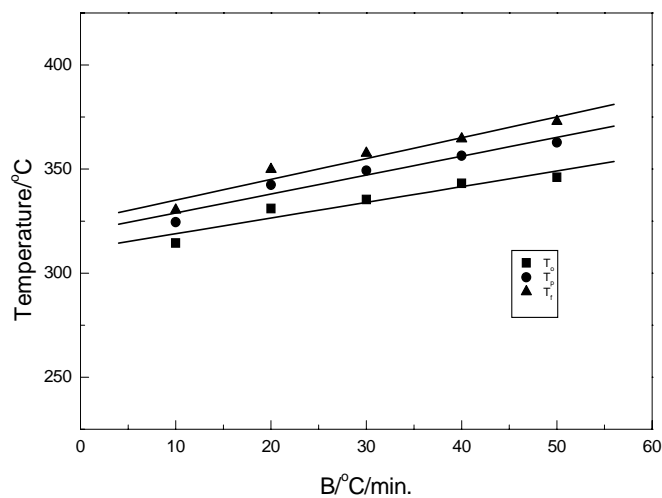


**Figure 3.3 Relation of thermal degradation temperatures and  $B$  for PHB thermal degradation.**

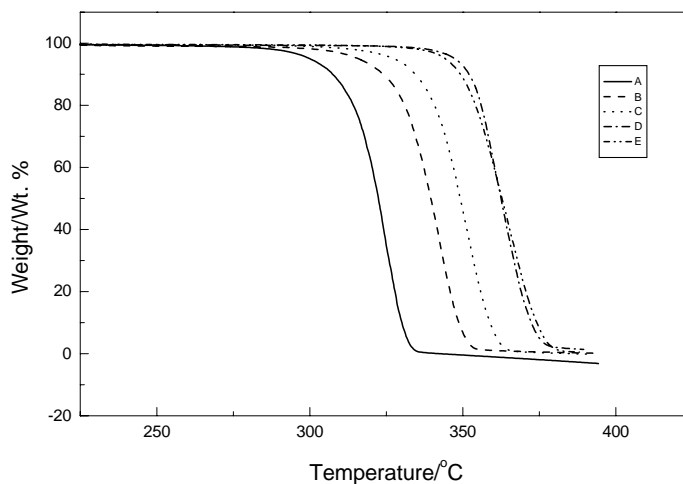


**Figure 3.4 TG curves of P(HB–HV) (70:30) thermal degradation: (A)  $B = 10^{\circ}\text{C min}^{-1}$ , (B)  $B = 20^{\circ}\text{C min}^{-1}$ , (C)  $B = 30^{\circ}\text{C min}^{-1}$ , (D)  $B = 40^{\circ}\text{C min}^{-1}$ , and (E)  $B = 50^{\circ}\text{C min}^{-1}$ . The weight is expressed on the vertical axis as a percentage of the initial weight (wt %). The temperature ( $^{\circ}\text{C}$ ) is expressed on the horizontal axis.**

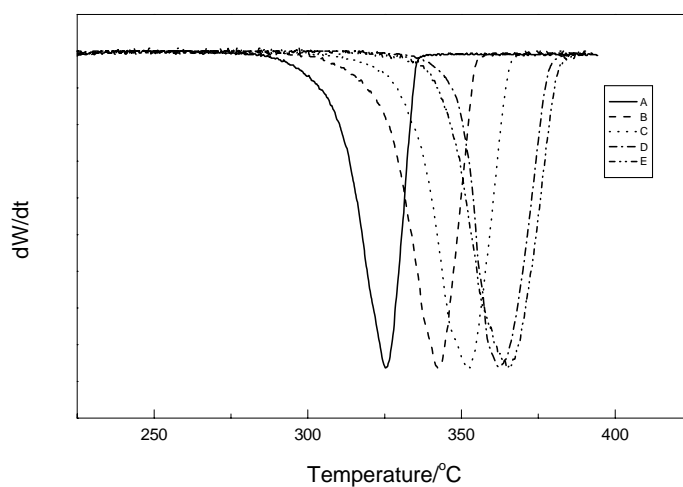


**Figure 3.5** DTG curves of P(HB–HV) (70:30) thermal degradation: (A)  $B = 10^{\circ}\text{C min}^{-1}$ , (B)  $B = 20^{\circ}\text{C min}^{-1}$ , (C)  $B = 30^{\circ}\text{C min}^{-1}$ , (D)  $B = 40^{\circ}\text{C min}^{-1}$ , and (E)  $B = 50^{\circ}\text{C min}^{-1}$ .  $dW/dt$  is shown on the vertical axis. The temperature ( $^{\circ}\text{C}$ ) is expressed on the horizontal axis.

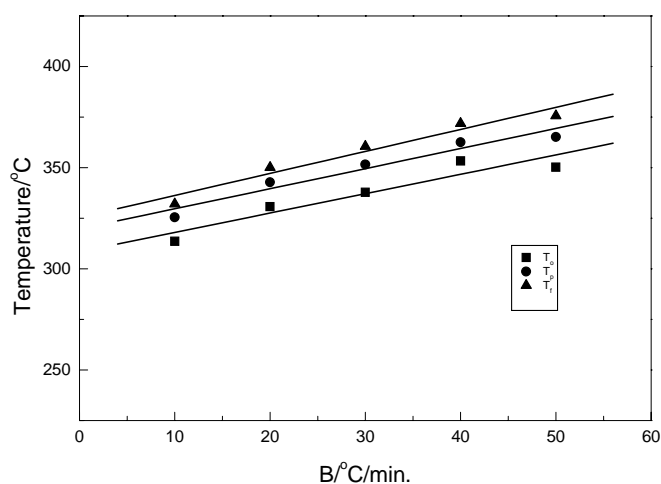


**Figure 3.6** Relation of thermal degradation temperatures and  $B$  for P(HB–HV) (70:30) thermal degradation

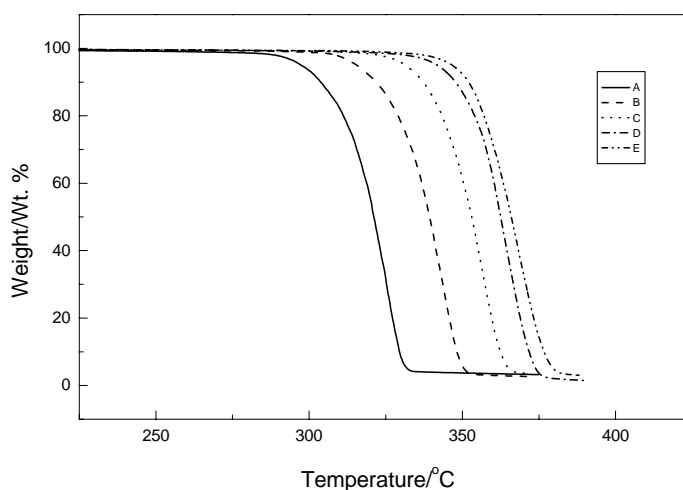


**Figure 3.7** TG curves of P(HB-HHx) (85:15) thermal degradation: (A)  $B = 10^{\circ}\text{C min}^{-1}$ , (B)  $B = 20^{\circ}\text{C min}^{-1}$ , (C)  $B = 30^{\circ}\text{C min}^{-1}$ , (D)  $B = 40^{\circ}\text{C min}^{-1}$ , and (E)  $B = 50^{\circ}\text{C min}^{-1}$ . The weight is expressed on the vertical axis as a percentage of the initial weight (wt %). The temperature ( $^{\circ}\text{C}$ ) is expressed on the horizontal axis.

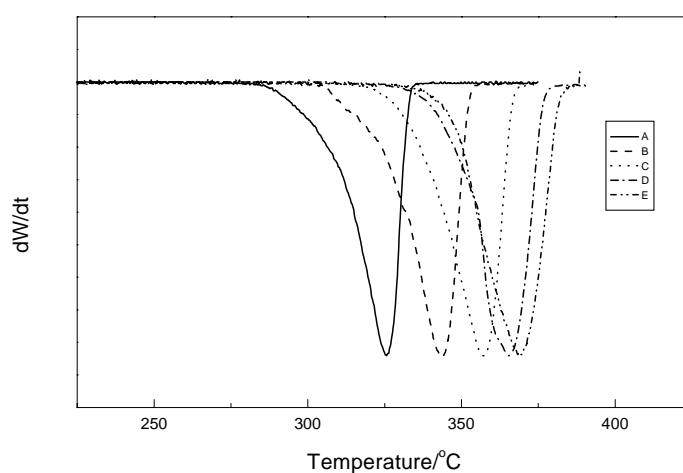


**Figure 3.8** DTG curves of P(HB-HHx) (85:15) thermal degradation: (A)  $B = 10^{\circ}\text{C min}^{-1}$ , (B)  $B = 20^{\circ}\text{C min}^{-1}$ , (C)  $B = 30^{\circ}\text{C min}^{-1}$ , (D)  $B = 40^{\circ}\text{C min}^{-1}$ , and (E)  $B = 50^{\circ}\text{C min}^{-1}$ .  $dW/dt$  is shown on the vertical axis. The temperature ( $^{\circ}\text{C}$ ) is expressed on the horizontal axis.

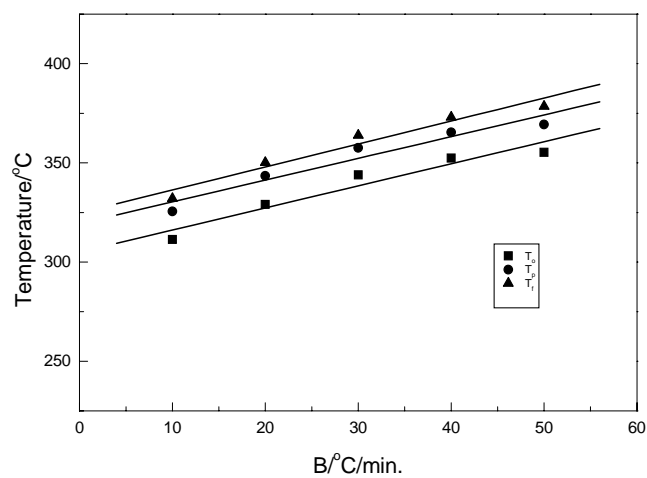


**Figure 3.9 Relation of thermal degradation temperatures and  $B$  for P(HB-HHx) (85:15) thermal degradation.**

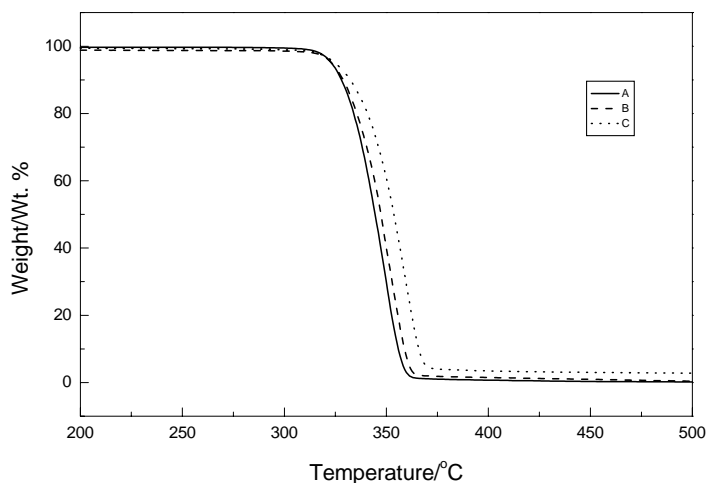


**Figure 3.10 TG curves of PHB, P(HB-HV), and P(HB-HHx) thermal degradation at  $40^{\circ}\text{C min}^{-1}$ : (A) PHB, (B) P(HB-HV), and (C) P(HB-HHx). The weight is expressed on the vertical axis as a percentage of the initial weight (wt %). The temperature ( $^{\circ}\text{C}$ ) is expressed on the horizontal axis.**

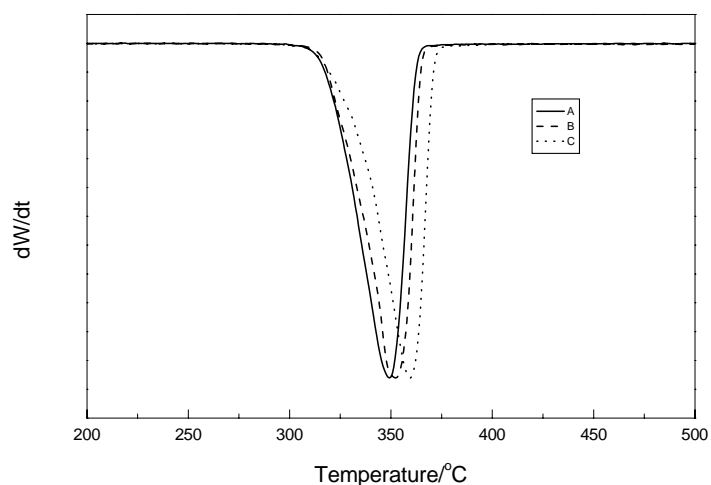


**Figure 3.11** DTG curves of PHB, P(HB–HV), and P(HB–HHx) thermal degradation at  $40^{\circ}\text{C min}^{-1}$ : (A) PHB, (B) P(HB–HV), and (C) P(HB–HHx).  $dW/dt$  is shown on the vertical axis. The temperature ( $^{\circ}\text{C}$ ) is expressed on the horizontal axis.

**Table 3.1** Thermal Degradation Temperatures of PHB, P(HB–HV), and P(HB–HHx) at a  $B$  of  $40^{\circ}\text{C min}^{-1}$

|                         | PHB | P(HB–HV)<br>(70 : 30) | P(HB–HHx)<br>(85 : 15) |
|-------------------------|-----|-----------------------|------------------------|
| $T_o(^{\circ}\text{C})$ | 331 | 334                   | 339                    |
| $T_p(^{\circ}\text{C})$ | 349 | 352                   | 359                    |
| $T_f(^{\circ}\text{C})$ | 358 | 364                   | 369                    |

**Table 3.2**  $T_g$  and  $T_m$  of PHB, P(HB–HV), and P(HB–HHx)

|                         | PHB  | P(HB–HV)<br>(70 : 30) | P(HB–HHx)<br>(85 : 15) |
|-------------------------|------|-----------------------|------------------------|
| $T_g(^{\circ}\text{C})$ | 5.73 | 2.11                  | 3.22                   |
| $T_m(^{\circ}\text{C})$ | 179  | 111                   | 109                    |

$T_g$ : the samples (30 mg) were heated from room temperature to  $200^{\circ}\text{C}$  at a  $20^{\circ}\text{C min}^{-1}$  under  $\text{N}_2$  gas flow; after 2 min, the melted samples were rapidly cooled to  $-50^{\circ}\text{C}$  by liquid  $\text{N}_2$ , and then the frozen samples were heated at a constant scanning rate of  $10^{\circ}\text{C min}^{-1}$  under a  $\text{N}_2$  purge.  $T_m$ : the samples (10 mg) were heated from room temperature to  $200^{\circ}\text{C}$  at a constant scanning rate of  $10^{\circ}\text{C min}^{-1}$  under  $\text{N}_2$  atmosphere.

# **Chapter 4**

## **Thermal Degradation Kinetics and Mechanism of Poly(3-hydroxybutyrate) and Poly(3-hydroxybutyrate-co-3-hydroxyvalerate) as Studied by TG, TG–FTIR, and Py–GC/MS**

### **Introduction**

PHB and P(HB–HV) are the most commonly found members of the PHA family. PHAs are hydrolyzed by extracellular depolymerases, which are secreted by many bacteria in microbially active environments.<sup>[88]</sup> All PHA depolymerases are comprised of an N-terminal catalytic domain, a C-terminal substrate binding domain, and a linkage region connecting the two domains. The first step in enzymatic degradation is adsorption of the PHA depolymerase on the biopolymer surface by the substrate binding domain of the enzyme; the second step is hydrolysis of the polymer chains by the active site (catalytic domain) of the enzyme into water-soluble products.<sup>[89]</sup> The enzymatic hydrolysis of PHB produces HB dimers as the major product, along with a mixture monomers and oligomers. The oligomers are hydrolyzed to monomers by oligomer hydrolases.<sup>[88-91]</sup> Enzymatic degradation of PHA requires the presence of a crystalline phase because depolymerases do not bind well with the mobile amorphous phase to induce hydrolysis.<sup>[92-94]</sup> At a more

fundamental level there is considerable potential for design and bioengineering of PHAs for applications in drug delivery, but PHB has a narrow thermal processing window, so it is important to know the thermal properties in order to improve the thermal processing of these biopolymers.

The objective of this study was to investigate the thermal degradation of PHB and P(HB–HV) with dynamic thermogravimetry (TG), thermogravimetry–Fourier transform infrared spectroscopy (TG–FTIR), and pyrolysis–gas chromatography/mass spectroscopy (Py–GC/MS). The thermal degradation kinetics and mechanism of PHB and P(HB–HV) have also been considered.

## Results and Discussion

Figures 4.1 and 4.2 show the TG curves from the thermal degradation of PHB and P(HB–HV) at five heating rates, which shift toward higher temperatures with an increasing heating rate. Table 4.1 shows the correlation between the heating rate and the thermal degradation weight loss percentages of PHB and P(HB–HV). The  $C_p$  and  $C_f$  are the thermal degradation weight losses that correspond to  $T_p$  and  $T_f$ , respectively.  $C_p$  is the weight loss percentage at  $T = T_p$ , and  $C_f$  is the weight loss percentage at  $T = T_f$ . The average  $C_p$  and  $C_f$  of PHB are  $80.0\% \pm 0.6\%$  and  $99.5\% \pm 0.5\%$ , respectively. The average  $C_p$  and  $C_f$  of P(HB–HV) are  $71.6\% \pm 3.4\%$  and  $99.1\% \pm 0.5\%$ , respectively. The thermal degradation of PHB under nitrogen may be regarded as complete degradation.

Table 4.2 shows the kinetic parameters in PHB degradation. The mean value of all  $n$  values measured at different values of  $B$  is 0.7. The frequency factor,  $A$ , and activation energy,  $E$ , decrease linearly with the increment of  $B$ . By the linear regression least-squares method,  $E = 308 - 0.22B$ , and the apparent activation energy,  $E_o$ , at  $B = 0^\circ\text{C min}^{-1}$  is  $308 \text{ kJ mol}^{-1}$ . Table 4.3 shows the kinetics parameters in the thermal degradation of P(HB–HV). The mean value of  $n$  is 1.3,  $E = 376 - 0.15B$ , and  $E_o$  is  $376 \text{ kJ mol}^{-1}$ . However, too much physical significance should not be attached to the differences in  $A$ ,  $E_o$  and  $n$  because the solid-state reaction rate kinetic parameters obtained from linear regression are very sensitive to the conditions surrounding the solid samples.<sup>[95]</sup>

The thermal degradation phenomena of PHB and P(HB–HV) can be observed directly from the stack plot of the coupling TG and FTIR measurements by analyzing the gas spectra from the thermal degradation of the polymers.<sup>[96, 97]</sup> Figures 4.3 and 4.4 show the stack plots of TG–FTIR for PHB and P(HB–HV), respectively, under nitrogen at a heating rate of  $40^\circ\text{C min}^{-1}$ . The horizontal axis represents the FTIR wave numbers of released gas from the TG furnace, the vertical axis the intensity of the absorption from the released gas, and the third axis the temperatures of the TG furnace.

Absorptions at  $3585$  and  $965 \text{ cm}^{-1}$  are of  $-\text{OH}$  vibration in the carboxyl group, those at  $1770$  and  $1760 \text{ cm}^{-1}$  are of  $-\text{C}=\text{O}$  stretching vibration in unsaturated ester and unsaturated carboxyl acid, which must be a consequence of the fact that the major product, a carboxylic acid, is monomeric in the gas phase.<sup>[98]</sup> Absorption at

1655  $\text{cm}^{-1}$  is of  $-\text{C}=\text{C}-$  stretching vibration, and absorptions at 1150 and 1095  $\text{cm}^{-1}$  are of  $-\text{C}-\text{O}-$  stretching vibration in esters. Figures 4.5 and 4.6 show the FTIR spectra of gases evolved from these samples at various temperatures. Figure 4.5 shows that there are many chemical groups, especially the  $-\text{C}=\text{O}$  group, at 295°C in PHB degradation products. At 310°C, the absorbance of  $-\text{C}=\text{C}-$ ,  $-\text{C}=\text{O}$ ,  $-\text{C}-\text{O}-$ , and  $-\text{OH}$  reach maximum. After 310°C the absorbance of the above groups decrease. So the products of PHB degradation should be unsaturated esters and unsaturated carboxyl acids.

There are absorption peaks at 3585, 2360, 1770, 1760, 1655, 1150, 1095, and 965  $\text{cm}^{-1}$  in the TG-FTIR spectra of P(HB-HV), which are similar to those of PHB. The maximum absorbance is at 325°C. The small absorption at 2360  $\text{cm}^{-1}$  is the characteristic absorption of  $\text{CO}_2$ . So the products of P(HB-HV) degradation should be unsaturated esters and unsaturated carboxyl acids and a small amount of  $\text{CO}_2$ .

Figures 4.7 and 4.8 show the gas chromatograms of the pyrolysis products of PHB and P(HB-HV) in nitrogen at 590°C. Table 4.4 shows the identification of the products in the Py-GC/MS of PHB and P(HB-HV). In the pyrolysis of PHB, the major pyrolysates were propene (6.73%), 2-butenic acid (45.78%), propenyl-2-butenate (24.66%), and butyric-2-butenate (21.73%). In the pyrolysis of P(HB-HV), the major pyrolysates were propene (6.20%), 2-butenic acid (45.47%), 2-pentenoic acid (25.81%), propenyl-2-butenate (11.57%), propenyl-2-pentenoate (5.39%), butyric-2-butenate (1.93%), and pentanoic-2-pentenoate (2.31%).

Analyses of the FTIR and GC/MS data show that the thermal degradation products of the two biopolymers were slightly different: the PHB yielded mainly four-carbon unsaturated carboxyl acids and unsaturated esters, whereas the P(HB–HV) yielded mainly five-carbon unsaturated carboxyl acids and unsaturated esters. The above results suggest that the thermal degradation of PHB and P(HB–HV) begins with chain scission of the ester linkages by *cis* elimination, which leads to the formation of unsaturated carboxyl acids and unsaturated esters (see Fig. 4.9).<sup>[99, 100]</sup>

## **Conclusions**

PHB and P(HB–HV) were thermally degraded at 250°C–400°C in nitrogen. The degradation products of PHB were mainly propene, 2-butenic acid, and propenyl-2-butenate. The degradation products of P(HB–HV) were mainly propene, 2-butenic acid, 2-pentenoic acid, propenyl-2-butenate, butyl-2-butenate, and CO<sub>2</sub>. The degradation was probably initiated from chain scission of the ester linkage.

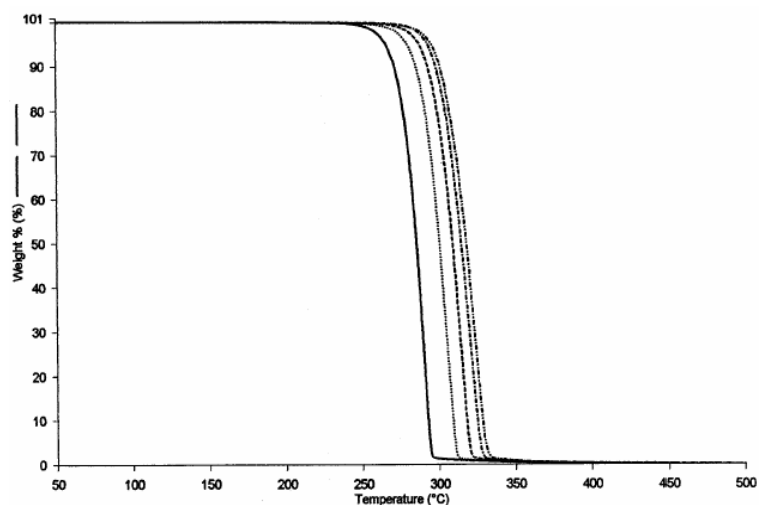


**Figure 4.1** TG curves of PHB thermal degradation at five heating rates (from left to right:  $B = 10, 20, 30, 40,$  and  $50^{\circ}\text{C min}^{-1}$ , respectively). The weight is expressed on the vertical axis as a percentage of the initial weight (wt %). The temperature ( $^{\circ}\text{C}$ ) is expressed on the horizontal axis.

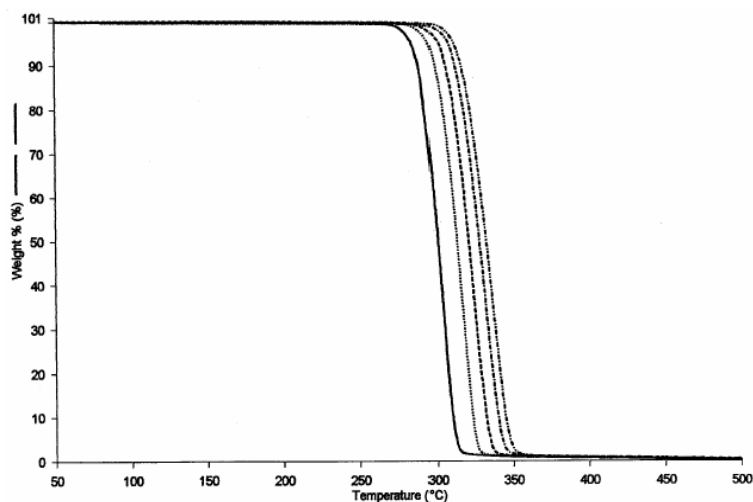


**Figure 4.2** TG curves of P(HB–HV) thermal degradation at five heating rates (from left to right:  $B = 10, 20, 30, 40,$  and  $50^{\circ}\text{C min}^{-1}$ , respectively). The weight is expressed on the vertical axis as a percentage of the initial weight (wt %). The temperature ( $^{\circ}\text{C}$ ) is expressed on the horizontal axis.

**Table 4.1 Relation between Heating Rate ( $B$ ) and Weight Loss Percentage ( $C$ ) for PHB and P(HB–HV) Degradation**

| $B$ ( $^{\circ}\text{C}/\text{min}$ ) | PHB            |                | P(HB–HV)       |                |
|---------------------------------------|----------------|----------------|----------------|----------------|
|                                       | $C_p$ (%)      | $C_f$ (%)      | $C_p$ (%)      | $C_f$ (%)      |
| 10                                    | 80.1           | 100.0          | 71.8           | 99.6           |
| 20                                    | 79.4           | 9.5            | 75.0           | 98.7           |
| 30                                    | 79.8           | 99.1           | 70.6           | 99.1           |
| 40                                    | 80.3           | 99.3           | 70.2           | 98.9           |
| 50                                    | 80.5           | 99.5           | 70.4           | 99.1           |
| Average                               | $80.0 \pm 0.6$ | $99.5 \pm 0.5$ | $71.6 \pm 3.4$ | $99.1 \pm 0.5$ |

**Table 4.2 Reaction Order and Activation Energy for PHB Degradation**

|                     | $B$ ( $^{\circ}\text{C}/\text{min}$ ) |      |      |      |       |
|---------------------|---------------------------------------|------|------|------|-------|
|                     | 10                                    | 20   | 30   | 40   | 50    |
| $n$                 | 0.7                                   | 0.6  | 0.7  | 0.8  | 0.7   |
| $E$ (kJ/mol)        | 307                                   | 303  | 300  | 299  | 298   |
| $A \times 10^{-23}$ | 443                                   | 50.4 | 17.4 | 9.42 | 0.481 |

**Table 4.3 Reaction Order and Activation Energy for P(HB–HV) Degradation**

|                     | $B$ ( $^{\circ}\text{C}/\text{min}$ ) |     |       |        |        |
|---------------------|---------------------------------------|-----|-------|--------|--------|
|                     | 10                                    | 20  | 30    | 40     | 50     |
| $n$                 | 1.3                                   | 1.2 | 1.3   | 1.3    | 0.7    |
| $E$ (kJ/mol)        | 374                                   | 373 | 371   | 370    | 368    |
| $A \times 10^{-23}$ | 45900                                 | 184 | 0.947 | 0.0558 | 0.0280 |

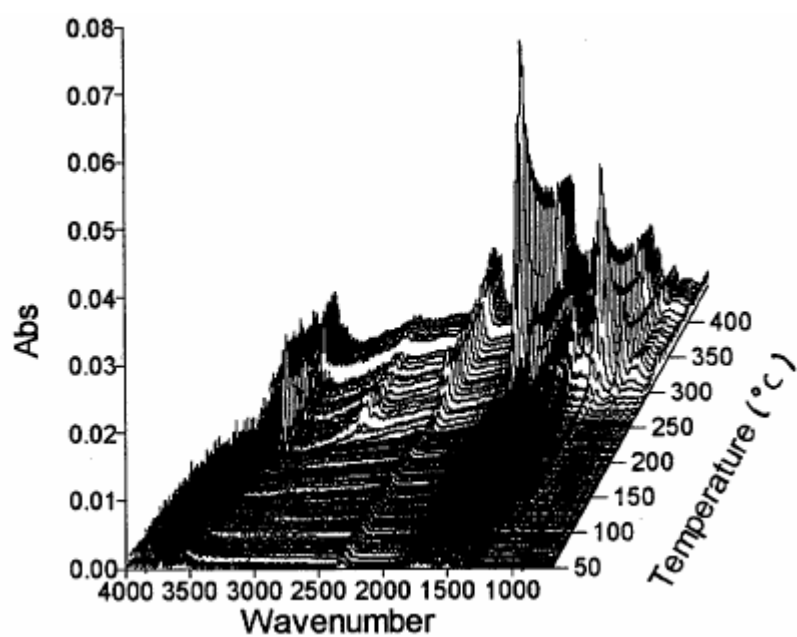


**Figure 4.3** TG–FTIR stack plots for PHB under nitrogen at a heating rate of  $40^{\circ}\text{C min}^{-1}$ . The horizontal axis represents the FTIR wave numbers of released gas from the TG furnace, the vertical axis the intensity of the absorption from the released gas, and the third axis the temperatures ( $^{\circ}\text{C}$ ) of the TG furnace.

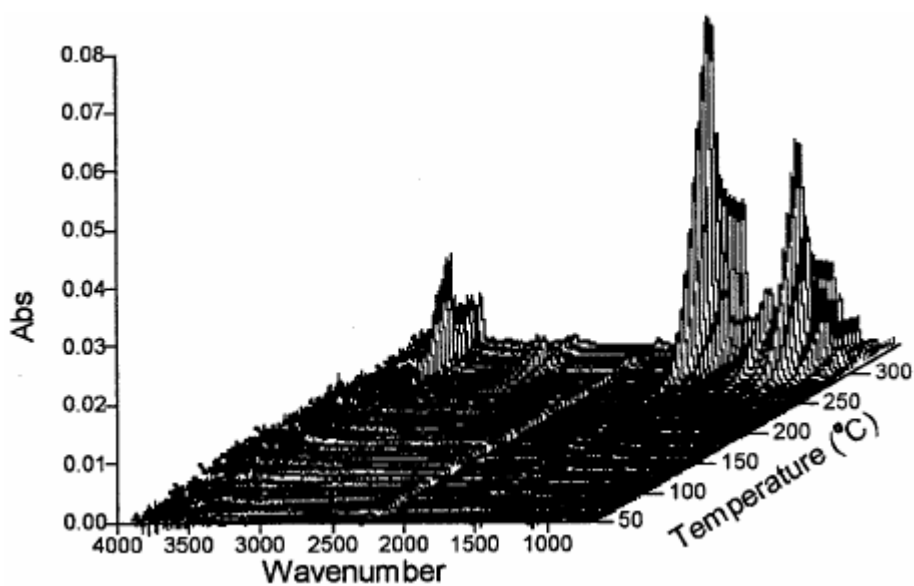


**Figure 4.4** TG-FTIR stack plots for P(HB-HV) under nitrogen at a heating rate of  $40^{\circ}\text{C min}^{-1}$ . The horizontal axis represents the FTIR wave numbers of released gas from the TG furnace, the vertical axis the intensity of the absorption from the released gas, and the third axis the temperatures ( $^{\circ}\text{C}$ ) of the TG furnace.

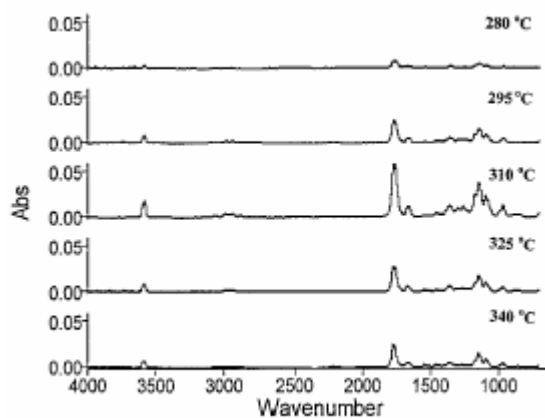


**Figure 4.5** FTIR spectra of gases evolved from PHB degradation at various temperatures. The intensity of absorption from chemical groups is shown on the vertical axis. The wavenumber ( $\text{cm}^{-1}$ ) is expressed on the horizontal axis.

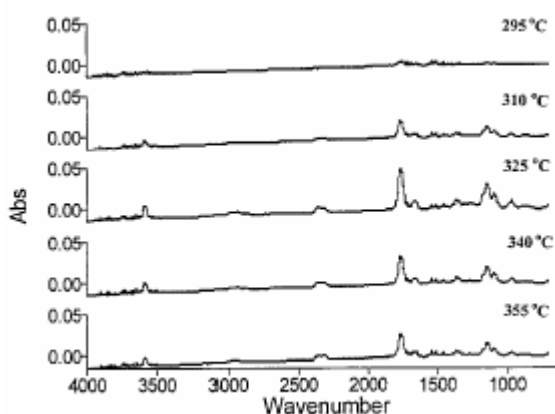


**Figure 4.6** FTIR spectra of gases evolved from P(HB-HV) degradation at various temperatures. The intensity of absorption from chemical groups is shown on the vertical axis. The wavenumber ( $\text{cm}^{-1}$ ) is expressed on the horizontal axis.

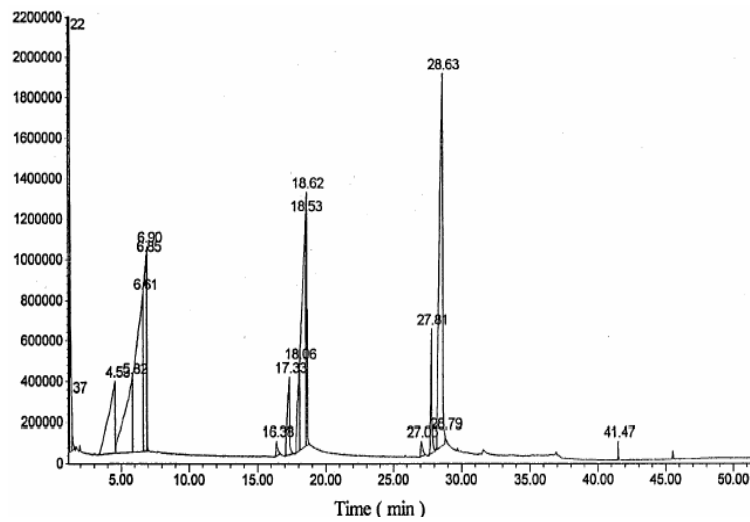


**Figure 4.7 Chromatograms of products from pyrolysis of PHB in nitrogen at 590°C.**

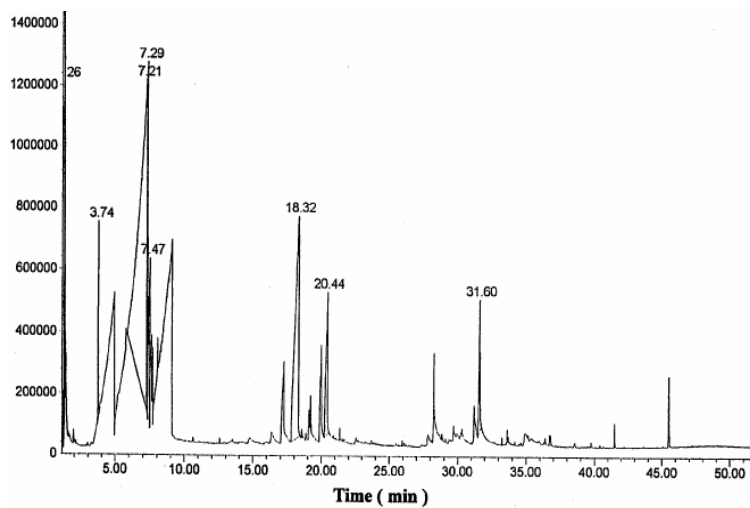


**Figure 4.8 Chromatograms of products from pyrolysis of P(HB-HV) in nitrogen at 590°C.**

**Table 4.4 Products in the Py–GC/MS of PHB and P(HB–HV) at 590°C in N<sub>2</sub>**

| Retention time (min) | Compound               | Molecular formula                              | Molecular weight | Content (%) |
|----------------------|------------------------|--|------------------|-------------|
| PHB                  |                        |  |                  |             |
| 1.23                 | Propene                | C <sub>3</sub> H <sub>6</sub>                  | 42               | 6.73        |
| 6.85                 | 2-Butenoic acid        | C <sub>4</sub> H <sub>6</sub> O <sub>2</sub>   | 86               | 45.78       |
| 18.62                | Propenyl-2-butenolate  | C <sub>7</sub> H <sub>10</sub> O <sub>2</sub>  | 126              | 24.66       |
| 28.63                | Butyric-2-butenolate   | C <sub>8</sub> H <sub>12</sub> O <sub>4</sub>  | 172              | 21.73       |
| P(HB-HV)             |                        |  |                  |             |
| 1.22                 | Propene                | C <sub>3</sub> H <sub>6</sub>                  | 42               | 6.20        |
| 7.29                 | 2-Butenoic acid        | C <sub>4</sub> H <sub>6</sub> O <sub>2</sub>   | 86               | 45.47       |
| 8.71                 | 2-Pentenoic acid       | C <sub>5</sub> H <sub>8</sub> O <sub>2</sub>   | 100              | 25.81       |
| 18.31                | Propenyl-2-butenolate  | C <sub>7</sub> H <sub>10</sub> O <sub>2</sub>  | 126              | 11.57       |
| 20.44                | Propenyl-2-pentenoate  | C <sub>8</sub> H <sub>12</sub> O <sub>2</sub>  | 140              | 5.39        |
| 28.25                | Butyric-2-butenolate   | C <sub>8</sub> H <sub>12</sub> O <sub>4</sub>  | 172              | 1.93        |
| 31.60                | Pentanoic-2-pentenoate | C <sub>10</sub> H <sub>16</sub> O <sub>4</sub> | 200              | 2.31        |



# Chapter 5

## Synthesis, Structure and Properties of Water-soluble

### Ethoxy [60]Fullerol

#### Introduction

$C_{60}$  and its derivatives have attracted great attention due to the outstanding physical and chemical properties of these compounds.<sup>[6, 101-104]</sup> Among the synthesized derivatives, the functionalized fullerenes have been greatly investigated.<sup>[105-125]</sup> A major effort in this area is the synthesis and characterization of fullerene derivatives with polar functionalities for biological applications.<sup>[24, 25, 45, 126-137]</sup> These fullerene derivatives display promising biological activities such as anti-HIV,<sup>[16, 20-22]</sup> DNA cleavage,<sup>[17-19, 138, 139]</sup> and cytotoxicity.<sup>[17, 23]</sup> A therapeutic agent must possess the ability to pass through both hydrophobic and hydrophilic domains. Thus, the development of methods to synthesize amphiphilic fullerene derivatives is not only a great challenge to synthetic chemist but also practically important.

Fullerenol, which has mainly been used in medical applications,<sup>[140-147]</sup> is one of the most interesting objects in the fullerene chemistry.<sup>[14, 148-152]</sup> Polyhydroxylated derivatives of  $C_{60}$  exhibit compatibility with water and polar solvents, but are insoluble in nonpolar solvents. The structure and components of

these fullerenolic compounds prepared by different methods differ slightly from each other, depending upon the variation of reagents and conditions used in the reaction.

Biodistribution studies<sup>[153]</sup> in mice and imaging of rabbits indicated that <sup>99m</sup>Tc-labeling C<sub>60</sub>(OH)<sub>x</sub> was widely distributed in all tissues. A significant percentage of total activity was retained for 48 h, particularly in the kidneys, bone, spleen and liver. All tissues displayed slow clearance over 48 h, except for bone, which showed slightly increasing localization within 24 h. The clearance pathways, tissue retention and tissue distribution for C<sub>60</sub>(OH)<sub>x</sub> make it and other fullerol-like materials potential therapeutic agents for treating leukemia, bone cancer and bone pain.

In this study, a novel amphiphilic ethoxy [60]fullerol was synthesized through the substitution of bromine atoms from C<sub>60</sub>Br<sub>24</sub> in CH<sub>3</sub>CH<sub>2</sub>OH/H<sub>2</sub>O/NaOH solution at ambient temperature (23°C). The structure of this compound was determined on the basis of its spectral data, and its antioxidant activity and cytotoxic property were evaluated with different assays.

## Results and Discussion

### Synthesis and Characterization of C<sub>60</sub>Br<sub>24</sub>

The icosahedral C<sub>60</sub> ([60-I<sub>h</sub>]fullerene) consists of 12 pentagons, 20 hexagons and 30 double bonds. Due to the spherical shape of the unsaturated carbon network, the C-atoms are pyramidalized. The bonds at the junctions of two hexagons ([6,6]-bonds) are shorter than the bonds at the junctions of a hexagon and a pentagon ([5,6]-bonds). As a consequence, in the lowest energy Kekulé structure of C<sub>60</sub>, the double bonds are placed at the junctions of the hexagons and there are no double bonds in the pentagonal rings. Topologically, each hexagon in C<sub>60</sub> exhibits a cyclohexatriene and each pentagon a [5]radialene character. The aliphatic character of the bonds of C<sub>60</sub> allowed the formation of halogen derivatives,<sup>[154-156]</sup> that is, a radical addition procedure. C<sub>60</sub>Br<sub>24</sub> was obtained from the bromination of C<sub>60</sub> with neat bromine. It is reported that each of the Br atoms of C<sub>60</sub>Br<sub>24</sub> is attached to a carbon atom of C<sub>60</sub> with a C-Br bond.<sup>[76]</sup> These bonds reduce slightly the symmetry of C<sub>60</sub> from I<sub>h</sub> to T<sub>h</sub> in C<sub>60</sub>Br<sub>24</sub>.

Figure 5.1 shows FTIR spectrum of C<sub>60</sub>Br<sub>24</sub>, which is very similar to those previously published.<sup>[76, 156]</sup> The main bands occur at 546, 606, 720, 751, 776, 849, 912, 946, 1049, 1117, 1244 and 1613 cm<sup>-1</sup>.

Figure 5.2 shows the solid-state <sup>13</sup>C-NMR spectrum of C<sub>60</sub>Br<sub>24</sub>. It was measured at ambient temperature using a single <sup>13</sup>C 90° pulse of 5.0 μs and the pre-delay recycle time of 50 s. The spin rate was 4000 Hz. The peak at δ 40.4 was

reasonable for  $sp^3$  carbons attached to bromine. The sharp peak at  $\delta$  141.0 was assigned to  $sp^2$ -hybridized carbons. The peaks located at  $\delta$  60.9,  $\delta$  100.5,  $\delta$  179.9 and  $\delta$  200.1 were assigned to the spinning sidebands of the peak at  $\delta$  141.0. Relative intensities of  $sp^2$  and  $sp^3$  regions were nearly 3:2, in agreement with the highly symmetrical structure of  $C_{60}Br_{24}$ . Results of elemental analysis: C 25.59%, Br 70.93%, which gave an average composition of  $C_{60}Br_{25.5}$ . The indicated  $C_{60}Br_{24}$  therefore matches the analysis, but with some molecules of bromine occluded in the lattice.

In liquid samples, the rapid and random molecular rotation has the effect of averaging the dipole-dipole interaction between nuclear spins and chemical shift anisotropy (CSA) to zero, leading to sharp lines. In solid samples, the motion of atoms and molecules is restricted, so that the effect of the dipole-dipole interaction does not average to zero. Since the resonance frequency of a particular nucleus depends on the magnetic field at its site, and since the local field due to neighboring spins varies appreciably from place to place throughout the sample owing to a variation in the orientation of the neighboring spins, there will be a significant spread in the resonance frequencies, resulting in a line broader by several orders of magnitude than a typical line from a liquid sample. Another source of NMR line broadening in solid samples is CSA. Using the MAS (magic angle spinning) technique can lead to a significant narrowing of a broadline spectrum. However, the spinning rate must exceed the magnitude of the interactions to be removed. Because of the large magnitude of some interactions, sufficiently high spinning rates are

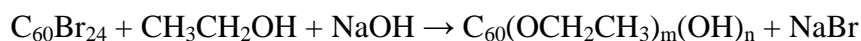
difficult to achieve. Taking 220 ppm as the maximum anisotropy expected for  $sp^2$  hybridized carbons, a spinning rate of 22 kHz is necessary to remove the shift anisotropy completely. Given the spinning rate of 4.0 kHz, it is not possible to average the anisotropy. Spinning frequencies smaller than the shift anisotropy result in the spectrum showing sidebands separated by the spinning frequency symmetrically placed about the isotropic average peak. So, the peak at  $\delta$  141.0 appeared to possess four spinning sidebands. As the spinning rate is increased, the number of sidebands decreases and the relative intensity of the central isotropic peak increases.

Figure 5.3 shows the solid-state  $^{13}\text{C}$ -NMR spectrum of  $\text{C}_{60}$  at ambient temperature. It was determined under the same conditions as Figure 5.2. The observation of a single NMR line for  $\text{C}_{60}$  provides direct evidence for its highly symmetrical soccer ball-like structure in which all 60 carbon atoms are in identical environments.<sup>[157]</sup> The molecules in a powder are randomly oriented, but  $\text{C}_{60}$  molecules reorient rapidly in the solid state at room temperature, its chemical shift in an external magnetic field is isotropic. Compared to  $\text{C}_{60}$ , the chemical shift of  $\text{C}_{60}\text{Br}_{24}$  is anisotropic. Therefore, the observed spectrum is a broad but characteristic band, which is the superposition of the signals from molecules having all possible orientations.

## Synthesis and Characterization of Ethoxy [60]Fullerol

The reaction of  $C_{60}$  and liquid bromine formed  $C_{60}Br_{24}$ , a crystalline compound isolated as a bromine solvate,  $C_{60}Br_{24}(Br_2)_x$ . The result of its single crystal x-ray determination<sup>[68]</sup> shows a new pattern of addition to the carbon skeleton that imparts a rare high symmetry. Twenty-four bromine atoms envelop the carbon core, shielding the 18 remaining double bonds from addition.  $C_{60}Br_{24}$  has a higher stability, and is insoluble in general organic solvents, which inhibit further reaction.

Novel fullerene derivative ethoxy [60]fullerol was synthesized through the substitution of bromine atoms from  $C_{60}Br_{24}$  in  $CH_3CH_2OH/H_2O/NaOH$  solution at ambient temperature. The reaction equation is as follows:



$C_{60}Br_{24}$  is insoluble in aqueous solution, adding  $CH_3CH_2OH$  into reaction system increases its miscibility, while a large amount of  $NaOH$  greatly improves its reactivity. In the meantime,  $NaOH$  easily reacts with  $CH_3CH_2OH$  to form  $CH_3CH_2ONa$ . The substitution of bromine atoms seems to be a cascade process,<sup>[156]</sup> i.e., firstly all the bromine is lost and then substituted.  $C_{60}$  should have not only perfect symmetry, but also energy as well as memory function.

Figure 5.4 shows FTIR spectrum of ethoxy [60]fullerol, which contains characteristic bonds for  $-C-O-$ ,  $-O-H$ ,  $-C=C-$  and  $-C-C-$  vibrations.<sup>[142, 143]</sup> The wide peak at  $3440\text{ cm}^{-1}$  is characteristic of stretching vibrations of the hydroxyl group. Bands at  $1625\text{ cm}^{-1}$  and  $1393\text{ cm}^{-1}$  represent the stretching vibrations of the  $-$

C=C– and –C–C– bonds, and the band at  $1076\text{ cm}^{-1}$  is characteristic of the –C–O– stretching vibrations.

Figure 5.5 shows the solid-state  $^{13}\text{C}$ -NMR spectrum of ethoxy [60]fullerol. It was measured using cross-polarization with magic-angle sample spinning (CP/MAS). The pre-delay recycle time was 5.0 s. The  $^1\text{H}$   $90^\circ$  pulse width was  $5.8\ \mu\text{s}$ . The CP contact-time was 3.0 ms. The spin rate was 5000 Hz. The spectrum exhibited a broad peak centered at  $\delta$  146.3, a strong, broad peak centered at  $\delta$  77.2, and two strong, sharp peaks centered at  $\delta$  63.2 and  $\delta$  15.7 corresponding to olefinic carbons, monooxygenated carbons, –CH<sub>2</sub>– and –CH<sub>3</sub> carbons, respectively.<sup>[142]</sup> The peaks located at  $\delta$  96.7,  $\delta$  203.9 and  $\delta$  246.4 were assigned to the spinning sidebands of the peak at  $\delta$  146.3.

Figure 5.6 shows the  $^1\text{H}$ -NMR spectrum of unpurified ethoxy [60]fullerol in  $\text{CDCl}_3$ , which exhibited many peaks that were attributed to impurity materials. Figure 5.7 shows the  $^1\text{H}$ -NMR spectrum of purified ethoxy [60]fullerol in  $\text{CDCl}_3$ , which exhibited a broad peak centered at  $\delta$  3.87, two strong peaks centered at  $\delta$  1.26 and  $\delta$  1.69 corresponding to –CH<sub>2</sub>– and –CH<sub>3</sub> protons in ethyl group and protons in hydroxyl group. Figure 5.8 shows the  $^1\text{H}$ -NMR spectrum of purified ethoxy [60]fullerol in  $\text{CDCl}_3$  with one drop  $\text{D}_2\text{O}$ , which exhibited nearly the same peaks as Figure 5.7, but without a peak centered at  $\delta$  1.69. That means the peak centered at  $\delta$  1.69 in Figure 5.7 belongs to the C<sub>60</sub>-bound hydroxyl group.<sup>[142]</sup> Figure 5.9 shows the  $^{13}\text{C}$ -NMR spectrum of ethoxy [60]fullerol in  $\text{C}_6\text{D}_6$ , which was measured at ambient temperature with the use of broadband decoupling of protons for 24 h. It

exhibited a broad peak centered at  $\delta$  148.0, a weak, broad peak centered at  $\delta$  77.8, a strong, broad peak centered at  $\delta$  64.1 and a strong, sharp peak centered at  $\delta$  16.6 corresponding to olefinic carbons, monooxygenated carbons,  $-\text{CH}_2-$  and  $-\text{CH}_3$  carbons. Both the results of FTIR and NMR determination showed that the hydroxyl groups and ethoxy groups were bonded to the [60]fullerene cage.

### Evaluation of Ethoxy [60]Fullerol Composition

Figure 5.10 shows the  $^{13}\text{C}$ -NMR spectrum of ethoxy [60]fullerol in  $\text{C}_6\text{D}_6$  with Lorentzian line fitting. Usually, proton-decoupling technique easily produces the nuclear Overhauser effect (NOE), but the carbons on the spherical cage are not linked with protons. As a result, the fitting lines of NMR spectrum thus obtained could be integrated. The relative integration areas of peaks at  $\delta$  148.0,  $\delta$  77.8,  $\delta$  64.1 and  $\delta$  16.6 are 36.00, 24.66, 31.56 and 54.04, respectively. The result suggests that the relative number of  $sp^2$  carbons at  $\delta$  148.0 and monooxygenated  $sp^3$  carbons at  $\delta$  77.8 that make up the [60]fullerene cage is nearly 3 : 2 also.

Figure 5.11 shows the  $^1\text{H}$ -NMR spectrum of ethoxy [60]fullerol in  $\text{CDCl}_3$  with Lorentzian line fitting. The relative integration areas of peaks at  $\delta$  3.87,  $\delta$  1.69, and  $\delta$  1.26 are 2.00, 3.60 and 3.06, respectively. The peaks at  $\delta$  3.87 and  $\delta$  1.26 are assigned to  $-\text{CH}_2-$  and  $-\text{CH}_3$  protons in the ethyl group. In Figure 5.8, the peak at  $\delta$  2.18 is assigned to  $-\text{CH}_3$  protons in acetone, i.e., there was a small amount of acetone in the sample, which was absorbed due to hydrogen bonding between  $\text{C}=\text{O}$

and –OH. Results of elemental analysis: C 66.74%, H 4.66%. Taking the following three molecular formulae of fullerol:  $C_{60}(OCH_2CH_3)_9(OH)_{16}$  (containing one molecule of acetone: C 66.80%, H 4.60%);  $C_{60}(OCH_2CH_3)_8(OH)_{16}$  (containing two molecules of acetone: C 67.03%, H 4.66%);  $C_{60}(OCH_2CH_3)_7(OH)_{17}$  (containing three molecules of acetone: C 66.48%, H 4.71%), the indicated stoichiometry would match the analysis. But from Figure 5.8, the relative integration areas of peaks at  $\delta$  3.87 and  $\delta$  2.18 are 2.00 and 1.50, in agreement with the formula of  $C_{60}(OCH_2CH_3)_8(OH)_{16} : CH_3COCH_3 = 1 : 2$  (molar ratio). In this case, the relative integration areas of peaks at  $\delta$  3.87,  $\delta$  1.69 and  $\delta$  1.26 should be 2.00, 2.00 and 3.00, respectively. So, the area of peak at  $\delta$  1.69 can be attributed not only to protons in hydroxyl group, but also residual water in  $CDCl_3$ .

### **Antioxidant Activity of Ethoxy [60]Fullerol**

Table 5.1 shows the antioxidant activity of ethoxy [60]fullerol, five kinds of Chinese medicinal herb, ascorbic acid and BHT. In the DPPH assay, percentage free radical scavenging capacity (SR%) of fullerol was assayed at a concentration of  $7.5 \text{ mg ml}^{-1}$ . In the FRAP assay, the total antioxidant power of fullerol was calculated as its FRAP value in  $\mu\text{mol g}^{-1}$ . Comparison to ascorbic acid and BHT, the antioxidant activity of ethoxy [60]fullerol is very weak.

## **Antitumor Activity of Ethoxy [60]Fullerol**

The cytotoxic property of ethoxy [60]fullerol was evaluated on human breast carcinoma (cell line: MCF-7), which is expressed as the concentration of the drug required to produce 50% inhibition of cell growth (ED50) by MTT 72 h assay. The cytotoxicity assay of fullerene derivatives usually proceeds under UV light,<sup>[17, 23]</sup> Table 5.2 shows that UV light has no effect on the antitumor activity of ethoxy [60]fullerol.

Doxorubicin (DOX) is an antitumor drug, which is used singly or in combination with other chemotherapeutic agents.<sup>[158]</sup> DOX demonstrates cytotoxic effects when bioactivated to free radical form. Compared with DOX, the value of ethoxy [60]fullerol is still lower.

## **Conclusions**

Novel fullerene derivative  $C_{60}(OCH_2CH_3)_8(OH)_{16}$  could be synthesized through the substitution of bromine atoms from  $C_{60}Br_{24}$  in  $CH_3CH_2OH/H_2O/NaOH$  solution at ambient temperature (23°C). Both the results of FTIR and NMR determination showed that the hydroxyl groups and ethoxy groups were bonded to the [60]fullerene cage. The antioxidant activity of ethoxy [60]fullerol is very weak. Ethoxy [60]fullerol has antitumor activity.

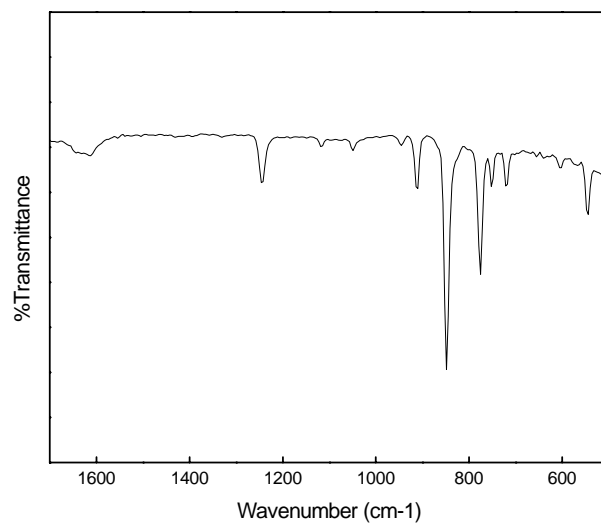


**Figure 5.1** FTIR spectrum of  $C_{60}Br_{24}$ . The percent transmittance of chemical groups is shown on the vertical axis. The wavenumber ( $cm^{-1}$ ) is shown on the horizontal axis.

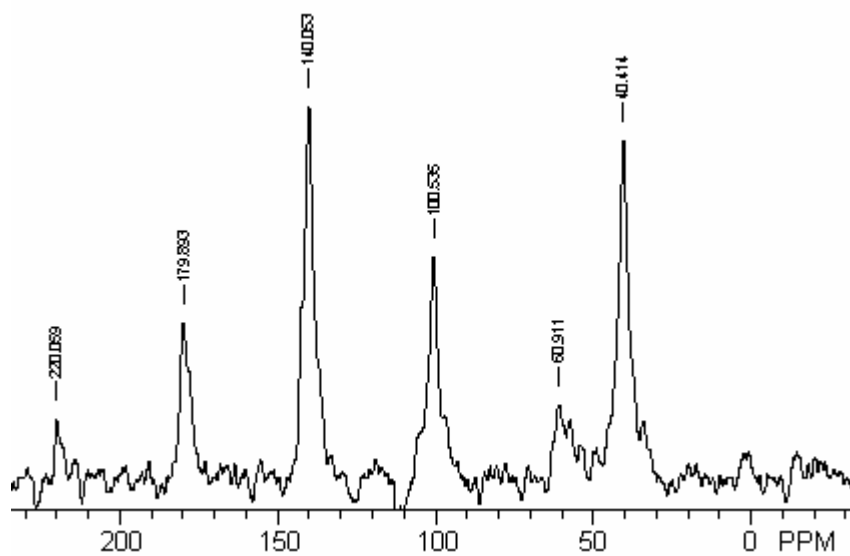


**Figure 5.2** Solid-state  $^{13}C$ -NMR spectrum of  $C_{60}Br_{24}$  at spinning rate of 4 kHz.

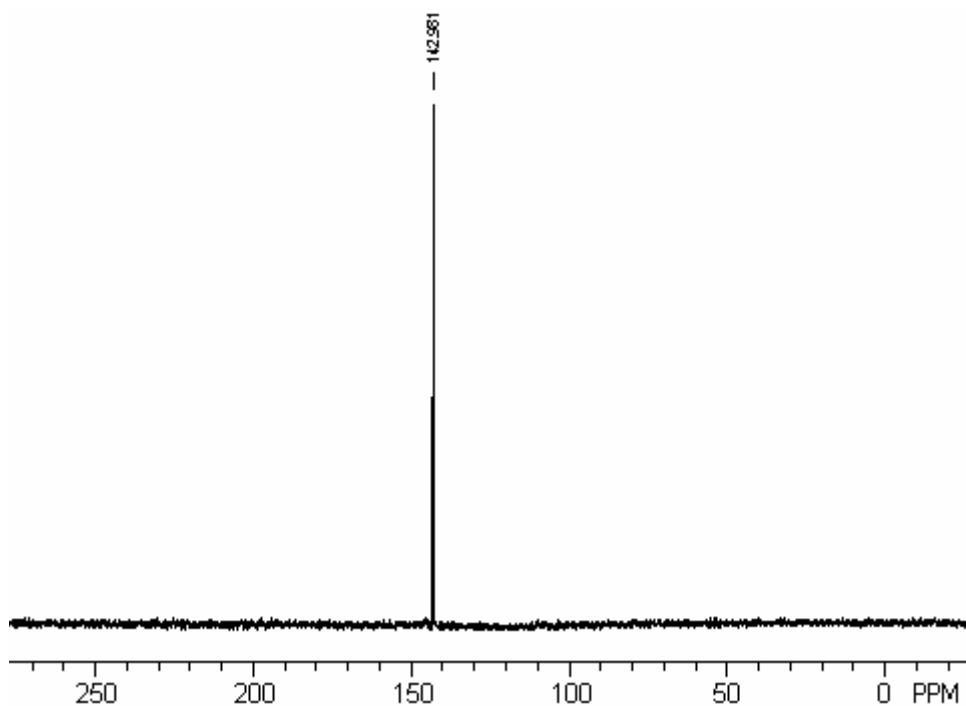


**Figure 5.3** Solid-state  $^{13}\text{C}$ -NMR spectrum of  $\text{C}_{60}$  at spinning rate of 4 kHz.

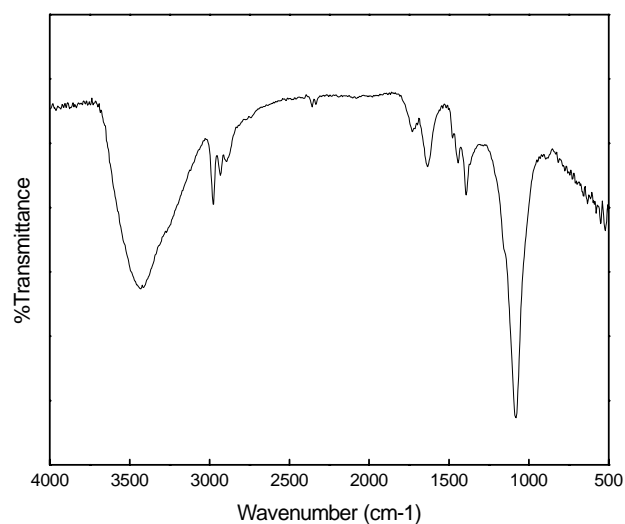


**Figure 5.4** FTIR spectrum of ethoxy [60]fullerol. The percent transmittance of chemical groups is shown on the vertical axis. The wavenumber ( $\text{cm}^{-1}$ ) is shown on the horizontal axis.

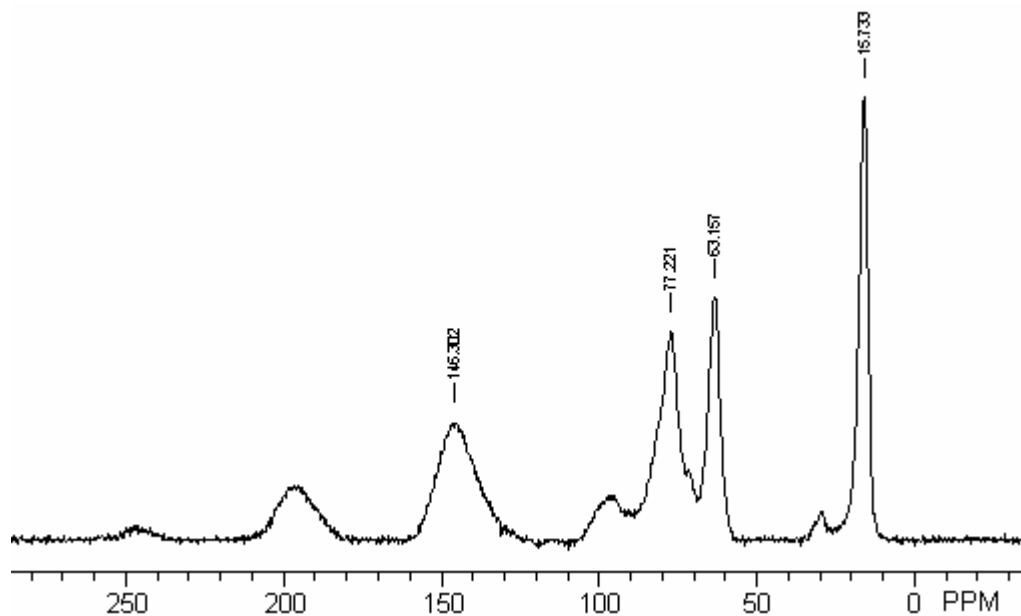


Figure 5.5  $^{13}\text{C}$  CP/MAS spectrum of ethoxy [60]fullerol at MAS rate of 5 kHz.

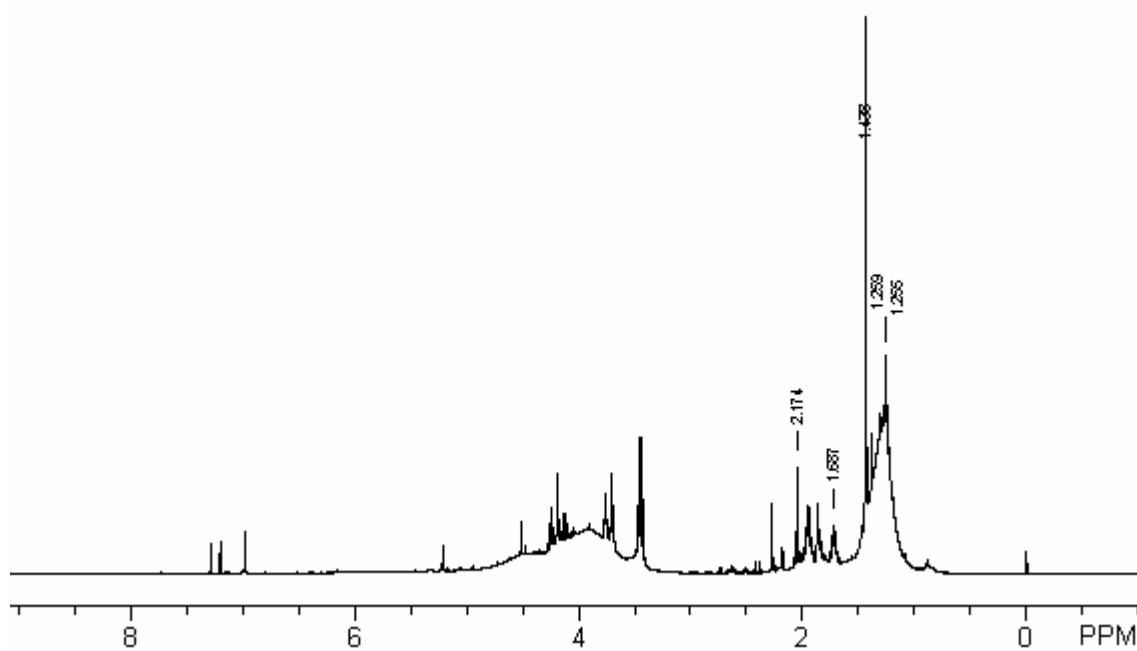


Figure 5.6  $^1\text{H}$ -NMR spectrum of unpurified ethoxy [60]fullerol in  $\text{CDCl}_3$ .

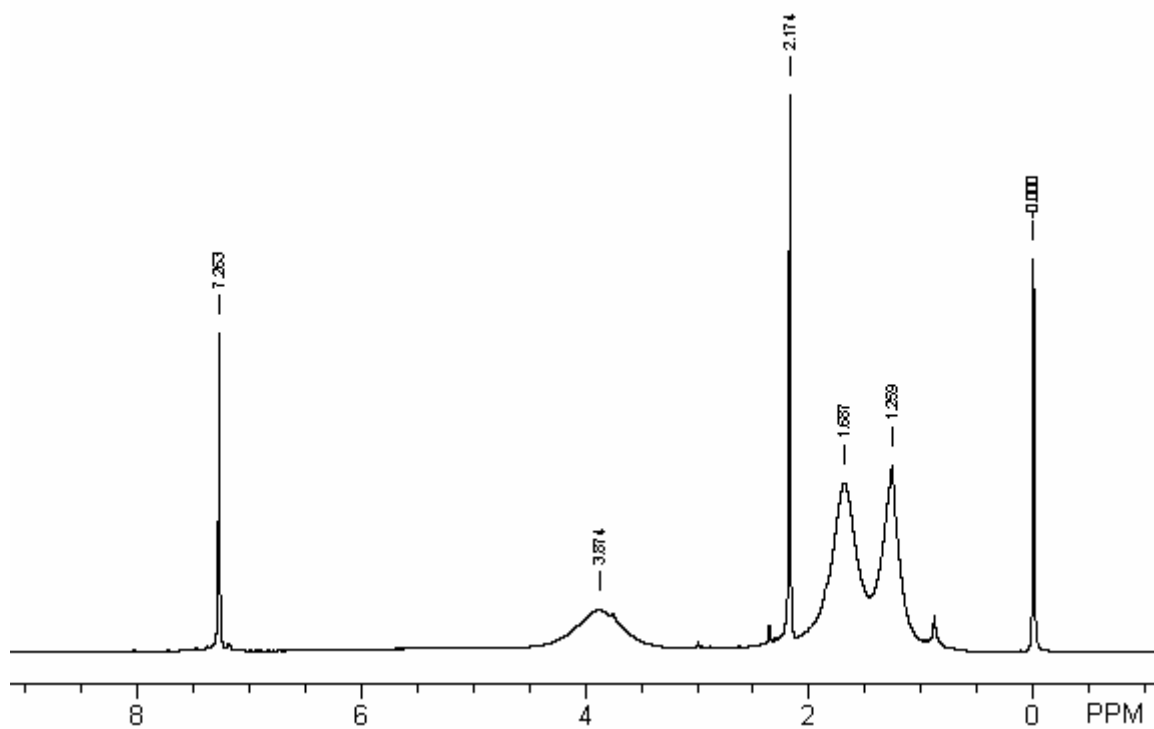
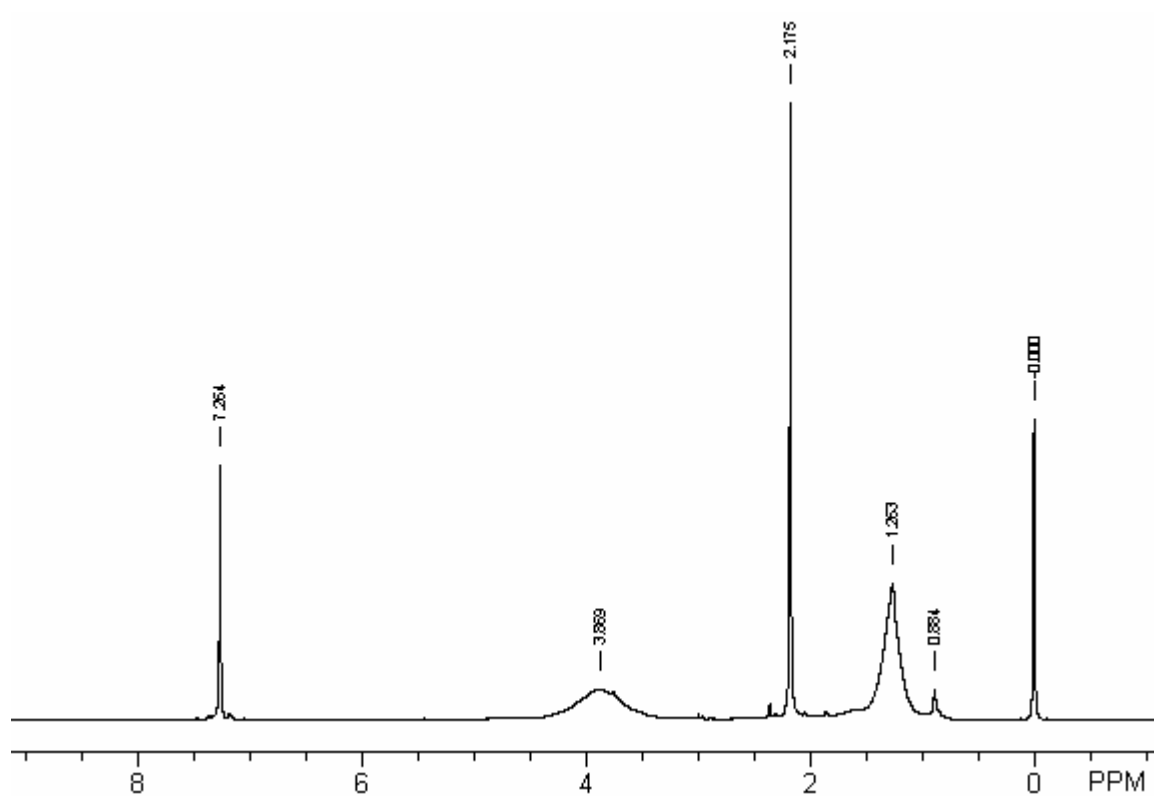
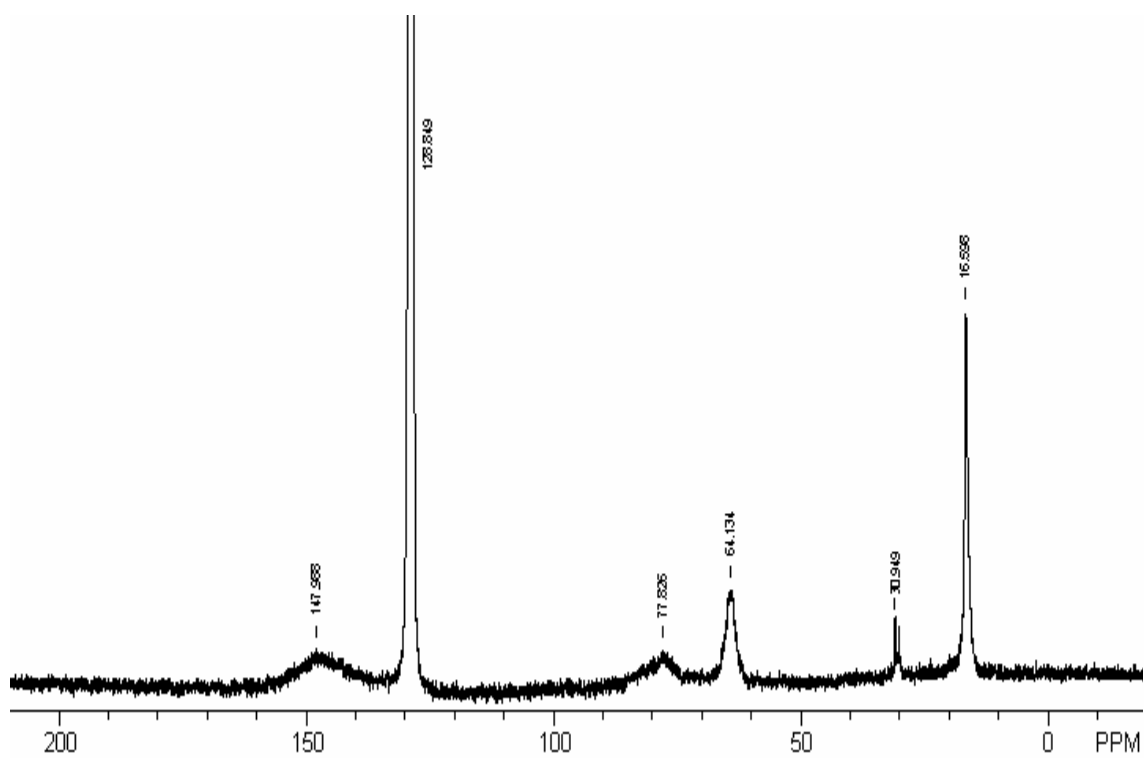


Figure 5.7  $^1\text{H-NMR}$  spectrum of purified ethoxy [60]fullerol in  $\text{CDCl}_3$ .



**Figure 5.8**  $^1\text{H-NMR}$  spectrum of purified ethoxy [60]fullerol in  $\text{CDCl}_3$  with one drop  $\text{D}_2\text{O}$ .



**Figure 5.9**  $^{13}\text{C}$ -NMR with proton decoupling spectrum of ethoxy [60]fullerol in  $\text{C}_6\text{D}_6$ .

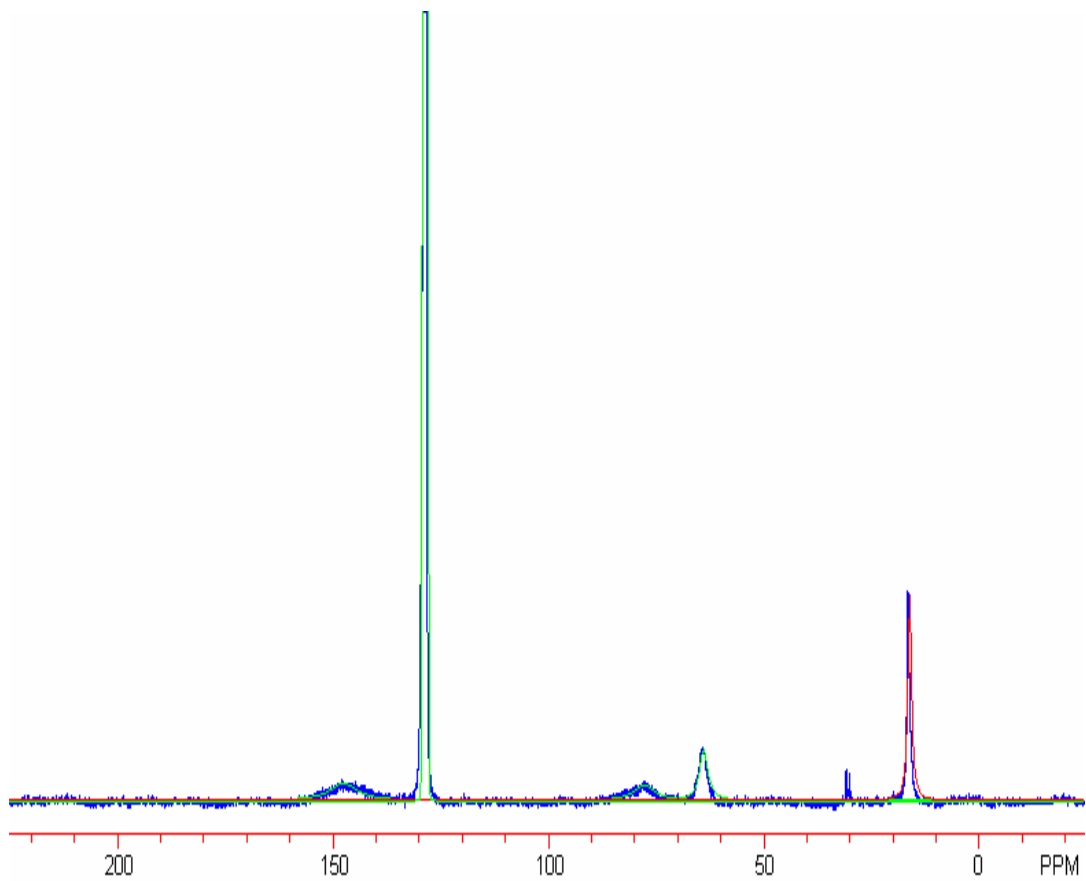


**Figure 5.10**  $^{13}\text{C}$ -NMR spectrum of ethoxy [60]fullerol in  $\text{C}_6\text{D}_6$  with Lorentzian line fitting.

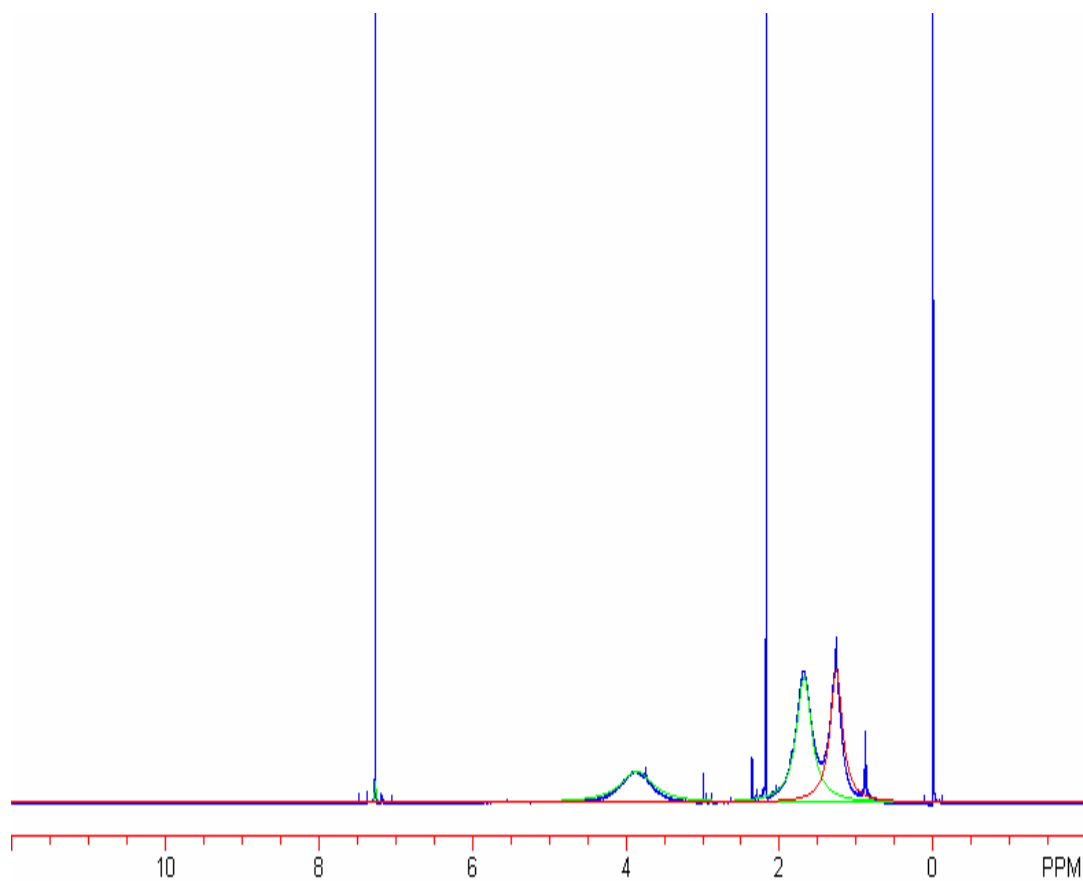


**Figure 5.11**  $^1\text{H-NMR}$  spectrum of purified ethoxy [60]fullerol in  $\text{CDCl}_3$  with Lorentzian line fitting

**Table 5.1 Antioxidant Activity of Ethoxy [60]Fullerol\***

|                           | Percentage free radical scavenging capacity (SR%) | Total phenolics content (mg g <sup>-1</sup> ) | FRAP value of the extracts (μmol g <sup>-1</sup> ) |
|---------------------------|---|---|--|
| Fullerol                  | 5.54  | 7.82  | 48.35  |
| <i>Radix Sanguisorbae</i> | 2.87 ± 0.26 (PEE)                                 | 87.89 ± 2.84 (CEE)                            | 5202.15 ± 68.18 (WE)                               |
| <i>Radix Rhapontici</i>   | 2.50 ± 0.19 (PEE)                                 | 17.36 ± 0.81 (CEE)                            | 37.17 ± 3.50 (PEE)                                 |
| <i>Fructus Crataegi</i>   | 0.49 ± 0.37 (PEE)                                 | 40.18 ± 1.11 (CEE)                            | 305.69 ± 10.02 (PEE)                               |
| <i>Cortex Cinnamomi</i>   | 7.50 ± 0.73 (PEE)                                 | 4.15 ± 0.16 (PEE)                             | 23.39 ± 0.65 (PEE)                                 |
| <i>Herba Taxilli</i>      | 1.82 ± 0.58 (PEE)                                 | 28.46 ± 0.37 (CEE)                            | 280.35 ± 5.92 (CEE)                                |
| Ascorbic Acid             | -   | -   | 11334.69   |
| BHT                       | -   | -   | 781.42   |

**Note:** PEE – petroleum ether extract; CEE – chloroform-ethyl acetate extract; WE – water extract. \* Private communication from Li, S. and Kwok, C. Y. in Dr. Peter H. Yu's group.

**Table 5.2 Cytotoxic Property of Ethoxy [60]Fullerol against Human Breast Carcinoma (cell line: MCF-7)**

|                             | ED50 doxorubicin/<br>μM | ED50 fullerol/μM |
|-----------------------------|-------------------------|------------------|
| No UV light                 | 0.06                    | 33.65            |
| UV light exposed for 30 min | -                       | 33.72            |

## Chapter 6

### Suggestions for Further Work

#### 6.1 Research of Molecular Recognition by Vancomycin

##### 6.1.1 Chemical Structure and Resistance

Vancomycin<sup>[159-162]</sup>(Fig. 6.1) is a vital therapeutic agent used worldwide for the treatment of infections with Gram-positive bacteria. The emergence of vancomycin-resistant *Enterococci* (VRE)<sup>[163]</sup> and vancomycin-intermediate resistant

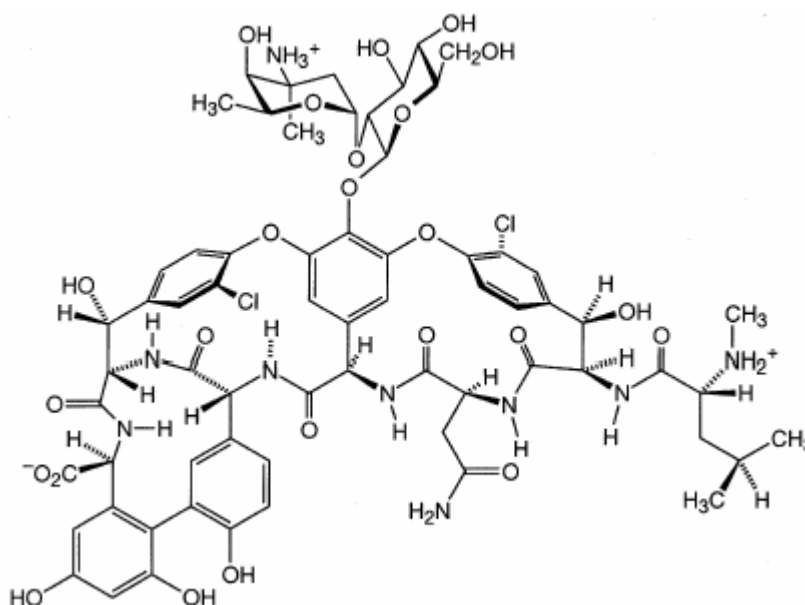
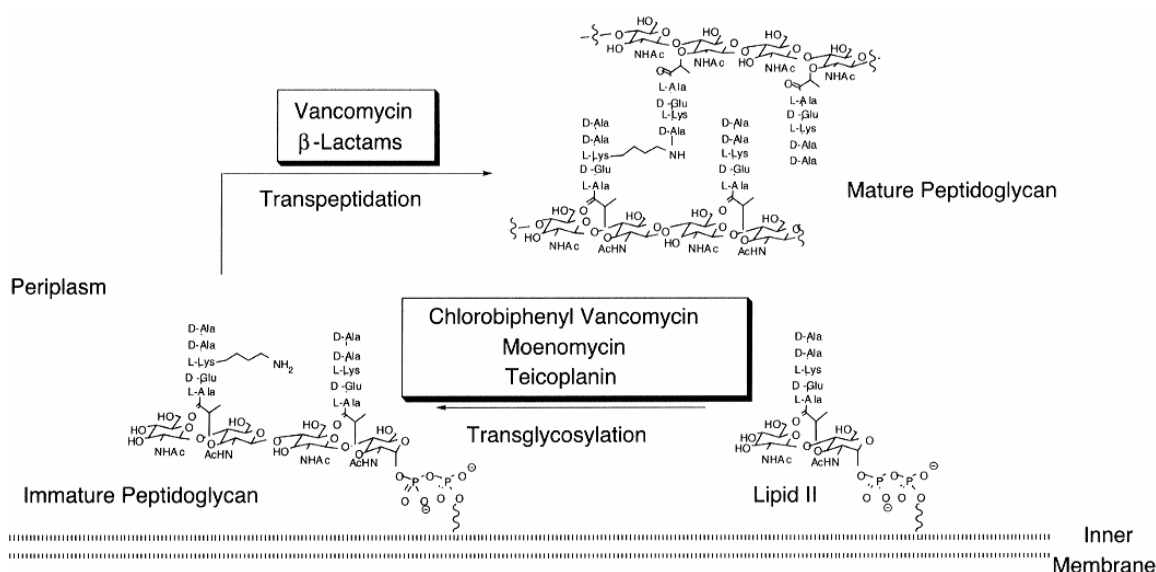


Figure 6.1 Chemical structure of vancomycin

*Staphylococcus aureus* (VISA)<sup>[164]</sup> is a major public health threat.<sup>[165]</sup> So, it is very important to develop novel antibacterial drugs with activity against VRE and VISA.<sup>[166, 167]</sup> The antibacterial activity of vancomycin results from its ability to inhibit bacterial cell-wall peptidoglycan biosynthesis (Fig. 6.2).<sup>[168-171]</sup> Vancomycin binds to the terminal D-Ala-D-Ala fragment of the immature cell wall through an intricate network of five hydrogen bonds and thereby inhibits cell wall construction,<sup>[172]</sup> which eventually leads to bacterial death due to the weakened cell wall's loss of ability to withstand high osmotic pressure. Vancomycin resistance is



**Figure 6.2 Final stage of peptidoglycan biosynthesis. Transglycosylase enzymes polymerize lipid II into long polysaccharide chains (immature peptidoglycan), which are then cross-linked by transpeptidases. Chlorobiphenyl vancomycin, moenomycin, and teicoplanin inhibit the transglycosylation step; vancomycin and β-lactams inhibit the transpeptidation step.**<sup>[169]</sup>

primarily conferred through the mutation of the terminal D-Ala-D-Ala to a terminal D-Ala-D-Lac.<sup>[173, 174]</sup> This structural change results in the loss of one hydrogen bond from the vancomycin-peptide complex, thereby decreasing vancomycin's affinity for the cell wall by a thousand-fold, and as a consequence, rendering the antibiotic ineffective against such mutants.

## **6.1.2 Rational Modification**

### **6.1.2.1 Modify the Binding Surface**

One of the most obvious tactics to reach this target is to modify the binding surface between vancomycin and its ligand within the cell wall. Its implementation appears at present as synthetically complex, although a number of attempts along these lines have been made.<sup>[175-177]</sup>

### **6.1.2.2 Semi-synthetic Derivatives**

Scientists have explored more practical approach to restoring antibacterial activity to vancomycin-type structures.<sup>[178-185]</sup> The vancomycin derivatives with a hydrophobic substituent on the carbohydrate moiety are active against vancomycin-resistant strains even though they contain the same peptide-binding pocket as vancomycin. The functional mechanism of these derivatives may be fundamentally different from that of vancomycin, but they retain activity against both vancomycin-

sensitive and vancomycin-resistant strains even when the peptide-binding pocket is damaged<sup>[186]</sup>. Specifically, lipophilic anchors such as those present on the naturally occurring glycopeptide antibiotic teicoplanin<sup>[187, 188]</sup> facilitate the delivery of the molecule at its site of action within the cell wall and thus improve its effectiveness against bacteria.

### **6.1.2.3 Covalent Dimers**

Some glycopeptide antibiotics naturally occur the tendency to form dimers with desirable characteristics, which has led several investigators to explore the properties of covalently linked dimers.<sup>[189-192]</sup> Beyond dimers, the binding of trimeric ligands to trimeric vancomycin has also been described.<sup>[193]</sup> In this case, the binding affinity was almost threefold that of the monomer, making its affinity higher than that of avidin-biotin.<sup>[194]</sup>

## **6.2 Ethoxy [60]Fullerol as Carrier with Vancomycin**

Vancomycin easily forms dimers by itself, which decreases its utility. Through the reactions of carboxyl group on vancomycin, ethoxy [60]fullerol would be used as carrier with it. Because of suitable chemical and biological properties of fullerol,<sup>[153]</sup> it could increase the utility and decrease the toxicity of this therapeutic compound and deliver it to the desirable focus tissue directly.

### **6.3 Purification and Structure Determination of [60]Fullerene Derivatives**

Purification of organic compounds is one of the most important problems in materials chemistry and biological research interest. Simple precipitation and filtration allow separating out the product mixture from the reactants but final purification of the fullerene derivatives by liquid chromatography<sup>[195, 196]</sup> is needed. Structural determination by MS, UV–Vis, FTIR, and NMR etc. is then carried out. If the pure compound can be crystallized, x-ray structural determination could be good method.

### **6.4 Antibacterial Activity of [60]Fullerene Derivatives**

The antibacterial activity of these compounds is to be assessed according to normal procedures.

### **6.5 Anticancer Bioactivity of [60]Fullerene Derivatives**

The effectiveness of these compounds in photodynamic therapy would be assessed with or without light irradiation.<sup>[17, 23]</sup>

## References

- (1) Pouton, C. W., and Akhtar, S. "Biosynthetic polyhydroxyalkanoates and their potential in drug delivery". *Advanced Drug Delivery Reviews*, Vol. 18(2), pp133-162 (1996)
- (2) Zinn, M., Withol, B., and Egli, T. "Occurrence, synthesis and medical application of bacterial polyhydroxyalkanoate". *Advanced Drug Delivery Reviews*, Vol. 53(1), pp5-21 (2001)
- (3) Hanggi, U. J. *In Novel Biodegradable Microbial Polymers*, Kluwer Academic Publishers, Netherlands, pp65 (1990)
- (4) Byrom, D. "Production of poly- $\beta$ -hydroxybutyrate: poly- $\beta$ -hydroxyvalerate copolymers". *FEMS Microbiology Review*, Vol. 103(2-4), pp247-250 (1992)
- (5) Kroto, H. K., Heath, J. R., O'Brien, S. C., Curl, R. F., and Smalley, R. E. "C<sub>60</sub>-Buckminsterfullerene". *Nature*, Vol. 318(6042), pp162-163 (1985)
- (6) Taylor, R., and Walton, D. R. M. "The chemistry of fullerenes". *Nature*, Vol. 363(6431), pp685-695 (1993)
- (7) Andersson, T., Nilsson, K., Sundahl, M., Westman, G., and Wennerström, O. "C<sub>60</sub> embedded in  $\gamma$ -cyclodextrin: a water-soluble fullerene". *Journal of the Chemical Society, Chemical Communications*, Issue 8, pp604-606 (1992)
- (8) Boulas, P., Kutner, W., Jones, M. T., and Kadish, K. M. "Bucky(basket)ball: stabilization of electrogenerated C<sub>60</sub><sup>-</sup> radical monoanion in water by means

- of cyclodextrin inclusion chemistry". *The Journal of Physical Chemistry*, Vol. 98(4), pp1282-1287 (1994)
- (9) Priyadarsini, K. I., Mohan, H., Tyagi, A. K., and Mittal, J. P. "Inclusion complex of  $\gamma$ -cyclodextrin- $C_{60}$ : formation, characterization and photophysical properties in aqueous solutions". *The Journal of Physical Chemistry*, Vol. 98(17), pp4756-4759 (1994)
- (10) Zhang, D. D., Liang, Q., Chen, W. J., Li, M. C., and Wu, S. H. "Study on the preparation and structure of inclusion complex of  $\gamma$ -cyclodextrin- $C_{60}$ ". *Chinese Science Bulletin*, Vol. 39(4), pp383-384 (1994)
- (11) Williams, R. M., and Verhoeven, J. W. "Supramolecular encapsulation of  $C_{60}$  in a water-soluble calixarene—a core-shell charge-transfer complex". *Journal of the Royal Netherlands Chemical Society*, Vol. 111(12), pp531-532 (1992)
- (12) Atwood, J. L., Koutsantonis, G. A., and Raston, C. L. "Purification of  $C_{60}$  and  $C_{70}$  by selective complexation with calixarenes". *Nature*, Vol. 368(6468), pp229-231 (1994)
- (13) Scrivens, W. A., Tour, J. M., Creek, K. E., and Pirisi, L. "Synthesis of  $^{14}C$ -labeled  $C_{60}$ , its suspension in water, and its uptake by human keratinocytes". *Journal of the American Chemical Society*, Vol. 116(10), pp4517-4518 (1994)
- (14) Chiang, L. Y., Upasani, R. B., and Swirczewski, J. W. "Versatile nitronium

- chemistry for C<sub>60</sub> fullerene functionalization”. *Journal of the American Chemical Society*, Vol. 114(26), pp10154-10157 (1992)
- (15) Burley, G. A., Keller, P. A., and Pyne, S. G. “[60]Fullerene amino acids and related derivatives”. *Fullerene Science and Technology*, Vol. 7(6), pp973-1001 (1999)
- (16) Marcorin, G. L., Ros, T. D., Castellano, S., Stefancich, G., Bonin, I., Miertus, S., and Prato, M. “Design and synthesis of novel [60]fullerene derivatives as potential HIV aspartic protease inhibitors”. *Organic Letters*, Vol. 2(25), pp3955-3958 (2000)
- (17) Tokuyama, H., Yamago, S., Nakamura, E., Shiraki, T., and Sugiura, Y. “Photoinduced biochemical activity of fullerene carboxylic acid”. *Journal of the American Chemical Society*, Vol. 115(17), pp7918-7919 (1993)
- (18) Nakamura, E., Tokuyama, H., Yamago, S., Shiraki, T., and Sugiura, Y. “Biological activity of water-soluble fullerenes. Structural dependence of DNA cleavage, cytotoxicity, and enzyme inhibitory activities including HIV-protease inhibition”. *Bulletin of the Chemical Society of Japan (in English)*, Vol. 69, pp2143-2151 (1996)
- (19) Takenaka, S., Yamashita, K., Takagi, M., Hatta, T., and Tsuge, O. “Photo-induced DNA cleavage by water-soluble cationic fullerene derivatives”. *Chemistry Letters*, Issue 4, pp321-322 (1999)
- (20) Friedman, S. H., DeCamp, D. L., Sijbesma, R. P., Srdanov, G., Wudl, F., and Kenyon, G. L. “Inhibition of the HIV-1 protease by fullerene derivatives:

- model building studies and experimental verification”. *Journal of the American Chemical Society*, Vol. 115(15), pp6506-6509 (1993)
- (21) Sijbesma, R., Srdanov, G., Wudl, F., Castoro, J. A., Wilkins, C., Friedman, S. H., DeCamp, D. L., and Kenyon, G. L. “Synthesis of a fullerene derivative for the inhibition of HIV enzymes”. *Journal of the American Chemical Society*, Vol. 115(15), pp6510-6512 (1993)
- (22) Rajagopalan, P., Wudl, F., Schinazi, R. F., and Boudinot, F. D. “Pharmacokinetics of a water-soluble fullerene in rats”. *Antimicrobial Agents and Chemotherapy*, Vol. 40(10), pp2262-2265 (1996)
- (23) Yang, X. L., Fan, C. H., and Zhu, H. S. “Photo-induced cytotoxicity of malonic acid [C<sub>60</sub>]fullerene derivatives and its mechanism”. *Toxicology in Vitro*, Vol. 16, pp41-46 (2002)
- (24) Ros, T. D. and Prato, M. “Medicinal chemistry with fullerenes and fullerene derivatives”. *Journal of the Chemical Society, Chemical Communications*, Issue 8, pp663-669 (1999)
- (25) Nakamura, E., and Isobe, H. “Functionalized fullerenes in water. The first 10 years of their chemistry, biology, and nanoscience”. *Accounts of Chemical Research*, Vol. 36(11), pp807-815 (2003)
- (26) Arbogast, J. W., Foote, C. S., and Kao, M. “Electron-transfer to triplet C<sub>60</sub>”. *Journal of the American Chemical Society*, Vol. 114(6), pp2277-2279 (1992)
- (27) Arbogast, J. W., Darmany, A. P., Foote, C. S., Rubin, Y., Diederich, F., Alvarez, M. M., Anz, S. J., and Whetten, R. L. “Photophysical properties of C<sub>60</sub>”. *Journal of Physical Chemistry*, Vol. 95(1), pp11-12 (1991)

- (28) Liu, Y., Wang, L. F., and Zhang, D. D. "Study on the water-soluble inclusion complex of  $\beta$ -cyclodextrin polymer- $C_{60}$ ". *Chinese Science Bulletin*, Vol. 40(9), pp863 (1995)
- (29) Murthy, C. N., and Geckeler, K. E. "The water-soluble  $\beta$ -cyclodextrin-[60]fullerene complex". *Journal of the Chemical Society, Chemical Communications*, Issue 13, pp1194-1195 (2001)
- (30) Samal, S., Choi, B.-J., and Geckeler, K. E. "The first water-soluble main-chain polyfullerene". *Journal of the Chemical Society, Chemical Communications*, Issue 15, pp1373-1374 (2000)
- (31) Hungerbühler, H., Guldi, D. M., and Asmus, K.-D. "Incorporation of  $C_{60}$  into artificial lipid membranes". *Journal of the American Chemical Society*, Vol. 115(8), pp3386-3387 (1993)
- (32) Yamakoshi, Y. N., Yagami, T., Fukuhara, K., Sueyoshi, S., and Miyata, N. "Solubilization of fullerene into water with polyvinylpyrrolidone applicable to biological tests". *Journal of the Chemical Society, Chemical Communications*, Issue 4, pp517-518 (1994)
- (33) Naim, A., and Shevlin, B. S. "Reversible addition of hydroxide to the fullerenes". *Tetrahedron Letters*, Vol. 33(47), pp7097-7100 (1992)
- (34) Schneider, N. S., Darwish, A. D., Kroto, H. W., Taylor, R., Walton, D. R. M. "Formation of fullerols via hydroboration of fullerene- $C_{60}$ ". *Journal of the Chemical Society, Chemical Communications*, Issue 4, pp463-464 (1994)

- (35) Li, J., Takeuchi, A., Ozawa, M., Li, X. H., Saigo, K., and Kitazawa, K. "C<sub>60</sub> fullerol formation catalyzed by quaternary ammonium hydroxides". *Journal of the Chemical Society, Chemical Communications*, Issue 23, pp1784-1785 (1993)
- (36) Li, T. B., Huang, K. X., Li, X. H., Jiang, H. Y., Li, J., Yan, X. Z., Li, J., and Zhao, S. K. "Studies on the rapid preparation of fullerols and its formation mechanism". *Chemical Journal of Chinese Universities*, Vol. 19(6), pp858-860 (1998)
- (37) Zhou, D. J., Gan, L. B., Xu, L. B., Luo, C. P. and Huang, C. H. "Glycine C<sub>60</sub> adduct and its rare earth complexes". *Fullerene Science and Technology*, Vol. 3(2), pp127-131 (1995)
- (38) Gan, L. B., Luo, C. P., Xu, L. B., Zhou, D. J., Huang, C. H., and Zhao, S. K. "Water-soluble fullerene derivatives. Synthesis and characterization of  $\beta$ -alanine C<sub>60</sub> adducts". *Chinese Chemical Letters*, Vol. 5(4), pp275-278 (1994)
- (39) Kotelnikova, R. A., Kotelnikov, A. I., Bogdanov, G. N., Romanova, V. S., Kuleshova, E. F., Parnes, Z. N., and Vol'pin, M. E. "Membranotropic properties of the water soluble amino acid and peptide derivatives of fullerene C<sub>60</sub>". *FEBS Letters*, Vol. 389, pp111-114 (1995)
- (40) Prato, M., Bianco, A., Maggini, M., Scorrano, G., Toniolo, C., and Wudl, F. "Synthesis and characterization of the first fullerene-peptide". *Journal of Organic Chemistry*, Vol. 58(21), pp5578-5580 (1993)

- (41) Samal, S. and Geckeler, K. E. "Cyclodextrin-fullerenes: a new class of water-soluble fullerenes". *Journal of the Chemical Society, Chemical Communications*, Issue 13, pp1101-1102 (2000)
- (42) Bergamin, M., Da Ros, T., Spalluto, G., Boutorine, A., and Prato, M. "Synthesis of a hybrid fullerene-trimethoxyindole-oligonucleotide conjugate". *Journal of the Chemical Society, Chemical Communications*, Issue 1, pp17-18 (2001)
- (43) Ros, T. D., Prato, M., Novello, F., Maggini, M., and Banfi, E. "Easy access to water-soluble fullerene derivatives via 1,3-dipolar cycloadditions of azomethine ylides to C<sub>60</sub>". *Journal of Organic Chemistry*, Vol. 61(25), pp9070-9072 (1996)
- (44) Richardson, C. F., Schuster, D. I., and Wilson, S. R. "Synthesis and characterization of water-soluble amino fullerene derivatives". *Organic Letters*, Vol. 2(8), pp1011-1014 (2000)
- (45) Brettreich, M., and Hirsch, A. "A highly water-soluble dendro[60]fullerene". *Tetrahedron Letters*, Vol. 39(18), pp2731-2734 (1998)
- (46) Jain, R. A. "The manufacturing techniques of various drug loaded biodegradable poly(lactide-co-glycolide) (PLGA) devices". *Biomaterials*, Vol. 21, pp2475-2490 (2000)
- (47) Johansen, P., Men, Y., Merkle, H. P., and Gander, B. "Revisiting PLA/PLGA microspheres: an analysis of their potential in parenteral vaccination". *European Journal of Pharmaceutics and Biopharmaceutics*, Vol. 50(1), pp129-146 (2000)

- (48) Anderson, A. J. and Dawes, E. A. "Occurrence, metabolism, metabolic role, and industrial uses of bacterial polyhydroxyalkanoates". *Microbiological Reviews*, Vol. 54(4), pp450-472 (1990)
- (49) Brandl, H., Cross, R. A., Lenz, R. W., and Fuller, R. C. "Pseudomonas oleovorans as a source of poly( $\beta$ -hydroxyalkanoate) for potential applications as biodegradable polyesters". *Applied and Environmental Microbiology*, Vol. 54(8), pp1977-1982 (1988)
- (50) Lee, S. Y. "Bacterial polyhydroxyalkanoates". *Biotechnology and Bioengineering*, Vol. 49(1), pp1-14 (1996)
- (51) Chen, G. Q., Koenig, K. H., and Lafferty, R. M. "Occurrence of poly-D(-)-3-hydroxyalkanoates in the genus *Bacillus*". *FEMS Microbiology Letters*, Vol. 84(2), pp173-176 (1991)
- (52) Lupke, T., Radusch, H. J., and Metzner, K. "Solid-state processing of PHB powders". *Macromolecular Symposia*, Vol. 127, pp227-240 (1998)
- (53) Steinbuchel, A., Fuchtenbusch, B., Gorenflo, V., Hein, S., Jossek, R., Langenbach, S., and Rehm, B. H. A. "Biosynthesis of polyesters in bacteria and recombinant organisms". *Polymer Degradation and Stability*, Vol. 59(1-3), pp177-182 (1998)
- (54) Koller, I., and Owen, A. "Starch-filled PHB and PHB/HV copolymer". *Polymer International*, Vol. 39, pp175-181 (1996)
- (55) Kusaka, S., Iwata, T., and Doi, Y. "Microbial synthesis and physical properties of ultra-high-molecular-weight poly[(R)-3-hydroxybutyrate]".

- Journal of Macromolecular Science, Pure and Applied Chemistry*, Vol. A35(2), pp319-335 (1998)
- (56) Lee, S. Y., Chang, H. N., and Chang, Y. K. *In Better Living Through Innovative Biochemical Engineering*, Singapore University Press, Singapore, pp53 (1994)
- (57) Shirai, Y., Yamaguchi, N., and Kusubayashi, N. *In Better Living Through Innovative Biochemical Engineering*, Singapore University Press, Singapore, pp263 (1994)
- (58) Shimizu, H., Sonoo, S., and Shioya, S. *In Biochemical Engineering for 2001*, Springer-Verlag, Tokyo, pp195 (1992)
- (59) Wang, T., Ye, L., and Song, Y. R. "Progress of PHA production in production in transgenic plants". *Chinese Science Bulletin*, Vol. 44(19) pp1729-1736 (1999)
- (60) Yoon, J. S., Lee, W. S., Jin, H. J., Chin, I. J., Kim, M. N., and Go, J. H. "Toughening of poly(3-hydroxybutyrate) with poly(*cis*-1, 4-isoprene)". *European Polymer Journal*, Vol. 35(5), pp781-788 (1999)
- (61) Ha, C.-S., and Cho, W.-J. "Miscibility, properties, and biodegradability of microbial polyester containing blends". *Progress in Polymer Science*, Vol. 27(4), pp759-809 (2002)
- (62) Yu, P. H., Chua, H., Huang, A. L., Lo, W., and Chen, G. Q. "Conversion of food industrial wastes into bioplastics". *Applied Biochemistry and Biotechnology*, Vol. 70-72, pp603-614 (1998)

- (63) King, P. P. "Biotechnology. An industrial view". *Journal of Chemical Technology and Biotechnology*, Vol. 32(1), pp2-8 (1982)
- (64) Chen, G. Q., Konig, K. H., and Lafferty, R. M. "Production of poly-D(-)-3-hydroxybutyrate and poly-D(-)-3-hydroxyvalerate by strains of *Alcaligenes latus*". *Antonie van Leeuwenhoek*, Vol. 60(1), pp61-66 (1991)
- (65) Chen, G. Q., and Page, W. J. "Production of poly- $\beta$ -hydroxybutyrate by *Azotobacter vinelandii* in a two-stage fermentation process". *Biotechnology Techniques*, Vol. 11(5), pp347-350 (1997)
- (66) Holden, G., Legge, N. R., Quirk, R., and Schroeder, H. E. *In Thermoplastic Elastomers*, 2<sup>nd</sup> Ed, Hanser Publishers, New York, pp465-485 (1996)
- (67) Bluhm, T. L., Hamer, G. K., Marchessault, R. H., Fyfe, C. A., and Veregin, R. P. "Isodimorphism in bacterial poly( $\beta$ -hydroxybutyrate-co- $\beta$ -hydroxyvalerate)". *Macromolecules*, Vol. 19, pp2871-2876 (1986)
- (68) Bloembergen, S., Holden, D. A., Hamer, G. K., Bluhm, T. L., and Marchessault, R. H. "Studies of composition and crystallinity of bacterial poly( $\beta$ -hydroxybutyrate-co- $\beta$ -hydroxyvalerate)". *Macromolecules*, Vol. 19, pp2865-2871 (1986)
- (69) Doi, Y., Kanesawa, Y., Kunioka, M., and Saito, T. "Biodegradation of microbial copolyesters: poly(3-hydroxybutyrate-co-3-hydroxyvalerate) and poly(3-hydroxybutyrate-co-4-hydroxybutyrate)". *Macromolecules*, Vol. 23(1), pp26-31 (1990)
- (70) Mergaert, J., Webb, A., Anderson, C., and Swings, J. "Microbial degradation of poly(3-hydroxybutyrate) and poly(3-hydroxybutyrate-co-3-

- hydroxyvalerate) in soils". *Applied and Environmental Microbiology*, Vol. 59(10), pp3233-3238 (1993)
- (71) Mitomo, H., Barham, P. J., and Keller, A. "Temperature dependence of mechanical properties of poly( $\beta$ -hydroxybutyrate- $\beta$ -hydroxyvalerate)". *Polymer Communications*, Vol. 29(4), pp112-115 (1988)
- (72) Hu, P., Chen, G. Q., Zhang, Z. M., and Wu, Q. "Production and characterization of biodegradable plastics - polyhydroxyalkanoates (PHA)". *Hecheng Shuzhi Ji Suliao*, Vol. 14(2), pp45-49 (1997)
- (73) Chua, H., Yu, P. H. F., and Lo, W. "Accumulation of biodegradable copolyesters of 3-hydroxybutyrate and 3-hydroxyvalerate in *Alcaligenes eutrophus*". *Applied Biochemistry and Biotechnology*, Vol. 70-72, pp929-935 (1998)
- (74) Xi, J. X., Wu, Q., Yan, Y. B., Zhang, Z. M., Yu, P. H. F., Cheung, M. K., Zhang, R. Q., and Chen, G. Q. "Hyperproduction of polyesters consisting of medium-chain-length hydroxyalkanoate monomers by strain *Pseudomonas stutzeri* 1317". *Antonie van Leeuwenhoek International Journal of General and Molecular Microbiology*, Vol. 78(1), pp43-49 (2000)
- (75) Coats, A. W., and Redfern, J. P. "Kinetic parameters from thermogravimetric data". *Nature*, Vol. 201(4914), pp68-69 (1964)
- (76) Tebbe, F. N., Harlow, R. L., Chase, D. B., Thorn, D. L., Campbell, G. C., Calabrese, J. C., Herron, N., Young, R. J., and Wasserman, E. "Synthesis and single-crystal x-ray structure of a highly symmetrical C<sub>60</sub> derivative, C<sub>60</sub>Br<sub>24</sub>". *Science*, Vol. 256, pp822-825 (1992)

- (77) Brand-Williams, W., Cuvelier, M. E., and Berset, C. "Use of a free radical method to evaluate antioxidant activity". *Lebensmittel-Wissenschaft und – Technologie*, Vol. 28(1), pp25-30 (1995)
- (78) Weber, V., Coudert, P., Rubat, C., Duroux, E., Leal, F., and Couquelet, J. "Antioxidant properties of novel lipophilic ascorbic acid analogues". *Journal of Pharmacy and Pharmacology*, Vol. 52(5), pp523-530 (2000)
- (79) Benzie, I. F. F., and Strain, J. J. "Ferric reducing antioxidant power assay: direct measure of total antioxidant activity of biological fluids and modified version for simultaneous measurement of total antioxidant power and ascorbic acid concentration". *Oxidants and Antioxidants, Part A: Methods in Enzymology*, Vol. 299, pp15-27 (1999)
- (80) Benzie, I. F. F., and Strain, J. J. "The ferric reducing ability of plasma (FRAP) as a measure of 'antioxidant power': the FRAP assay". *Analytical Biochemistry*, Vol. 239(1), pp70-76 (1996)
- (81) Singleton, V. L., Orthofer, R., and Lamuela-Raventos, R. M. "Analysis of total phenols and other oxidation substrates and antioxidants by means of Folin-Ciocalteu reagent". *Oxidants and Antioxidants, Part A: Methods in Enzymology*, Vol. 299, pp152-178 (1999)
- (82) Doi, Y. *Microbial Polyesters*, VCH: New York (1990)
- (83) Jedlinski, Z., Kowalczyk, M., Adamus, G., Sikorska, W., and Rydz, J. "Novel synthesis of functionalized poly(3-hydroxybutanoic acid) and its copolymers". *International Journal of Biological Macromolecules*, Vol. 25(1-3), pp247-253 (1999)

- (84) Mergaert, J., Anderson, C., Wouters, A., Swings, J., and Kersters, K. "Biodegradation of polyhydroxyalkanoates". *FEMS Microbiology Reviews*, Vol. 103(2-4), pp317-321 (1992)
- (85) Verhoogt, H., Ramsay, B. A., and Favis, B. D. "Polymer blends containing poly(3-hydroxyalkanoate)s". *Polymer*, Vol. 35(24), pp5155-5169 (1994)
- (86) Barham, P. J., and Keller, A. "The relationship between microstructure and mode of fracture in polyhydroxybutyrate". *Journal of Polymer Science Part B: Polymer Physics*, Vol. 24(1), pp69-77 (1986)
- (87) Billingham, N. C., Henman, T. J., and Holmes, P. A. *In Developments in Polymer Degradation*, Grassie, N., Ed., Elsevier: London, Vol. 7, pp81 (1987)
- (88) Jendrossek, D., Schirmer, A., and Schlegel, H. G. "Biodegradation of polyhydroxyalkanoic acids". *Applied Microbiology and Biotechnology*, Vol. 46(5-6), pp451-463 (1996)
- (89) Sudesh, K., Abe, H., and Doi, Y. "Synthesis, structure and properties of polyhydroxyalkanoates: biological polyesters". *Progress in Polymer Science*, Vol. 25(10), pp1503-1555 (2000)
- (90) Shirakura, Y., Fukui, T., Saito, T., Okamoto, Y., Narikawa, T., Koide, K., Tomita, K., Takemasa, T., and Masamune, S. "Degradation of poly(3-hydroxybutyrate) by poly(3-hydroxybutyrate) depolymerase from *Alcaligenes faecalis* T1". *Biochimica et Biophysica Acta*, Vol. 880(1), pp46-53 (1986)

- (91) Scandola, M., Focarete, M. L., and Frisoni, G. "Simple kinetic model for the heterogeneous enzymatic hydrolysis of natural poly(3-hydroxybutyrate)". *Macromolecules*, Vol. 31(12), pp3846-3851 (1998)
- (92) Scandola, M., Focarete, M. L., Gazzano, M., Matuszowicz, A., Sikorska, W., Adamus, G., Kurcok, P., Kowalczyk, M., and Jedlinski, Z. "Crystallinity-induced biodegradation of novel [(R,S)-beta-butyrolactone]-b-pivalolactone copolymers". *Macromolecules*, Vol.30 (25), pp7743-7748 (1997)
- (93) Abe, H., Matsubara, I., and Doi, Y. "Physical-properties and enzymatic degradability of polymer blends of bacterial poly[(R)-3-hydroxybutyrate] and poly[(R,S)-3-hydroxybutyrate] stereoisomers". *Macromolecules*, Vol. 28 (4), pp844-853 (1995)
- (94) He, Y., Shuai, X. T., Cao, A., Kasuya, K., Doi, Y., and Inoue, Y. "Enzymatic biodegradation of synthetic atactic poly(R, S-3-hydroxybutyrate) enhanced by an amorphous nonbiodegradable polymer". *Polymer Degradation and Stability*, Vol. 73(2), pp193-199 (2001)
- (95) Hatakeyama, T., and Quinn, F. X. *Thermal Analysis: Fundamentals and Applications to Polymer Science*, 2<sup>nd</sup> Ed, Wiley: New York (1999)
- (96) Promoda, K. P., Chung, T. S., Liu, S. L., Oikawa, H., and Yamaguchi, A. "Characterization and thermal degradation of polyimide and polyamide liquid crystalline polymers". *Polymer Degradation and Stability*, Vol. 67(2), pp365-374 (2000)
- (97) Herrera, M., Matuschek, G., and Kettrup, A. "Comparative studies of polymers using TA-MS, macro TA-MS and TA-FTIR". *Thermochimica*

- Acta*, Vol. 361(1-2), pp69-76 (2000)
- (98) Silverstein, R. M., and Webster, F. X. *Spectrometric Identification of Organic Compounds*, 6<sup>th</sup> Ed, John Wiley & Sons, Inc., New York, pp96 (1998)
- (99) Morikawa, M., and Marchessault, R. H. "Pyrolysis of bacterial polyalkanoates". *Canadian Journal of Chemistry*, Vol. 59(15), pp2306-2313 (1981)
- (100) Aoyagi, Y., Yamashita, K., and Doi, Y. "Thermal degradation of poly[(R)-3-hydroxybutyrate], poly[epsilon-caprolactone], and poly[(S)-lactide]". *Polymer Degradation and Stability*, Vol. 76(1), pp53-59 (2002)
- (101) Andreoni, W. *The Physics of Fullerene-based and Fullerene-related Materials*, Kluwer Academic Publishers: Boston (2000)
- (102) Wudl, F. "Fullerene materials". *Journal of Materials Chemistry*, Vol. 12(7), pp1959-1963 (2002)
- (103) Hirsch, A. "New cages and unusual guests: fullerene chemistry continues to excite". *Angewandte Chemie Internatioal Edition*, Vol. 40(7), pp1195-1197 (2001)
- (104) Guldi, D. M. "Fullerenes: three dimensional electron acceptor materials". *Journal of the Chemical Society, Chemical communications*, Issue 5, pp321-327 (2000)
- (105) Hirsch, A. *The Chemistry of the Fullerenes*, Thieme: Stuttgart (1994)
- (106) Foote, C. S. "Photophysical and photochemical properties of fullerenes". *Topics in Current Chemistry*, Vol. 169, pp347-363 (1994)

- (107) Diederich, F., and Thilgen, C. "Covalent fullerene chemistry". *Science*, Vol. 271(5247), pp317-323 (1996)
- (108) Diederich, F., Isaacs, L., and Philp, D. "Syntheses, structures, and properties of methanofullerenes". *Chemical Society Reviews*, Vol. 23(4), pp243-255 (1994)
- (109) Prato, M. "[60]Fullerene chemistry for materials science applications". *Journal of Materials Chemistry*, Vol. 7(7), pp1097-1109 (1997)
- (110) Hirsch, A. "Addition reactions of buckminsterfullerene (C<sub>60</sub>)". *Synthesis*, Issue 8, pp895-913 (1995)
- (111) Balch, A. L., and Olmstead, M. M. "Reactions of transition metal complexes with fullerenes (C<sub>60</sub>, C<sub>70</sub>, etc.) and related materials". *Chemical Reviews*, Vol. 98(6), pp2123-2165 (1998)
- (112) Hsiao, T.-Y., Santhosh, K. C., Liou, K.-F., and Cheng, C.-H. "Nickel-promoted first ene-diyne cycloaddition reaction on C<sub>60</sub>: Synthesis and photochemistry of the fullerene derivatives". *Journal of the American Chemical Society*, Vol. 120(47), pp12232-12236 (1998)
- (113) Pyo, S., Shu, L. H., and Echegoyen, L. "Preparation of a [60]fullerene derivative containing a fused seven-membered ring". *Tetrahedron Letters*, Vol. 39(42), pp7653-7656 (1998)
- (114) Cassell, A. M., Scrivens, W. A., and Tour, J. M. "Assembly of DNA/fullerene hybrid materials". *Angewandte Chemie International Edition*, Vol. 37(11), pp1528-1531 (1998)

- (115) Atwood, J. L., Barbour, L. J., Raston, C. L., and Sudria, I. B. N. "C<sub>60</sub> and C<sub>70</sub> compounds in the pincerlike jaws of calix[6]arene". *Angewandte Chemie International Edition*, Vol. 37(7), pp981-983 (1998)
- (116) Nierengarten, J.-F., Schall, C., and Nicoud, J.-F. "A tetraphenylporphyrin with four fullerene substituents". *Angewandte Chemie International Edition*, Vol. 37(13-14), pp1934-1936 (1998)
- (117) Habicher, T., Nierengarten, J.-F., Gramlich, V., and Diederich, F. "Pt<sup>II</sup>-directed self-assembly of a dinuclear cyclophane containing two fullerenes". *Angewandte Chemie International Edition*, Vol. 37(13-14), pp1916-1919 (1998)
- (118) Nierengarten, J.-F., Oswald, L., and Nicoud, J.-F. "Dynamic cis/trans isomerisation in a porphyrin-fullerene conjugate". *Journal of the Chemical Society, Chemical Communications*, Issue 15, pp1545-1546 (1998)
- (119) Dietel, E., Hirsch, A., Eichhorn, E., Rieker, A., Hackbarth, S., and Roder, B. "A macrocyclic [60]fullerene-porphyrin dyad involving pi-pi stacking interactions". *Journal of the Chemical Society, Chemical Communications*, Issue 18, pp1981-1982 (1998)
- (120) Isobe, H., Tokuyama, H., Sawamura, M., and Nakamura, E. "Synthetic and computational studies on symmetry-defined double cycloaddition of a new tris-annulating reagent to C<sub>60</sub>". *Journal of Organic Chemistry*, Vol. 62(15), pp5034-5041 (1997)
- (121) Nierengarten, J.-F., Gramlich, V., Cardullo, F., and Diederich, F. "Regio- and diastereoselective bisfunctionalization of C<sub>60</sub> and enantioselective

- synthesis of a C<sub>60</sub> derivative with a chiral addition pattern”. *Angewandte Chemie International Edition*, Vol. 35(18), pp2101-2103 (1996)
- (122) Taki, M., Sugita, S., Nakamura, Y., Kasashima, E., Yashima, E., Okamoto, Y., and Nishimura, J. “Selective functionalization on [60]fullerene governed by tether length”. *Journal of the American Chemical Society*, Vol. 119(5), pp926-932 (1997)
- (123) Shen, C. K.-F., Chien, K. M., Juo, C. G., Her, G. R., and Luh, T. Y. “Chiral bisazafulleroids”. *Journal of Organic Chemistry*, Vol. 61(26), pp9242-9244 (1996)
- (124) Nakamura, E., Isobe, H., Tokuyama, H., and Sawamura, M. “Regio- and diastereo-controlled double cycloaddition to [60]fullerene: one-step synthesis of C<sub>s</sub> and C<sub>2</sub> chiral organofullerenes with new tris-annulating reagents”. *Journal of the Chemical Society, Chemical Communications*, Issue 15, pp1747-1748 (1996)
- (125) Isaacs, L., Haldimann, R. F., and Diederich, F. “Tether-directed remote functionalization of buckminsterfullerene-regiospecific hexaadduct formation”. *Angewandte Chemie International Edition*, Vol. 33(22), pp2339-2342 (1994)
- (126) Friedman, S. H., Ganapathi, P. S., Rubin, Y., and Kenyon, G. L. “Optimizing the binding of fullerene inhibitors of the HIV-1 protease through predicted increases in hydrophobic desolvation”. *Journal of Medicinal Chemistry*, Vol. 41(13), pp2424-2429 (1998)

- (127) Chen, H. C., Yu, C., Ueng, T. H., Chen, S. D., Chen, B. J., Huang, K. J., and Chiang, L. Y. "Acute and subacute toxicity study of water-soluble polyalkylsulfonated C-60 in rats". *Toxicologic Pathology*, Vol. 26(1), pp143-151 (1998)
- (128) Miyata, N., and Yamakoshi, Y. *Fullerenes: Recent Advances in the Chemistry and Physics of Fullerenes and Related Materials*, Kadish, K. M., Ruoff, R. S., Eds., The Electrochemical Society: Pennington, NJ, Vol. 5, pp345 (1995)
- (129) An, Y.-Z., Anderson, J. L., and Rubin, Y. "Synthesis of  $\alpha$ -amino acid derivatives of C<sub>60</sub> from 1,9-(4-hydroxycyclohexano)-buckminsterfullerene". *Journal of Organic Chemistry*, Vol. 58(18), pp4799-4801 (1993)
- (130) Skiebe, A., and Hirsch, A. "A facile method for the synthesis of amino-acid and amido derivatives of C<sub>60</sub>". *Journal of the Chemical Society, Chemical Communications*, Issue 3, pp335-336 (1994)
- (131) Jensen, A. W., Wilson, S. R., and Schuster, D. I. "Biological applications of fullerenes". *Bioorganic & Medicinal Chemistry*, Vol. 4(6), pp767-779 (1996)
- (132) Nierengarten, J. F., Schall, C., Nicoud, J. F., Heinrich, B., and Guillon, D. "Amphiphilic cyclic fullerene bisadducts: synthesis and Langmuir films at the air-water interface". *Tetrahedron Letters*, Vol. 39(32), pp5747-5750 (1998)
- (133) Chen, C., Li, J., Ji, G., Zheng, Q., and Zhu, D. "Synthesis of a C<sub>60</sub> functionalized calix[4]-spiro-bis-crown". *Tetrahedron Letters*, Vol. 39(40), pp7377-7380 (1998)

- (134) Gan, L., Jiang, J., Su, Y., Shi, Y., Huang, C., Pan, J., Lu, M., and Wu, Y. "Synthesis of pyrrolidine ring-fused fullerene multicarboxylates by photoreaction". *Journal of Organic Chemistry*, Vol. 63(13), pp4240-4247 (1998)
- (135) Bourgeois, J., Echegoyen, L., Fibbioli, M., Pretsch, E., and Diederich, F. "Regioselective synthesis of trans-1 fullerene bis-adducts directed by a crown ether tether: alkali metal cation modulated redox properties of fullerene crown ether conjugates". *Angewandte Chemie International Edition*, Vol. 37(15), pp2118-2121 (1998)
- (136) Schergna, S., Ros, T. D., Linda, P., Ebert, C., Gardossi, L., and Prato, M. "Enzymatic modification of fullerene derivatives". *Tetrahedron Letters*, Vol. 39(42), pp7791-7794 (1998)
- (137) Kurz, A., Halliwell, C. M., Davis, J. J., Hill, H. A. O., and Canters, G. W. "A fullerene-modified protein". *Journal of the Chemical Society, Chemical Communications*, Issue 3, pp433-434 (1998)
- (138) Boutorine, A. S., Tokuyama, H., Takasugi, M., Isobe, H., Nakamura, E., and Helene, C. "Fullerene-oligonucleotide conjugates – photoinduced sequence-specific DNA cleavage". *Angewandte Chemie International Edition*, Vol. 33(23-24), pp2462-2465 (1994)
- (139) An, Y.-Z., Chen, C.-H. B., Anderson, J. L., Sigman, D. S., Foote, C. S., and Rubin, Y. "Sequence-specific modification of guanosine in DNA by a C<sub>60</sub>-linked deoxyoligonucleotide: evidence for a non-singlet oxygen mechanism". *Tetrahedron*, Vol. 52(14), pp5179-5189 (1996)

- (140) Jin, H., Chen, W. Q., Tang, X. W., Chiang, L. Y., Yang, C. Y., Schloss, J. V., and Wu, J. Y. "Polyhydroxylated C<sub>60</sub>, fullerenols, as glutamate receptor antagonists and neuroprotective agents". *Journal of Neuroscience Research*, Vol. 62(4), pp600-607 (2000)
- (141) Lai, H. S., Chen, W. J., and Chiang, L. Y. "Free radical scavenging activity of fullereneol on the ischemia-reperfusion intestine in dogs". *World Journal of Surgery*, Vol. 24(4), pp450-454 (2000)
- (142) Huang, H. M., Ou, H. C., Hsieh, S. J., and Chiang, L. Y. "Blockage of amyloid  $\beta$  peptide-induced cytosolic free calcium by fullereneol-1, carboxylate C<sub>60</sub> in PC12 cells". *Life Sciences*, Vol. 66(16), pp1525-1533 (2000)
- (143) Lai, Y. L., Chiou, W. Y., Lu, F. J., and Chiang, L. Y. "Roles of oxygen radicals and elastase in citric acid-induced airway constriction of guinea-pigs". *British Journal of Pharmacology*, Vol. 126(3), pp778-784 (1999)
- (144) Lu, L. H., Lee, Y. T., Chen, H. W., Chiang, L. Y., and Huang, H. C. "The possible mechanisms of the antiproliferative effect of fullereneol, polyhydroxylated C<sub>60</sub>, on vascular smooth muscle cells". *British Journal of Pharmacology*, Vol. 123(6), pp1097-1102 (1998)
- (145) Ueng, T. H., Kang, J. J., Wang, H. W., Cheng, Y. W., and Chiang, L. Y. "Suppression of microsomal cytochrome P450-dependent monooxygenases and mitochondrial oxidative phosphorylation by fullereneol, a polyhydroxylated fullerene C<sub>60</sub>". *Toxicology Letters*, Vol. 93(1), pp29-37 (1997)

- (146) Lai, Y. L., and Chiang, L. Y. "Water-soluble fullerene derivatives attenuate exsanguination-induced bronchoconstriction of guinea-pigs". *Journal of Autonomic Pharmacology*, Vol. 17(4), pp229-235 (1997)
- (147) Tsai, M. C., Chen, Y. H., and Chiang, L. Y. "Polyhydroxylated C<sub>60</sub>, fullerenol, a novel free-radical trapper, prevented hydrogen peroxide- and cumene hydroperoxide-elicited changes in rat hippocampus in-vitro". *Journal of Pharmacy and Pharmacology*, Vol. 49(4), pp438-445 (1997)
- (148) Chiang, L. Y., Swirczewsky, J. W., Hsu, C. S., Chowdhury, S. K., Cameron, S., and Creegan, K. "Multihydroxy additions onto C<sub>60</sub> fullerene molecules". *Journal of the Chemical Society, Chemical Communications*, Issue 24, pp1791-1793 (1992)
- (149) Chiang, L. Y., Upasani, R. B., Swirczewsky, J. W., and Soled, S. "Evidence of hemiketals incorporated in the structure of fullerols derived from aqueous acid chemistry". *Journal of the American Chemical Society*, Vol. 115(13), pp5453-5457 (1993)
- (150) Chiang, L. Y., Wang, L. Y., and Swirczewsky, J. W. "Efficient synthesis of polyhydroxylated fullerene derivatives via hydrolysis of polycyclosulfated precursors". *Journal of Organic Chemistry*, Vol. 59(14), pp3960-3968 (1994)
- (151) Chiang, L. Y., Bhonsle, J. B., Wang, L. Y., Shu, S. F., Chang, T. M., and Hwu, J. R. "Efficient one-flask synthesis of water-soluble [60]fullerenols". *Tetrahedron*, Vol. 52(14), pp4963-4972 (1996)

- (152) Chen, B. H., Huang, J. P., Wang, L. Y., Shiea, J., Chen, T. L., and Chiang, L. Y. "Facile sulfation of C<sub>60</sub> using P<sub>2</sub>O<sub>5</sub> as an oxidation promoter". *Journal of the Chemical Society, Perkin Transactions 1*, Issue 7, pp1171-1173 (1998)
- (153) Li, Q. N., Xiu, Y., Zhang, X. D., Liu, R. L., Du, Q. Q., Shun, X. G., Chen, S. L., and Li, W. X. "Preparation of <sup>99m</sup>Tc-C<sub>60</sub>(OH)<sub>x</sub> and its biodistribution studies". *Nuclear Medicine and Biology*, Vol. 29(6), pp707-710 (2002)
- (154) Hitchcock, P. B., and Taylor, R. "Single crystal X-ray structure of tetrahedral C<sub>60</sub>F<sub>36</sub>: the most aromatic and distorted fullerene". *Journal of the Chemical Society, Chemical Communications*, Issue 18, pp2078-2079 (2002)
- (155) Adamson, A. J., Holloway, J. H., Hope, E. G., and Taylor, R. "Halogen and interhalogen reactions with [60]fullerene: preparation and characterization of C<sub>60</sub>Cl<sub>24</sub> and C<sub>60</sub>Cl<sub>18</sub>F<sub>14</sub>". *Fullerene Science and Technology*, Vol. 5(4), pp629-642 (1997)
- (156) Birkett, P. R., Hitchcock, P. B., Kroto, H. W., Taylor, R., and Walton, D. R. M. "Preparation and characterization of C<sub>60</sub>Br<sub>6</sub> and C<sub>60</sub>Br<sub>8</sub>". *Nature*, Vol. 357(6378), pp479-481 (1992)
- (157) Tycko, R., Dabbagh, G., Fleming, R. M., Haddon, R. C., Makhija, A. V., and Zahurak, S. M. "Molecular dynamics and phase transition in solid C<sub>60</sub>". *Physical Review Letters*, Vol. 67(14), pp1886-1889 (1991)
- (158) Stewart, C. F., and Ratain, M. J. *Pharmacology of Cancer Chemotherapy*, 6<sup>th</sup> Ed, Lippincott Williams and Wilkins, Philadelphia, pp1-16 (2001)

- (159) Williams, D. H., and Bardsley, B. "The vancomycin group of antibiotics and the fight against resistant bacteria". *Angewandte Chemie International Edition*, Vol. 38(9), pp1173-1193 (1999)
- (160) Nicolaou, K. C., Boddy, C. N. C., Bräse, S., and Winssinger, N. "Chemistry, biology, and medicine of the glycopeptide antibiotics". *Angewandte Chemie International Edition*, Vol. 7(17), pp3798-3823 (1999)
- (161) Nagarajan, R. *Glycopeptide Antibiotics*, Marcel Dekker, New York. (1994)
- (162) Levine, J. F. "Vancomycin - a review". *Medical Clinics of North America*, Vol. 71 (6), pp1135-1145 (1987)
- (163) Leclercq, R., Derlot, E., Duval, J., and Courvalin, P. "Plasmid-mediated resistance to vancomycin and teicoplanin in *Enterococcus-faecium*". *New England Journal of Medicine*, Vol. 319(3) pp157-161 (1988)
- (164) Hiramatsu, K. "Vancomycin resistance in Staphylococci". *Drug Resistance Updates*, Vol. 1(2) pp135-150 (1998)
- (165) Smith, T. L., Pearson, M. L., Wilcox, K. R., Cruz, C., Lancaster, M. V., Robinson-Dunn, B., Tenover, F. C., Zervos, M. J., Band, J. D., White, E., and Jarvis, W. R. "Emergence of vancomycin resistance in *Staphylococcus aureus*". *New England Journal of Medicine*, Vol. 340(7), pp493-501 (1999)
- (166) Felmingham, D. "Towards the ideal glycopeptide". *Journal of Antimicrobial Chemotherapy*, Vol. 32(5), pp663-666 (1993)
- (167) Zhu, J. P. "Recent developments in reversing glycopeptide-resistant pathogens". *Expert Opinion on Therapeutic Patents*, Vol. 9(8), pp1005-1019 (1999)

- (168) Hältje J.-V. "Growth of the stress-bearing and shape-maintaining murein sacculus of *Escherichia coli*". *Microbiology Molecular Biology Reviews*, Vol. 62, pp181-203 (1998)
- (169) Eggert, U. S., Ruiz, N., Falcone, B. V., Branstrom, A. A., Goldman, R. C., Silhavy, T. J., and Kahne, D. "Genetic basis for activity differences between vancomycin and glycolipid derivatives of vancomycin". *Science*, Vol. 294, pp361-364 (2001)
- (170) Sahm, D. F., Kissinger, J., Gilmore, M. S., Murray, P. R., Mulder, R., Solliday, J., and Clarke, B. "*In vitro* susceptibility studies of vancomycin-resistant *Enterococcus faecalis*". *Antimicrobial Agents and Chemotherapy*, Vol. 33, pp1588-1591 (1989)
- (171) Shankar, N., Baghdayan, A. S., and Gilmore, M. S. "Modulation of virulence within a pathogenicity island in vancomycin-resistant *Enterococcus faecalis*". *Nature*, Vol. 417, pp746-750 (2002)
- (172) Williams D. H., Williamson M. P., Butcher D. W., and Hammond S. J. "Detailed binding-sites of the antibiotics vancomycin and ristocetin-A - determination of intermolecular distances in antibiotic substrate complexes by use of the time-dependent NOE". *Journal of the American Chemical Society*, Vol. 105(5), pp1332-1339 (1983)
- (173) Walsh, C. T., Fisher, S. L., Park, I. S., Prahalad, M., and Wu, Z. "Bacterial resistance to vancomycin: five genes and one missing hydrogen bond tell the story". *Chemistry & Biology*, Vol. 3(1), pp21-28 (1996)

- (174) Wright, G. D., and Walsh, C. T. "D-Alanyl-D-alanine ligases and the molecular mechanism of vancomycin resistance". *Accounts of Chemical Research*, Vol. 25(10), pp468-473 (1992)
- (175) Cristofaro, M. F., Beauregard, D. A., Yan, H. S., Osborn, N. J., and Williams, D. H. "Cooperativity between nonpolar and ionic forces in the binding of bacterial-cell wall analogs by vancomycin in aqueous-solution". *The Journal of Antibiotics*, Vol. 48(8), pp805-810 (1995)
- (176) Xu, R., Greiveldinger, G., Marenus, L., Cooper, A., and Ellman, A. "Combinatorial library approach for the identification of synthetic receptors targeting vancomycin-resistant bacteria". *Journal of the American Chemical Society*, Vol. 121(20), pp4898-4899 (1983)
- (177) Nicolaou, K. C., Hughes, R., Cho, S. C., Winssinger, N., Smethurst, C., Labischinski, H., and Endermann, R. "Target-accelerated combinatorial synthesis and discovery highly potent antibiotics effective against vancomycin-resistant bacteria". *Angewandte Chemie International Edition*, Vol. 39(21), pp3823-3828 (2000)
- (178) Nagarajan, R., Schabel, A. A., Occolowitz, J. L., Counter, F. T., Ott, J. L., and Felty-Duckworth, A. M. "Synthesis and antibacterial evaluation of N-alkyl vancomycins". *The Journal of Antibiotics*, Vol. 42(1), pp63-72 (1989)
- (179) Nicasti, T. I., Cole, C. T., Preston, D. A., Schabel, A. A., and Nagarajan, R. "Activity of glycopeptides against vancomycin-resistant gram-positive bacteria". *Antimicrobial Agents and Chemotherapy*, Vol. 33(9), pp1477-1481 (1989)

- (180) Nagarajan, R., Schabel, A. A., Occolowitz, J. L., Counter, F. T., and Ott, J. L. "Synthesis and antibacterial activity of N-acyl vancomycins". *The Journal of Antibiotics*, Vol. 41(10), pp1430-1438 (1988)
- (181) Nagarajan, R. "Structure-activity-relationships of vancomycin-type glycopeptide antibiotics". *The Journal of Antibiotics*, Vol. 46(8), pp1181-1195 (1993)
- (182) Beauregard, D. A., Williams, D. H., Gwynn, M. N., and Knowles, D. J. C. "Dimerization and membrane anchors in extracellular targeting of vancomycin group antibiotics". *Antimicrobial Agents and Chemotherapy*, Vol. 39(3), pp781-785 (1995)
- (183) Cooper, R. D. G., Snyder, N. J., Zweifel, M. J., Staszak, M. A., Wilkie, S. C., Nicas, T. I., Mullen, D. L., Butler, T. F., Rodriguez, M. J., Huff, B. E., and Thompson, R. C. "Reductive alkylation of glycopeptide antibiotics: synthesis and antibacterial activity". *The Journal of Antibiotics*, Vol. 49(6), pp575-581 (1996)
- (184) Rodriguez, M. J., Snyder, N. J., Zweifel, M. J., Wilkie, S. C., Stack, D. R., Cooper, R. D. G., Nicas, T. I., Mullen, D. L., Butler, T. F., and Thompson, R. C. "Novel glycopeptide antibiotics: N-alkylated derivatives active against vancomycin-resistant enterococci". *The Journal of Antibiotics*, Vol. 51, pp560-569 (1998)
- (185) Sharman, G. J., Try, A. C., Dancer, R. J., Cho, Y. R., Staroske, T., Bardsley, B., Maguire, A. J., Cooper, M. A., O'Brien, D. P., and Williams, D. H. "The role of dimerization and membrane anchoring in activity of glycopeptide

- antibiotics against vancomycin-resistant bacteria". *Journal of the American Chemical Society*, Vol. 119, pp12041-12047 (1997)
- (186) Ge, M., Chen, Z., Onishi, H. R., Kohler J., Silver, L. L., Kerns, R., Fukuzawa, S., Thompson, C., and Kahne, D. "Vancomycin derivatives that inhibit peptidoglycan biosynthesis without binding D-Ala-D-Ala". *Science*, Vol. 284(5413), pp507-511 (1999)
- (187) Somma, S., Gastaldo, L., and Corti, A. "Teicoplanin, a new antibiotic from actinoplanes-teichomyceticus NOV-SP". *Antimicrobial Agents and Chemotherapy*, Vol. 26(6), pp917-923 (1984)
- (188) Barna, J. C. J., Williams, D. H., Stone, D. J. M., Leung, T. W. C., and Doddrell, D. M. "Structure elucidation of the teicoplanin antibiotics". *Journal of the American Chemical Society*, Vol. 106(17), pp4895-4902 (1984)
- (189) Sundram U. N., and Griffin, J. H. "Novel vancomycin dimer with activity against vancomycin-resistant *Enterococci*". *Journal of the American Chemical Society*, Vol. 118, pp13107-13108 (1996)
- (190) Rao, J. H., and Whitesides G. M. "Using capillary electrophoresis to study the electrostatic interactions involved in the association of D-Ala-D-Ala with vancomycin". *Journal of the American Chemical Society*, Vol. 119, pp9336-9340 (1997)
- (191) Rao, J. H., and Whitesides G. M. "Tight binding of a dimeric derivative of vancomycin with dimeric L-Lys-D-Ala-D-Ala". *Journal of the American Chemical Society*, Vol. 119, pp10286-10290 (1997)

- (192) Rao, J. H., Yan L., Xu, B., and Whitesides G. M. "Using surface plasmon resonance to study the binding of vancomycin and its dimer to self-assembled monolayers presenting D-Ala-D-Ala". *Journal of the American Chemical Society*, Vol. 121, pp2629-2630 (1999)
- (193) Rao, J. H., Lahiri, J., Weis, R. M., and Whitesides, G. M. "Design, synthesis, and characterization of a high-affinity trivalent system derived from vancomycin and L-Lys-D-Ala-D-Ala". *Journal of the American Chemical Society*, Vol. 122(12), pp2698-2710 (2000)
- (194) Rao, J. H., Lahiri, J., Isaacs, L., Weis, R. M., and Whitesides, G. M. "A trivalent system from vancomycin center dot D-Ala-D-Ala with higher affinity than avidin center dot biotin". *Science*, Vol. 280(5364), pp708-711 (1998)
- (195) Jinno, K. *Separation of Fullerenes by Liquid Chromatography*, Royal Society of Chemistry, UK (1999)
- (196) Taylor, R. "Fluorinated fullerenes". *Chemistry – A European Journal*, Vol. 7(19), pp4075-4083 (2001)

## Appendices

### Appendix 1. Elemental analysis of C<sub>60</sub>Br<sub>24</sub>

# MEDAC LTD

Analytical and chemical consultancy services

## A N A L Y T I C A L   R E P O R T

Date            16 June, 2004

Name            Jidong He

Sample ID    CBr

Formula

**MEDAC LTD**  
Brunel Science Centre  
Cooper's Hill Lane  
Englefield Green  
Egham  
Surrey TW20 0JZ  
United Kingdom

[www.medacLtd.com](http://www.medacLtd.com)

Tel/Fax No. 01784 434299  
Email: [MedacLtd@aol.com](mailto:MedacLtd@aol.com)

| ELEMENT   | C     | H     | N     | S | Cl | Br    | I |  |  |
|-----------|-------|-------|-------|---|----|-------|---|--|--|
| % Theory  |       |       |       |   |    |       |   |  |  |
| % Found 1 | 25.59 | <0.10 | <0.10 |   |    | 70.91 |   |  |  |
| % Found 2 | 25.59 | <0.10 | <0.10 |   |    | 70.95 |   |  |  |

## Appendix 2. Elemental analysis of ethoxy [60]fullerol

# MEDAC LTD

Analytical and chemical consultancy services

## A N A L Y T I C A L   R E P O R T

Date        16 June, 2004

Name        Jidong He

Sample ID   CDH

Formula

**MEDAC LTD**  
Brunel Science Centre  
Cooper's Hill Lane  
Englefield Green  
Egham  
Surrey TW20 0JZ  
United Kingdom

[www.medacLtd.com](http://www.medacLtd.com)

Tel/Fax No. 01784 434299  
Email: [MedacLtd@aol.com](mailto:MedacLtd@aol.com)

| ELEMENT   | C     | H    | N     | S | Cl | Br | I |  |  |
|-----------|-------|------|-------|---|----|----|---|--|--|
| % Theory  |       |      |       |   |    |    |   |  |  |
| % Found 1 | 66.75 | 4.59 | <0.10 |   |    |    |   |  |  |
| % Found 2 | 66.72 | 4.72 | <0.10 |   |    |    |   |  |  |

### Appendix 3. MALDI-TOF reflection mass spectrum of ethoxy [60]fullerol

Method: RDE2000K

Laser: 2840

Mode: Reflector

Scans Averaged: 30

Accelerating Voltage: 20000

Pressure: 5.32e-07

Grid Voltage: 72.000 %

Low Mass Gate: 400.0

Guide Wire Voltage: 0.030 %

Timed Ion Selector: 180.0 OFF

Delay: 100 ON

Negative Ions: OFF

